INHIBITION OF MONOCYTE/MACROPHAGE FUNCTIONS BY DEXAMETHASONE-LIPOSOMES IN ARTHRITIS

Influence on the expression of pro-inflammatory cytokines and effects in the adjuvant arthritis model

Hemmung von Monozyten/Makrophagen Funktionen durch Dexamethson-Liposomen in der Arthritis

Einfluss auf die Expression von pro-inflammatorischen Zytokinen und Effekte im Modell der Adjuvansarthritis

Dissertation

zur Erlangung des akademischen Grades

doctor medicinae (Dr. med.)

vorgelegt dem Rat der Medizinischen Fakultät

der Friedrich-Schiller-Universität Jena

von Rebecca Anderson de la Llana

geboren am 6. April 1983 in St Martin d'Hères

Gutachter

1. Professor R. W. Kinne, Orthopedics Department, Friedrich Schiller University, Jena
2. Professor R. Bräuer, Institute of Pathology, Friedrich Schiller University, Jena
3. Professor C. Castellote, Institute of Farmacology, Universityof Barcelona, Barcelona

Tag der öffentlichen Verteidigung: 7. April 2009

Abbreviations

AA	adjuvant arthritis
Ab	antibody
abs	absolute
AP-1	activator protein 1
APC	antigen presenting cell
approx	approximately
BSA	bovine serum albumin
ºC	centigrade Celsius
CD	cluster of differentiation
cDNA	complementary DNA
Chol	cholesterol
cNOS	constitutive nitric oxide synthase
COX	cyclooxygenase
CSF	colony stimulating factor
CSI	Cox specific inhibitor
CTGF	connective tissue growth factor
DMARD	disease modifying anti rheumatic drugs
DNA	deoxyribonucleic acid
DPPC	dipalmitoylphosphatidylcholin
DPPG	dipalmitoylphosphatidylglycerol
DTH	delayed type hypersensitivity
DxM	dexamethasone
e.g.	*exempli gratia* (Lat. = for instance)
ESR	erythrocyte sedimentation rate
expt.	experiment
fig.	figure
FOI	fluophore incorporation
g	gram
GAPDH	glycerol-aldehyde-3-phosphate dehydrogenase
GC	glucocorticoids
h	hour
HLA	human leukocyte antigen
HE	hematoxylin & eosin
Hum	human
i.e.	*id est* (Lat. = that is to say)
Ig	immunoglobulin
IFN	interferon
IL	interleukin
iNOS	inducible nitric oxide synthase
Iκ-B	inhibitor of NF-κB
i.v.	intravenous
k-	kilo-
l	liter
lipos	liposomes
kDa	kilo-Dalton
LN	lymph node

LPS	lipopolysaccharid
m-	milli-
µ-	micro-
MAPK	mitogen activated protein-kinase
Mb	Mycobacterium butyricum
MCSF	macrophage colony stimulating factor
Mφ	macrophages
MHC	major histocompatibility complex
min	minute
MIP	macrophage inhibiting protein
MPS	monocyte – phagocyte system
mRNA	messenger RNA
NF-κB	nuclear factor-kB
nm	nanometer
NO	nitric oxide
NSAID	non steroidal anti-inflammatory drugs
p-	pico-
PBMC	peripheral blood mononuclear cells
PBS	phosphate buffer saline
PEG	polyethylenglykol
PM	peritoneal macrophages
PMN	polymorphonuclear leukocytes
RA	rheumatoid arthritis
RES	reticulo-endothelial system
RNA	ribonucleic acid
rpm	rounds per minute
RT	room temperature
RT-PCR	reverse transcriptase polymerase chain reaction
s.c.	subcutaneous
tab.	table
TGF	transforming growth factor
TNF	tumor necrosis factor
vs.	versus
WBC	white blood count

Contents

1. ZUSAMMENFASSUNG

Hintergrund: Sowohl die Intensität der Makrophageninfiltration in die Synovialmembran als auch der Aktivierungsgrad dieser Zellen zeigen eine deutliche Korrelation mit der Schwere der Rheumatoiden Arthritis (RA). Makrophagen (Mφ) besitzen eine Vielzahl von pro-inflammatorischen und destruktiven Fähigkeiten die zur akuten und chronischen Erkrankung beitragen. Bei der RA zeigen neben den ortständigen Mφ auch die zirkulierenden Mφ Zeichen der Aktivierung. Demzufolge erweist sich das selektive Anti-Makrophagen-Prinzip als effektiver Ansatz um die lokale und systemische Entzündung zu hemmen sowie der daraus folgenden irreversiblen Gelenkdestruktion vorzubeugen.

Glukokortikoide (GK) gehören zu den wichtigsten und am häufigsten eingesetzten Therapeutika bei rheumatologischen Erkrankungen, und zeigen deutliche antiphlogistische und immunsuppressive Eigenschaften. Wegen ihrer unschätzbaren Effizienz und der Schwierigkeit sie durch andere Medikamente zu ersetzen, trotz der bedenklichen Vielzahl von systemischen Nebenwirkungen vor allem unter Langzeittherapie, besteht das Bedürfnis sicherere und verträglichere Darreichungsformen zu entwickeln. Durch spezifisches „Targeting" des entzündeten Gelenks gelingt es, die Effizienz der GK zu steigern und zusätzlich die systemischen Nebenwirkungen zu minimieren. Dieses Ziel wird seit den 1970er Jahren verfolgt, indem man versucht GK in liposomale Vehikel zu verpacken. Liposomen besitzen nämlich die Eigenschaft von aktivierten Mφ phagozytiert zu werden und demzufolge im entzündeten Gelenk zu kumulieren.

In einer vorherigen Studie wurden verschiedene Dexamethason-Liposomen (DxM-Lipos) mit unterschiedlichen Liposomengrößen und -zusammensetzungen, in Hinblick auf ihre Fähigkeit von Mφ aufgenommen zu werden und pro-inflammatorische Effektorfunktionen von Mφ zu inhibieren, in vitro verglichen. Daraufhin wurde die Formulierung, die diese Eigenschaften am besten erfüllte, für die vorliegende Arbeit ausgewählt.

Methoden und Ergebnisse: Zuerst wurden die Phagozytoserate und die Vitalität von humanen Blutmonozyten nach Inkubation mit DxM-Lipos untersucht, um die Liposomenaufnahme abzusichern und einen möglichen Effekt auf den Zelltod auszuschließen. Nachdem diese Vorraussetzungen erfüllt waren, wurde die differentielle Genexpression in LPS/IFN-γ stimulierten Monozyten nach Vorinkubation mit wirkstofffreien-PBS-Lipos oder DxM-Lipos mittels Microarrays untersucht. Durch diese Methode kann die Regulation der Expression tausender von Genen gleichzeitig ermittelt werden. Dadurch wurde ein Überblick der wichtigsten, durch DxM-Lipos hoch-

oder herunter-regulierten Genen erhalten. Die detaillierte Auswertung zeigte die signifikant verringerte Expression von einigen Interleukinen (TNF-α, IL-1β, IL-6, IL-1RA) und der Cyklooxygenase 1. Diese Ergebnisse wurden mittels RT-PCR, sowie durch Messung der Zytokinproduktion mittels ELISA validiert, wodurch die wirksame Hemmung von pro-inflammatorische Funktionen von Monozyten durch DxM-Lipos bestätigt werden konnte. Weiterhin zeigten diese Studien, dass Microarrays als Screening-Verfahren geeignet sind, um einen Überblick von relevanten Expressionänderungen bei Krankheit sowie unter Therapien zu erhalten, aber auch um weitere Untersuchungen gezielt auf die damit identifizierten Gene zu fokussieren.

Im zweiten Teil dieser Arbeit wurde die Wirksamkeit der DxM-Lipos im experimentellen Modell der Adjuvansarthritis (AA) der Ratte untersucht. Diese wurde am Tag 0 durch intradermale Injektion von Mycobacterium butyricum (Mb) ausgelöst, und nach Ausbruch der Erkrankung systemisch mit DxM-Lipos (3 x 1 mg/kg, i.v.; Tag 14, 15, 16) behandelt. Dies führte nicht nur zu einer hoch-wirksamen Unterdrückung der klinischen Zeichen der Arthritis, sondern auch zu einer signifikanten Hemmung der histologischen Zeichen. DxM-Lipos verursachten eine lang-anhaltende Verbesserung der AA, die auch signifikant stärker war als die Behandlung mit gleicher Dosis freien DxM oder PBS-Lipos. Weiterhin konnten Dosisabhängigkeitsstudien zeigen, dass durch die Verkapselung von DXM dessen Potenz mindestens um den Faktor 10 erhöht wurde.

Um festzustellen, ob DxM-Lipos auch systemische Entzündungszeichen beeinflussten, wurden hämatologische und immunologische Parameter untersucht. Dabei zeigte sich, dass DxM-Lipos im Gegensatz zu freiem DxM signifikant die Erhöhung der Blutsenkungsgeschwindigkeit, der Leukozytenzahl sowie der Lymphozytenzahl in Blut, Milz und lokalen, poplitealen Lymphknoten unterdrückten. Der markante Abfall der spezifischen anti-Mb-Antikörper und der zirkulierenden Lymphozyten wurde auf einen möglichen immunsupprimierenden Effekt zurückgeführt. Dennoch konnten diese Studien die wirksame Hemmung der systemischen Mφ-Aktivierung durch DxM-Lipos in den peritonealen Mφ zeigen, bei denen die Produktion von TNF-α, IL-1β und IL-6 signifikant reduziert wurde.

Der Vergleich von DxM-Lipos mit dem in Deutschland für schwere RA-Fälle zugelassenen, hoch-effizienten gegen TNF-α gerichteten Präparat Enbrel® (2 x 0.3 mg/kg, subkutane Applikation; Tag 14, 17) ergab im AA Modell eine signifikant höhere Wirksamkeit der DxM-Lipos.

Schlussfolgerung: Durch diese translationelle Forschung konnte gezeigt werden, dass die verkapselte GK-Formulierung das Potential besitzt, die therapeutische Wirksamkeit zu erhöhen sowie Nebenwirkungen zu vermindern. Sie stellt demzufolge eine erfolgsversprechende, sichere Therapiealternative in der zukünftigen Behandlung der RA dar.

2. INTRODUCTION

2.1 Rheumatoid arthritis

Rheumatologic diseases are subdivided into two main categories: the degenerative disorders, caused by a dysfunction of the cartilage metabolism, and the inflammatory diseases, characterized by synovial inflammation. Rheumatoid arthritis is the most common inflammatory arthritis affecting approx. 0.8% of the adult population worldwide. The prevalence in woman (estimated 83/100,000) is 2-3 times higher than in men (34/100,000; Symmons, 2002). The onset of the disease is most frequent in between the ages of 35 and 50 and the incidence is highest at the age of 60-75.

Rheumatoid arthritis is a complex and chronic systemic disorder of unknown etiology characterized by persistent synovial tissue inflammation in a symmetric distribution, leading to progressive destruction of cartilage, bone erosion and, over time, complete loss of joint integrity. Eventually, multiple organ systems may be affected. Due to the non-specific nature of the initial symptoms such as weakness, anorexia, sub-febrile temperatures, and vague musculo-skeletal symptoms, a certain period of observation is necessary before establishing the diagnosis. Characteristic clinical features typically develop within 1-2 years of disease onset: bilateral symmetric inflammatory polyarthritis with morning stiffness and movement restriction, subcutaneous nodules, the conversion to positive rheumatoid factor, and typical radiological findings such as juxtaarticular osteopenia, bone erosion, subchondral cysts, and ankylosis in end stages. In 1987 the American College of Rheumatology developed the revised criteria for the classification of RA (tab.1; Arnett et al., 1988), which allow a sensitivity of 91-94% and a specificity of 89% for the diagnosis of RA (Braunwald et al., 2001). However, failure to meet these criteria especially during early stages of the disease does not exclude the diagnosis.

The course of RA is variable, though often presents a poor outcome, with impaired quality of life, co-morbidity (Lazarević-Jovanović et al., 2004) and premature mortality (Pincus et al., 1984). Most patients experience persistent but fluctuating disease activity, accompanied by a variable degree of joint abnormalities and functional impairment. The economic impact of RA is multiplied by the high level of functional impairment it causes. Without adequate treatment, 20 to 30 percent of persons with rheumatoid arthritis become permanently work-disabled within three years of diagnosis, and even with appropriate treatment, approximately 50% of patients

will have work disability within 10 years. Furthermore, due to the stable increase of life expectance in the general population, RA incidence will continue to rise in the following years.

Tab.1 Revised American Rheumatism Association Criteria for Classification of Rheumatoid Arthritis

Criteria	Definition	Percentage with rheumatoid arthritis if sign or symptom is	
		Present	Absent
Morning stiffness	Morning stiffness in and around the joints, for at least 1 hour before maximal improvement	39	14
Arthritis of three or more joint areas	At least 3 joint areas simultaneously have had soft tissue swelling or fluid observed by a physician. The 14 possible areas are right or left PIP, MCP wrist, elbow, knee, ankle and MTP joints	32	13
Arthritis of hand joints	At least 1 area swollen (as defined above) in a wrist, MCP, or PIP joint	33	12
Symmetric arthritis	Simultaneous involvement of the same joint areas (as defined in 2) on both sides of the body (bilateral involvement of PIPs, MCPs, or MTPs is acceptable without absolute symmetry)	29	17
Rheumatoid nodules	Subcutaneous nodules, over bony prominences, or extensor surfaces, or in juxtaarticular regions	50	25
Serum rheumatoid factor	Demonstration of abnormal amounts of serum rheumatoid factor by any method for which the result has been positive in < 5% of normal control subjects	74	13
Radiographic changes	Radiographic changes typical of rheumatoid arthritis on popsteroanterior hand and wrist radiographs, which must include erosions or unequivocal bony decalcification localized in or most markedly adjacent to the involved joints (osteoarthritis changes alone do not qualify)	79	21

PIP= proximal interphalangeal; MCP= metacarpophalangeal; MTP= metatarsophalangeal.

* For classification purposes, a patient shall be said to have rheumatoid arthritis if he/she has satisfied at least 4 of these 7 criteria. Criteria 1 through 4 must have been present for at least 6 weeks. Patients with 2 clinical diagnoses are not excluded. Designation as classic, definite, or probable rheumatoid arthritis is *not* to be made.

2.1.1 Pathomechanism of rheumatoid arthritis

Little is known about the etiology of RA. In genetically predisposed individuals an autoimmune disease is induced which may occur secondary to the response to an infectious agent. This

autoimmune hypothesis is supported by different facts: 1) a genetic predisposition to RA with an association to several HLA-class II molecules has been verified: 80% of whites with rheumatoid arthritis express the HLA-DR1 or -DR4 subtypes, 2) the infiltration of the inflamed joint with T lymphocytes and with local immunoglobulin-producing B-lymphocytes, characteristic for an infectious process, and finally 3) the possibility of inducing a polyarthritis in animals by injecting auto-antibodies (collagen type II).
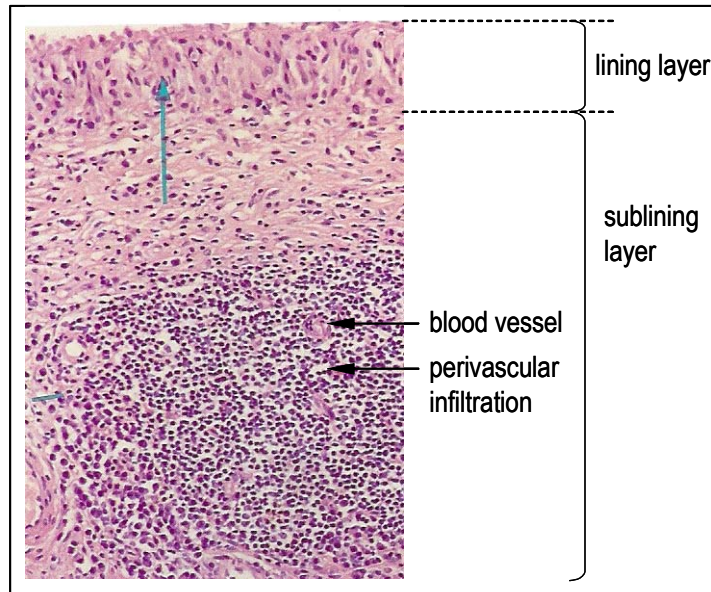
Fig. 1: Histology of the synovial membrane (HE x 150)

The characteristic features of rheumatoid inflammation: the lining layer is hyperplastic (⇑) with multiple cell layers and the sublining is marked with perivascular infiltrates of mononuclear cells (PMN, T cells, B cells, macrophages) forming a lymphoid follicle.
(from Atlas der Histopathologie, Curran; Springer Verlag, 2001)

Micro-vascular injury and an increase in the number of synovial lining cells appear to be the earliest lesions in rheumatoid synovitis (fig.1) followed by perivascular infiltration with mononuclear cells: auto-reactive T-helper cells, B-lymphocytes, plasma cells, dendritic cells (Pettit and Thomas, 1999), and mostly monocyte/macrophage (Mφ; Bresnihan, 1999). As the process continues, the synovium becomes edematous and protrudes into the joint cavity. The interaction between activated lymphocytes and Mφ plays the key role in enhancing the immunologic reaction, resulting in an increased production of pro-inflammatory cytokines, immunoglobulin (Ig), and antibodies against the Fc-portion of autologous IgG (=rheumatoid factors). The complement system is activated and immune complexes with IgG and rheumatoid factors are formed. Both undergo Mφ phagocytosis, amplifying the secretion of pro-inflammatory mediators as well as cartilage-degrading enzymes (metalloproteinases and elastases) and activating different cartilage cells and the capillary endothel. Invasion and proliferation of macrophage-derived Type A synoviocytes (Palmer et al., 1985) and fibroblast-like Type B synoviocytes (Cutolo et al., 1993) in the synovial lining induces the formation of a specific granulation tissue (the so-called pannus), which destroys the adjoining cartilage, joint capsule and periarticular tissue.

The result of this complex interaction between antigen, antigen-presenting-cells (APC), lymphocytes, Mφ, synovial fibroblasts, osteoclasts, and cytokines is a chronic joint inflammation with functional impairment, joint destruction and bone erosion.

2.1.2 Macrophages

2.1.2.1 Role in RA

Macrophages play an essential role in the pathogenesis of RA. They are involved in the maintenance of inflammation, bone destruction but also in systemic immunopathogenetic aspects in acute and chronic phases of arthritis (Kinne et al., 2000). In the inflamed synovium of patients with RA, Mφ abundance significantly correlates with the severity of the disease (Firestein et al., 1990; Mulherin et al., 1996) and the radiological progression of joint destruction. In addition, Mφ which mainly reside in the cartilage-pannus junction are activated, over-expressing major histocompatibility complex class II proteins, pro-inflammatory or regulatory cytokines, growth factors, and matrix-metalloproteinases (Bresnihan et al., 1999). Furthermore, Mφ have a key function in inducing angiogenesis, a characteristic feature of RA, by producing the chemokine IL-8 as well as soluble adhesion molecules (Koch et al., 1992).

The essential role of Mφ is also demonstrated by their central position in the interaction with other major actors of the inflammatory process: inflammation and cytokine production in the synovial membrane are enhanced and sustained by a both antigen-specific and antigen-independent T-cell-Mφ-interaction in acute and chronic phases of RA and Mφ are regarded as amplifiers of the pathogenic, destructive cascade especially via fibroblast activation rather than as primary effectors of tissue destruction (Scott et al., 1997).

Activation is not restricted to synovial Mφ, but extends to circulating monocytes and other cells of the mononuclear phagocyte system, such as differentiated Mφ within rheumatoid nodules, both associated with the severity of arthritis (Schulze-Koops et al., 1997). Activated circulating monocytes in different stages of differentiation show a gene activation pattern closely resembling the synovial activation spectrum, suggesting a rheumatoid phenotype imprinting of Mφ before their entry into the inflamed joint (Kinne et al., 2000). Deficiency of anti-inflammatory cytokines may shift the cytokine balance to a pro-inflammatory predominance and therefore accentuate the rheumatoid Mφ imprint.

One of the principal effects of Mφ activation is the up-regulation of NF-κB, which results in increased TNF-α, IL-1β, and IL-6 levels. Moreover, the incapability of inflammatory cells to

undergo apoptosis leads to their accumulation in the joints, thus maintaining the inflammatory process (Foxwell et al., 1998; Liu and Pope, 2003).

2.1.2.2 Pro- and anti-inflammatory mediators: NO and cytokines

The following inflammatory mediators are key effector molecules secreted by Mφ in RA:

Nitric oxide:

NO is a short-lived free radical produced from L-Arginin by the constitutive NO (cNOS) and the inducible NO synthase (iNOS). It is a potent intra- and inter-cellular signaling molecule that activates the intracellular guanylate cyclase and therefore increases cGMP levels. NO plays an important role in the modulation of inflammatory and immune reactions, and elevated concentrations have been detected in the synovial lining of RA patients (Sakurai et al., 1995). Mainly produced by chondrocytes, but also by Mφ of the synovial lining in RA, NO reacts with a number of enzymes and mediators, increases the TNF-α production of synovial cells, induces bone destruction, and activates cyclooxygenase 2 (COX-2). In inflammatory arthritis, protein kinase C expression (PKC) seems to play a key role for both iNOS induction and NO production in human monocytes (Pham et al., 2003), and NF-κB appears to be the most important transcription factor in regulating iNOS gene transcription (Xie et al., 1994).

Cytokines:

Cytokines (a general name for lymphokines, monokines, chemokines, interleukins and interferons) are small proteins which regulate immunity, inflammation and hematopoesis via autocrine, paracrine or endocrine action, by activating or inhibiting different signaling pathways in the target cells.

TNF-α: TNF-α is a 17.3 kDa protein, consisting of 157 amino acids and forming an homotrimer in its biologically active form. A large number of immune, non-immune, and tumor cells produce TNF-α. In RA, elevated concentrations have been found in the synovial fluid. TNF-α is mostly produced by Mφ in the synovial lining and at the pannus-cartilage junction, increases the expression of cytokines, adhesion molecules, and collagenases in synovial cells, and activates cartilage-degrading fibroblasts. Levels of this proximal cytokine in the inflammatory cascade correlate with the number of lining Mφ and the degree of radiologically assessed bone erosion. Transmembrane TNF-α is also involved in local cell-contact mediated processes (Kinne et al.,2000).

IL-1β: IL-1 exists in two different forms: IL-1α and IL-1β. IL-1β has a molecular weight of 17 kDa with 153 amino acids after being processed by caspase-1 (=IL-1 converting enzyme (ICE)), and is predominantly expressed by TNF-α-activated Mφ of the synovial lining. Intra-articular and systemic levels correlate with degree of joint inflammation (Arend et al., 1998). Believed to act in sequence after TNF-α, it stimulates the proliferation of T-cells, activates B-cells and fibroblasts, and enhances the production of prostaglandins (COX-2 mediated; Crofford et al. 1994) or acute-phase-proteins. It increases the secretion of TNF-α, IL-6, and IL-1β by a positive feedback mechanism. IL-1β mediates most of articular damage by inducing the production of metolloproteinases, degrading proteoglycans, and inhibiting their synthesis. It also induces bone resorption by activating osteoclasts. RA chronification may be promoted by the unbalance between IL-1β and its endogenous inhibitor IL-1 receptor antagonist.

IL-6: This 21 kDa protein (212 amino acids) plays a key role in the regulation of the innate immunity and the stimulation of B-cells. IL-6 is known to have both anti- and pro-inflammatory characteristics in RA (Dinarello and Moldawer. It is the most elevated cytokine in the synovial fluid, especially during the acute phase of RA, and is produced mostly by synovial fibroblasts in response to Mφ activation and only partially by Mφ themselves. In vitro, IL-1β stimulates IL-6 production and in vivo it contributes to the peak expression levels of IL-6 in the synovial membrane of experimental arthritis models (Schmidt-Weber et al., 1999). Its levels correlate with the degree of joint destruction, which is at least partially promoted by the generation of osteoclasts. Another pro-inflammatory effect is the induction of acute-phase-protein (i.e., C-reactive protein) and the subsequent systemic effects. Therefore, IL-6 contributes to the negative feedback-mechanisms of TNF-α and IL-1β, which stimulate IL-6 production, who in term inhibit TNF-α and IL-1β synthesis.

At the molecular level, IL-1β, IL-6 and TNF-α initiate a number of pro-inflammatory intracellular signaling events which include the activation of the transcriptional activities of activator protein-1 (AP-1) and nuclear factor-κB (NF-κB) by phosphorylation-dependent dissociation of I-κB.

IL-10: This biologically active homodimer contains 160 amino acids and has a molecular weight of 18-20 kDa. It is a macrophage-derived cytokine which reduces HLA-DR expression and antigen presentation in monocytes, inhibits the expression of pro-inflammatory cytokines like TNF-α and IL-1β in synovial Mφ, and reduces the production of NO as well as oxygen free radicals, functioning thereby as a negative regulator via autocrine regulation. This appears to

be mediated at least partially via an inhibitory effect on NF-κB (Wang et al., 1995). IL-10 levels are elevated in the synovial fluid of RA patients and seem to counteract both TNF-α and IL-1β. Despite its suppressive effects, the quantity of IL-10 is insufficient to neutralize the pro-inflammatory processes (Isomäki, P. et al., 1996)

IL-15: IL-15 levels are augmented in RA synovial fluid and this cytokine is produced by synovial cells, including Mφ. It contributes to a self-perpetuating pro-inflammatory loop, inducing IL-1β, IL-6, IL-8 & MCP-1 production in Mφ, via IL-15 stimulated T cells (Mc Innes et al., 1996).

IL-18: This 157 amino acid long cytokine is, like IL-1β, a product of the IL-1 converting enzyme. It belongs to the IL-1 family and was first identified as an "IFN-γ-inducing factor", because it enhances the production of IFN-γ in T-cells, alongside other cofactors. In addition, it augments the production of TNF-α and the cytotoxicity of NK-cells. In RA, IL-18 is mainly expressed by Mφ of lymphoid aggregates in the synovial membrane. It has clear pro-inflammatory effects, increasing the expression of iNOS and COX-2 in chondrocytes, and augmenting, in concert with IL-12 and IL-15, the production of cytokines and NO in synovial cells.

2.2 Therapies of rheumatoid arthritis

2.2.1 General principles

The goals of therapy in RA are 1) relief of pain, 2) reduction of inflammation, 3) protection of articular structures, 4) maintenance of mobility and function, and 5) control of systemic involvement. Actually, there is no cure for RA. Since the etiology of the disease is unknown and the mechanism of action of many therapeutic agents are uncertain, therapy remains empirical and palliative, aiming only at the relief of symptoms.

Medical treatment of RA involves three general approaches: aspirin and other nonsteroidal anti-inflammatory drugs (NSAID's) including the recently developed COX-2-specific inhibitors (CSI's), glucocorticoids (GC) and finally, the disease modifying or slow acting antirheumatic drugs (DMARD's) which also include immunosuppressive drugs (fig. 2). The principals of the medical management rely on the knowledge that RA is a chronic progressive disease with acute episodes. The usual approach, during acute inflammatory episodes, is to attempt to alleviate the patients symptoms with NSAID's, CSI's or GC in severe cases. Depending on the

aggressiveness of the disease as well as laboratory, and radiological findings, a continuous therapy with DMARD's or low dose GC during symptom-free intervals may be indicated to reduce progression of the joint destruction.
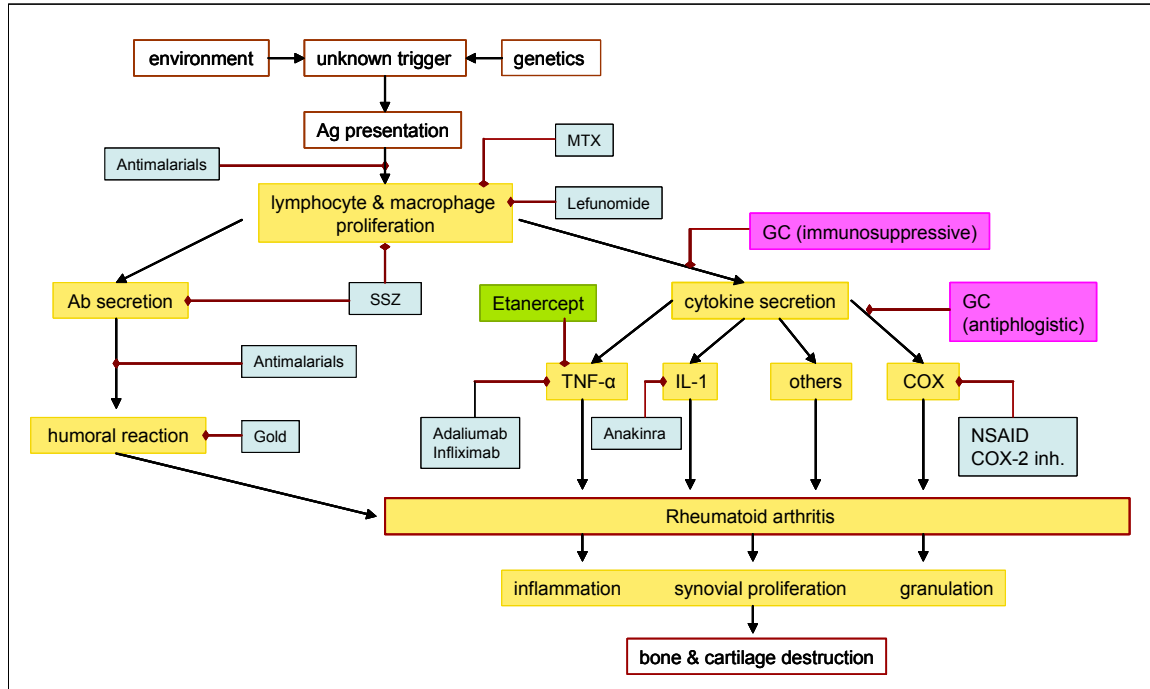
Fig. 2 Therapeutic targets in RA (from Clinical Pharmacology, M, Wehling; Thieme, 2005)
COX: cyclooxygenase, GC: glucocorticoids, MTX: methotrexate, SSZ: sulfasalszine
NSAID: non steroidal anti-inflammatory drugs

NSAID's, including CSI's, control symptoms of the local inflammation process by blocking the activity of the COX enzymes and the production of the resulting prostaglandins and prostacyclins. They therefore have analgesic, anti-inflammatory and antipyretic properties, but appear to exert minimal effect on the progression of the disease. These agents are associated with a wide range of toxic side-effects. Recent evidence indicates that inhibition of the constitutively expressed COX-1 leads to undesired loss of the cytoprotective effect of prostaglandins, whereas inhibition of the inducible COX-2 reduces inflammation symptoms. Therefore CSI's have been developed showing similar efficacy as classic NSAID's, but causing significantly less complications, such as gastroduodenal ulceration (Langman, 1999).

DMARD's include a number of agents that have the capacity to alter the course of RA: gold compounds, D-penicillamine, antimalarials, sulfasalazine, lefunomide, and cytostatic or immunosuppressive drugs such as methotrexate, azathioprine, cyclopoasphamide and cyclosporin. They exert minimal direct anti-inflammatory or analgesic effects, but interfere with different pathomechanical processes of RA. The onset of their therapeutic effect is usually

delayed for weeks or months, but evidence suggests that DMARD's retard the long term development of bone erosion (Fries et al., 1996). However, each of the DMARD's is associated with considerable toxicity and therefore careful monitoring of potential side effects is necessary.

2.2.2 Glucocorticoids

2.2.2.1 Therapeutic use of glucocorticoids in RA

Glucocorticoids (such as prednisolone, methylprednisolone, dexamethasone, etc.) are well-known, efficacious anti-arthritic drugs, widely used for the suppression of inflammation in chronic inflammatory diseases such as asthma, autoimmune diseases, and RA. GC have diverse forms of therapy in RA. Pulse treatment (> 250 mg/d prednisone i.v.) for a few days or intra-articular GC injections are very useful in acute disease-exacerbations in order to control excessive swelling and joint inflammation during these episodes. But most frequently GC are given as a low dose therapy (< 7.5 mg/d prednisone) in order to achieve a better symptomatic control upon concomitant therapy with DMARD's and as an initial bridge therapy before the onset of action of DMARD's (American College of Rheumatology, 2002). Recent evidence shows that low doses of GC also slow the radiological progression of articular disease. Furthermore, in patients with significant renal insufficiency or during pregnancy; in which the use of conventional DMARD's is contraindicated, GC represent the only possible therapy, underlining the difficulty in replacing them with other medications.

2.2.2.2 Mechanism of action

The mechanism of action of GC can be subdivided into genomic and non-genomic effects (Buttgereit, 2001; Barnes, 1998). The non-genomic effects, which occur very rapidly, may be related to alterations in the functional status of the cell membrane. These effects include analgesia and inhibition of adhesion molecule expression. Genomic effects (see fig. 3) are mediated via the glucocorticoid receptor (GC-R) which is found in an inactive form in the cytoplasm, and occurs in a complex with cell proteins (i.e. the heat shock protein 90 (hsp 90)). After binding to GC in the cytoplasm, the GC-R dissociates from the hsp90, dimerizes and translocates into the nucleus to bind to specific DNA motifs, the positive or negative GC response elements (GRE or nGRE). After binding to the GC-R, these motifs change the transcription rate, resulting in either induction or repression of the gene expression.

GC increase the transcription of genes coding for anti-inflammatory proteins, including lipocortin-1, IL-10 and IL-1 receptor antagonist. The anti-inflammatory effect of lipocortin-1 is

mediated through inhibition of phospholipo\ase A2, thereby inhibiting 1) arachidonic acid metabolites like prostaglandins, 2) the production of pro-inflammatory cytokines like IL-1, IL-2, IL-2 receptors, IFN-α, TNF-α, and 3) a variety of enzymes (collagenase, elastase…) The key mechanism, whereby GC exert their anti-inflammatory actions, is by interfering with transcription factors. Activated GC-R undergo a direct inhibitory interaction with activated transcription factors such as NF-κB and activator protein-1 (AP-1), which regulate the expression of a wide range of inflammatory and immune-regulatory genes. These protein-protein complexes prevent NF-κB and AP-1 from interacting with their recognitive DNA binding sites and therefore suppress the expression of pro-inflammatory cytokines, chemokines, iNOs, COX-2 and PLA2. On the other hand, GC up-regulate the production of IκB, which binds to NF-κB, thus sequestering it in the cytoplasm and inhibiting its nuclear translocation.
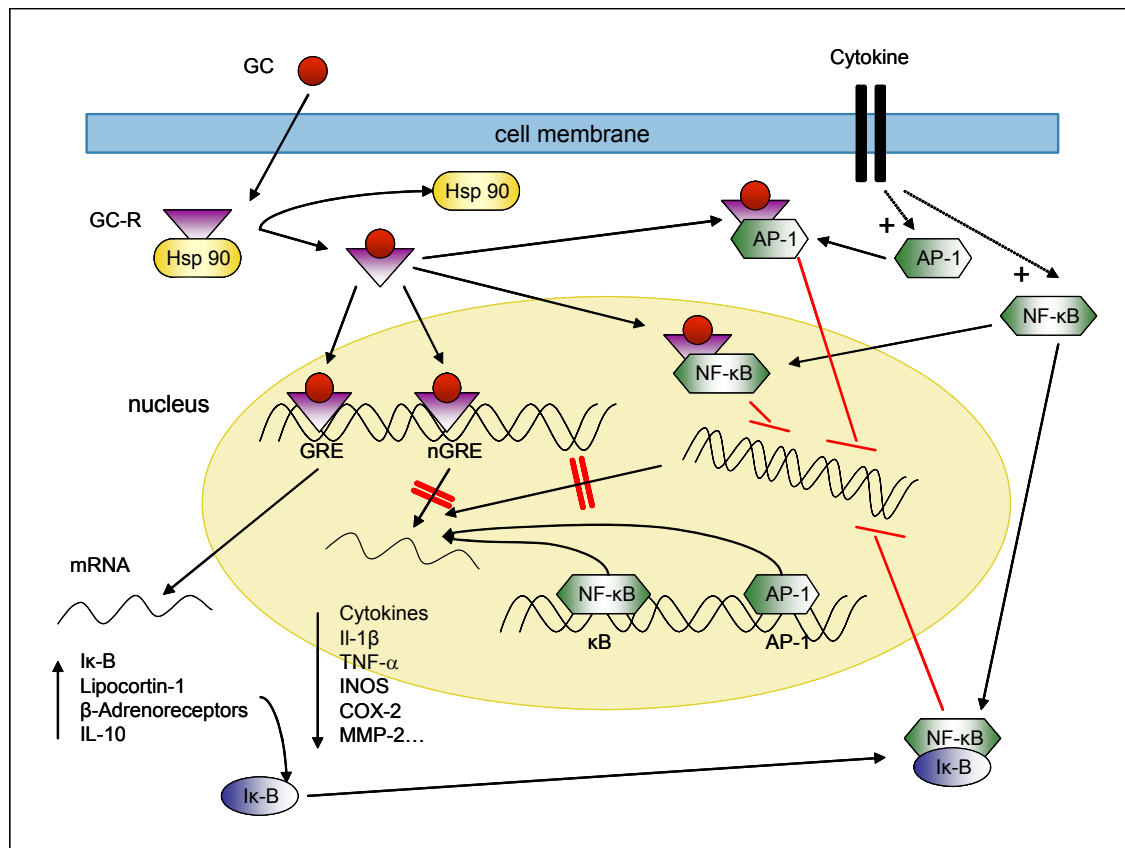
Fig. 3: Anti-inflammatory action of GC: molecular mechanisms

Glucocorticoids (GC) enters the cell, binds to a cytoplasmatic GC-receptor (GC-R) which is complexed with 2 heat shock proteins (hsp 90), translocates to the nucleus, and binds to GC recognition sequence of GC responsive genes (GRE or nGRE), or to transcription factors activator protein-1 (AP-1) or nuclear factor-κB (NF-κB). In this way GC may increase (via GRE) or decrease (via nGRE and binding on AP-1 or NF-κB) gene transcription. Adapted from Barnes; 1998.

Furthermore, GC lead to deacetylation of histones, resulting in tighter coiling of DNA and reduced access of transcription factors to their respective binding sites, thereby suppressing inflammatory gene expression (Wolffe, 1997). GC may also inhibit the protein synthesis of pro-inflammatory molecules by reducing the stability of mRNA via enhanced transcription of specific ribonucleases that break down mRNA containing AU-rich sequences. Through this mechanism GC inhibit the synthesis of GM-CSF, which plays a key role in the survival of inflammatory cells at the site of inflammation (Bickel et al., 1992).

However the anti-inflammatory, anti-angiogenic, and immunomodulatory potential of GC is limited by their considerable and well-known toxicity in particular upon long-term use. Osteoporosis, Cushing syndrome, increased susceptibility to infection, electrolyte alterations, and elevated risk of thrombosis are only some of the common side effects of GC. The aim of a steroid therapy, therefore must be the use of the lowest possible, but still efficacious dose.

2.2.3 New trends

The knowledge of the key role of Mφ in RA, and the correlation between the therapeutic effects of conventional anti-rheumatic drugs and the down-regulation of functions of the mononuclear phagocyte system have led to re-evaluation of the current treatment of RA in order to develop new therapeutic concepts, such as drugs directly targeting Mφ or their cytokine products. Another factor in support of targeting Mφ in RA is the differential activation of intracellular transduction pathways in different cells.

TNF-α neutralizing agents have recently become available for RA treatment: one of these is a chimeric mouse/human monoclonal antibody to TNF-α (infliximab) and the second is a TNF-α type II receptor fused to the Fc part of IgG (etanercept) known by the name of Enbrel®. Several positive clinical results have been described with TNF-α-blockers in RA (Moreland et al., 1999), as well as halting of the articular damage by etanercept (Genovese et al., 2002) and infliximab in combined therapy with methotrexate (Lipsky et al., 2000). Side effects include the increased risk of serious infections and the induction anti-DNA antibodies. More recently, IL-1 receptor antagonists (anakinra) have been developed and approved for RA therapy (Kawai, 2003). In contrast to the anti-TNF-α therapies, which bind free TNF-α molecules, thus preventing their interaction with cell surface receptors, anakinra competitively antagonizes IL-1by binding to the cellular IL-1-receptor.

Of great interest however, has been the idea of using the phagocytic activity of synovial Mφ and activated circulating monocytes, to target these cells by drugs, encapsulated in liposomes, (Hong et al., 1988)

2.3 Liposomes

2.3.1 Composition

Liposomes are phospholipid bi-layer vesicles ($\varnothing$ 25 nm-1 mm), with a structure similar to those of cellular membranes, encapsulating a hydrophilic space. Liposomes can be produced by dispersing phospholipids in hydrophilic solutions or by dissolving them in an organic solvent which is then removed by rotary evaporation (also reverse phase evaporation; Szoka et al., 1978). The lipid film forming on the wall of the container is then hydrated with buffer. This method allows the dilution of a number of products in the hydration buffer, which will then be encapsulated in the liposome, and a more accurate quantification of drug entrapment..

A large number of lipids are used to produce liposomes, resulting in different pharmacokinetic and pharmacodynamic characteristics of these vesicles. Commonly, derivates of phosphatidylcholine (PC) are used as basis components because their chemical structure induces the organization in light liposomes. The addition of cholesterol (Chol) in contrast, increases the stability of the membrane fluidity. By introducing specific functionalities to the bilayer, liposomes can acquire the ability to selectively accumulate at pathological target tissues, such as sites of inflammation and tumor, or escape biological elimination. Simply attaching water-soluble polymers to the surfaces of liposomes can modify their interactions: by coating liposomes with polyethylene glycol (PEG), Metselaar et al. obtained "long-circulating liposomes" with a half live of 50 h in circulation (Metselaar et al., 2003), which nonspecifically or passively target inflammatory sites. Other groups are intending to achieve specific active targeting of selected tissues, by including ligands and antibodies that recognize surface receptors of targeted cells.

These lipid vesicles have shown to be effective carriers or vehicles for different drugs. While lipophilic substances may be directly diluted with the lipids for the reverse phase evaporation method, hydrophilic medication must be diluted in the hydration buffer.

The structure and composition of liposomes resemble that of biological membranes, thus guaranteeing variable interactions with target cells and optimal tolerability in the organism. The

release of encapsulated drug into the cells is based on phagocytosis and fusion. In phagocytosis, the initial event in liposome-cell interaction is thought to be the absorption of intact vesicles to the cell surface, followed by active cellular endocytosis, fusion with a lysosome, and digestion of the liposome membrane by the enzymes. In the case of a fusion, the membranes of liposome and cell fuse directly, leading to the direct release of the contents into the cytoplasm. Other possible mechanisms include enzymatic degradation of the lipid bilayer, subsequent leakage of drug into the immediate vicinity of the cells and diffusion across the lipid membrane. However, the first mechanism seems to play a more significant role for hydrophilic drugs, specially in the case cells capable of phagocytosis.

2.3.2 Liposome uptake by macrophages

Activated Mφ are highly phagocytic and are therefore capable of ingesting liposomes. Uptake by Mφ is maximal for liposome formulations containing dipalmitoylphosphatidylcholin (DPPC) and the presence of negative charge enhances the interaction between the charged liposome bilayer and the cell membrane, via Scavanger receptors, which favors the accumulation inside Mφ (Nishikawa et al., 1990). There is no apparent difference in the uptake of liposomal formulations differing in their relative content of cholesterol (Katragadda et al., 2000). On the other hand, inclusion of PEG in the liposome surface leads to the formation of stearic barriers, which prevent opsonization and Mφ endocytosis (Cansell et al., 1999). Other authors hypothesize that the binding of PEG-Chol to the cell membranes induces a decrease in surface hydrophobicity and thereby leads to decreased phagocytic ingestion (Vertut-Doi et al., 1996). In addition, the inability of macromolecules to exit from normal blood vessels can be utilized to target tissues, in which vessels show enhanced permeability, for example in regions of inflammation and neoangiogenesis in RA (Torchilin et al., 2003). In this context, small unilamellar vesicles accumulate to a greater extent in paws of rats with adjuvant arthritis than large multilamellar liposomes (Lowe et al., 1989), and have less pro-inflammatory effects of their own. In addition, the uptake by macrophages is greater for liposomes with a size below 200 nm (Allen et al., 1991)

The quest for specific targeting has lead to the development of new PEG-ylated liposomes with a surface-conjugated cyclic Arg-Gly-Asp (RGD) peptide, which selectively home to inflamed skin (Koning et al., 2006). This is mediated by specific binding of RGD to the αvβ3 integrin, over-expressed in cells of neoangiogenic vessels.

2.3.3 Encapsulation of therapeutic drugs: dexamethasone

The characteristics of liposomes make them highly suitable for the employment as good drug carriers.

Dexamethasone-phosphate (9-fluor-16-methylprednisolone) is a water-soluble, halogenated, synthetic GC without any significant mineralocorticoid properties, but with potent glucocorticoid effects (4 x potency compared to prednisolone). Its pharmacokinetics are characterized by a long biological half-live. Since the middle of the 20th century, dexamethasone (DxM) has been successfully used for RA treatment , but its considerable number of side effects has reduced its use to a high dose therapy in acute episodes or to a low-dose continuous therapy. Moreover its toxicity, specially upon long-term use, continues to represent a severe problem.

The concept of encapsulating dexamethasone into liposomes has been intensively studied in a number of different immunological diseases such as RA.

MW = 392.45
9-fluor 16-methylprednisolone
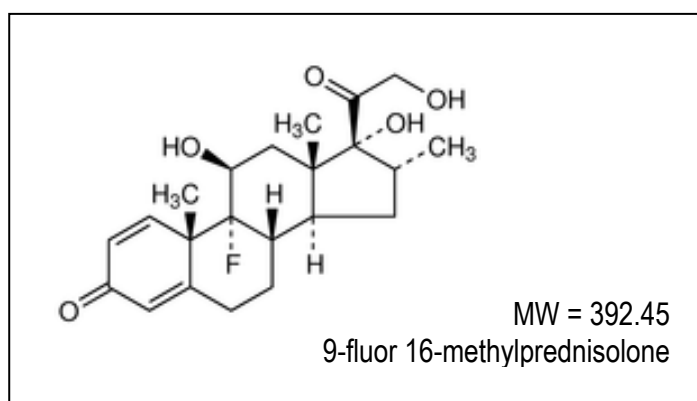
Fig. 4: Chemical structure of DxM

MW = molecular weight

Besides the enhanced accumulation in inflammation sites, Mφ and circulating monocytes acquire, in their activated form, an increased ability to phagocyte large molecules, such as liposomes. This unspecific targeting of the inflamed joint, and to a non-negligible extent of the liver and the spleen, is necessary to avoid undesirable side effects. In addition, encapsulation in serum-stable unilamellar liposomes is known to allow a slow drug delivery (reviewed by Allen, 1994). Therefore encapsulation not only increases the half-life in circulation, due to the resistance to kidney elimination, but also prolongs the retention time in joints, which may therefore allow reduction of administered dose (Barrera et al., 2000). Liposomal drug delivery has already been demonstrated to reduce the drug toxicity of doxorubicin, amphotericin B and MTX (Richards et al., 1999).

2.4 Animal models of arthritis: adjuvant arthritis

Several experimental models of arthritis have been established over the passed years in order to investigate pathomechanisms and new therapy concepts in RA. Basically we can distinguish two types of models: the ones directly inducing a systemic reaction to a single injection, like the adjuvant arthritis (AA), to which we oppose the models requiring a preliminary immunization in order to induce a local reaction to the injected antigen, such as the antigen induced arthritis, the collagen induced arthritis, bacterial or viral induced arthritis.

Adjuvant arthritis (AA) the first model described in 1956 by Pearson (reviewed in Billingham, 1995) is a severe experimental arthritis model for rats and mice with clinical and histopathological resemblances to RA. AA is induced by a intradermal injection of heat-killed *Mycobacterium butyricum* (Mb) and mineral oil. Like in RA, a systemic polyarticular disorder, characterized by increasing signs of tissue destruction and bone formation, follows the AA-induction. After a latent time of 6-10 days the course of AA presents an acute inflammation in the ankles, wrists, tarsals, and interphalangeal joints of rats. This disease is not limited to the joints, but has extra-articular manifestations, including tendonitis, iritis, nodular lesions in the visceral organs, urethritis, and diarrhoea. The rheumatoid factor is not produced in this experimental form of arthritis. The symptoms peak about 15-25 days after the injection, followed by a chronic stage of slow resolution. AA showed homologies in terms of histopathology and responses to several immunomodulatory drugs, in which T-cells and Mφ infiltrate the synovial membrane and assure a local production of TNF-α and IL-1ß (Carol et al., 2000; Simon et al., 2001). Furthermore, inflammatory processes also seem to be related with NF-κB activation in AA (Tsao et al., 1997). The immediate response to a single injection of Mb due to a cross-reaction between a joint macromolecule and the Mb-antigen, offers us the possibility to understand and investigate such types of immunologic disorders, therefore presenting an optimal model for studying Mφ-targeting drugs against RA.

2.5 Microarrays

Functional genomics is the study of gene function through parallel expression measurements of genomes, most commonly using microarrays technologies. Unlike PCR, in which the

expression of a single gene is measured, the whole genome is monitored in a single chip, therefore enabling the analysis of the expression of thousands of genes simultaneously.

Microarrays are artificially constructed grids of DNA, divided in spots, such that each one holds a DNA sequence that is complementary to a specific RNA sequence of the probes. Basically, the isolated RNA probes are copied while incorporating either fluorescent nucleotides or a tag that is later identified under fluorescent light. The labeled RNA is then hybridized to a microarray which is scanned under laser light, enabling a visualization of up- and down-regulated genes. There are two common types of microarrays: 1) microarrays, for which all probes have been designed to be theoretically similar with regard to hybridization temperature and binding affinity, thereby providing quantitative results, and 2) cDNA microarrays, for which each probe has a single hybridization characteristic, each microarray measuring two samples and providing a relative measurement for each RNA sample.

The degree of RNA purity influences the final result to a great extent, therefore exact quality controls of the samples should be performed before each experiment (Dumur et al., 2004; Mans, 2005). Dumur et al. described some basic quality principles for an optimal microarray experiment. All RNA samples must be free of DNA, the purity quotient 260/280 (absorbance measured at these wavelengths) must be greater then 1.8 and the 260/270 quotient shouldn't drop below 1.1. The fluophore-incorporation rate (FOI), which indicates the number of incorporated fluorescent-nucleotides per 1000 nucleotides during amplification, and therefore has a direct influence on the signal strength, must be normalized in the different RNA samples before hybridization.

Careful bio-informatic analysis and critical interpretation of the completed microarray scan is as important as the experiment itself. There are no fixed guidelines for normalization, calibration nor validation of microarray data, which increases the difficulty of interpretation (Smyth and Speed, 2003; Shannon et al., 2003). However, a number of software packages are available to help interpret the data and organize it in hierarchical clusters or self-organizing maps (Cluster©; SNOMAD©). International Databanks such as the Gene Expression Omnibus (GEO; http://ncbi.nlm.nih.gov/geo) from the National Center for Biotechnology Information (NCBI) have recently been created, in which gene expression data from different labs are collected, in order to compare and validate the results from different experiments and help the validation of functional-genomic hypothesis.

3. AIMS OF THE STUDY

Glucocorticoid-containing liposomes have been intensely studied since the 1970's with the aim of overcoming the limitations of long-term GC treatment in inflammatory diseases such as RA. A number of different liposome formulations and compositions have been manufactured and tested both *in vitro* and *in vivo*, aiming at passive and lately, active targeting of the main inflammation-promoting cells in RA, the monocyte/macrophage cell lineage. This served to optimize the anti-inflammatory efficacy of GC and thereby possibly reduce both therapeutic dose and side-effects. In a previous experimental series (Schulte, 2003), a total of five DxM-liposome formulations, manufactured by Novosom® and varying in liposome composition and size, were compared for their uptake, toxicity, and molecular effects in monocytes. According to these previous results, the liposome formulation chosen for the present study represented the best compromise between high uptake and efficacy.

The present study therefore focused on two separate complexes with the following aims:

o In vitro studies

- Assess the uptake of DxM-liposomes by Mφ and the lack of toxicity upon incubation of Mφ with DxM-liposomes

- Establish and test the microarray analysis for monocytes pre-incubated with PBS-liposomes or DxM-liposomes and subsequently stimulated with LPS/IFN-γ (to gain a better understanding of the therapeutic mechanism of action of DxM-liposomes by simultaneously investigating a large number of genes)

- Validate the array results by PCR investigations on selected genes and, in addition, by measuring the cytokine production by ELISA

o In vivo studies

- Test the therapeutic efficacy of systemic, i.v. administration of DxM-liposomes in the experimental adjuvant arthritis model and to analyze their effects on clinical and histological parameters of arthritis

- Assess the increase of therapeutic efficacy by liposomal encapsulation of DxM (by comparing free DxM and DxM-liposomes treatments and by analyzing the dose response)

- Analyze the systemic effects of i.v. administration of DxM-liposomes (to assess their effects on hematological and immune parameters, as well as possible side-effects)

- Compare systemic and local effects of DxM-liposomes with those of the clinically approved, anti-rheumatic biological Enbrel® (TNF-α receptor)

19

4. METHODS

4.1 Chemicals

<u>Hydration buffer:</u>

10 mM HEPES (Carl Roth GmbH, Karlsruhe, Germany)

150 mM NaCl (Carl Roth GmbH)

pH = 7.4 in Aqua bidest

<u>Lymphoprep</u>

Lymphocyte separation medium (PAA Laboratories GmbH, Pasching, Austria)

<u>Medium</u>

RPMI-1640 (Roswell Park Memorial Institute) with stable L- glutamine (PAA)

10% fetal calf serum (Invitrogen, Karlsruhe, Germany)

1% gentamycin (10 mg/ml; Invitrogen & PAA)

<u>PBS</u>

16 g NaCl (Carl Roth GmbH)

0.4 g KCl (Merck KG, Darmstadt, Germany)

2.88 g Na_2HPO_4 (Carl Roth GmbH)

0.48 g KH_2PO_4 (Merck KG, Darmstadt, Germany)

pH = 7.5 ad 1000 ml Aqua bidest

<u>PBS-Tween:</u>

PBS (see above)

0.1% Tween 20 (Carl Roth GmbH)

<u>LPS</u>

Lipopolysaccharide (E. coli; Serotype 0111:B4) 100 µg/ml (Sigma-Aldrich Chemie GmbH)

<u>IFN-γ</u>

Recombinant human interferon gamma, 100 µg/ml, (activity: 2×10^7 U/ml; Pepro Tech Inc., Rocky Hill, NJ)

<u>NP-40 Lysis buffer:</u>

1.58 g Tris (Carl Roth GmbH)

1.8 g NaCl (Carl Roth GmbH)

58.4 mg EDTA (Carl Roth GmbH)

2% Nonidet-P40 (Boehringer Mannheim GmbH, Mannheim, Germany)

pH = 7.5 ad 100 ml Aqua bidest

<u>GRIESS-Reagent:</u>

2.5% H_3PO_4 (Sigma-Aldrich Chemie GmbH, Germany)

1% sulfonilamide (Sigma-Aldrich Chemie GmbH)

0.1% N-(1-naphtyl)-ethylenediamine- dihydrochloride (Carl Roth GmbH)

in Aqua bidest

Rneasy® mini kit (Qiagen, Maryland, USA)

RNAse free water (Ambion),

RNA 6000 Nano LabChip kit (Agilent)

AminoAllyl MessageAmp aRNA Kit (Ambion)

Tri Reagent (Sigma-Aldrich Chemie GmbH)

Chloroform (Fluka Chemie, Buchs, Switzerland)

Isopropanol (Fluka Chemie)

Ethanol (Fluka Chemie)

Super Script II, reverse Transcriptase (Invitrogen)

Taq Polymerase (Invitrogen)

Agarose (agarose ultraPURE™; Gibco)

<u>10 × TBE:</u>

108 g Tris/HCl pH 8.0 (Carl Roth GmbH)

55 g boric acid (Merck KG)

10 g EDTA (Merck KG)

pH = 7.4 ad 1000ml Aqua bidest

Citrate buffer:

2.1 g citric acid monohydrate (Merck KG)

diluted in Aqua bidest ad NaOH (5 M)

pH = 4.8 ad 100 ml Aqua bidest

OPD-solution

30 mg o-Phenylenediamine (Sigma-Aldrich Chemie GmbH)

15 ml citrate buffer (see above)

300 µl H_2O_2 (3%)

4.2 Liposomes

4.2.1 Preparation of liposomes

All liposomes were manufactured and labeled by Novosom AG, Halle/Saale, Germany.

Serum-stable, unilamellar anionic liposomes were prepared using a lipid film composed of dipalmitoylphosphatidylcholin (DPPC), dipalmitoylphosphatidyl-glycerol (DPPG) and cholesterol (relative proportions of 50:10:40, respectively). Accurately weighed quantities of the respective lipids were transferred to a 10 ml round bottom flask and the contents dissolved using 1-2 ml chloroform/methanol (2:1). The water bath was heated to 50ºC to achieve a better solubility of unsaturated lipids. The organic solvent was then removed under vacuum in a rotary evaporator until a homogenous unilamellar lipid film was formed. The lipid film was dried over night by exsiccation. The hydration with hydration buffer was then performed for 45 min at room temperature (unsaturated lipids) or 50ºC (saturated lipids) under rotation. Final dilution/dispersion was achieved by short sonication (30 sec – 5 min), followed by three freeze and defreeze steps. A mean size of 200 nm was achieved by extrusion (Mini-Extruder, Avestin) through polycarbonate membranes of 400 nm diameter. Liposome size was determined with a Zetasizer 3000 Hsa, Malvern. Liposomes were free of PEG in order to avoid immunological complications such as allergic reactions characteristic of Stealth® lipososmes.

4.2.2 Fluorescence-labeled liposomes

Liposomes were labeled with the fluorescent dye TRITC (tetramethylrodamin-5,6-isothiocyanate)-dextran and prepared as described above. TRITC-dextran (25 mg/ml) was diluted in the hydration

buffer and added into the liposomes at a concentration of 0.29 µg TRITC-dextran/µl liposome. Free TRITC-dextran was removed by size exclusion chromatography with Sephadex G 75.

4.2.3 Dexamethasone-liposomes

The lipid film was prepared as described above and 25 mg/ml dexamethasone-phosphate (DxM) was added to the hydration buffer. Free DxM was removed by size exclusion chromatography with Sephadex G 25. Hydration of buffer containing liposomes was performed with PBS.

Liposomes were used in all experiments with the following designations: DxM-lipos, PBS-lipos and TRITC-lipos (tab. 4).

Designation	Formulation	mM Lipid	DxM in µg/ml	diameter in nm
DxM-lipos 1		12.88	512	288
PBS-lipos 1		100.00		246
DxM-lipos 2		12.56	598	267
PBS-lipos 2		73.21		284
DxM-lipos 3	DPPC/DPPG/Chol	10.50	500	263
PBS-lipos 3	50:10:40	10.50		264
DxM-lipos 4		11.14	500	284
PBS-lipos 4		11.14		215
DxM-lipos 5		12.06	500	242
PBS-lipos 5		12.06		193
TRITC-lipos	DPPC/DPPG/Chol	10.68	0.2892 µg TRITC-D/µl lipos	

Tab.4: Characteristics of different liposome formulations

DPPC: dipalmitoylphosphatidylcholin, DPPG: dipalmitoylphosphatidylglycerol, Chol: cholesterol,
TRICT-D: tetramethylrhodamin-5,6-isothiocyanat-dextran, DxM: dexamethasone

4.3 In vitro studies

4.3.1 Isolation of monocytes/macrophages

4.3.1.1 Isolation of human peripheral blood monocytes:

Buffy coats were prepared by centrifugation of peripheral blood from healthy donors in the Institute of Transfusion Medicine of the University Hospital, Jena, and processed immediately thereafter. After dilution in warm PBS (1:1), PBMC were obtained by density gradient centrifugation (2230

rpm) with Lymphoprep (30 ml sample over 15 ml Ficoll). Cells were isolated from the interphase between serum and Lymphoprep, resuspended in 50 ml PBS, and centrifuged for 10 min at 1420 rpm and RT. In order to eliminate thrombocytes, the cells were resuspended in 50 ml PBS and centrifuged twice for 10 min at 800 rpm. The cell pellet was resuspended in 10 ml RPMI medium and PBMC were counted in Neumann chamber slides. Cell suspensions were incubated for 2 h at 37ºC in a humidified 5% CO_2 atmosphere and non-adherent cells were eliminated by washing three times with warm PBS. For stabilization, cells were incubated for 20 h before further experiments. Remaining adherent cells normally consist of > 95% macrophages (Mφ; Yui et al., 1993). Buffy-coats were processed within 4 h after blood donation, assuring optimal viability and functional activity of monocytes.

4.3.1.2 Isolation of rat peritoneal macrophages

Male Lewis rats were anesthetized and sacrificed by CO_2 inhalation. Peritoneal macrophages (PM) were harvested by peritoneal lavage with 20 ml ice-cold PBS; cells were then centrifuged for 10 min at 4000 rpm, washed, and resuspended in RPMI medium at 2×10^6 cells/ml. Cells (1×10^6 cells) were seeded per well in 24-well plates, washed with warm PBS after 2 h incubation at 37ºC, 5% CO_2, and the adherent Mφ were then used for nitrite assays.

4.3.2 Experimental design:

4.3.2.1 Pre-incubation with liposomes

Isolated monocytes/macrophages were first incubated with liposomes and then stimulated for the time period indicated in table 5. Dexamethasone containing liposomes (DxM-lipos) were applied at a concentration 50 µM DxM. Drug-free liposomes (PBS-lipos) and fluorescence-labeled liposomes (TRITC-lipos) were applied at the same lipid concentration as DxM-liposomes. All experiments were completed within 4 weeks of liposome production to exclude possible changes in composition or dexamethasone "leaking". In vitro studies performed by Novosom® confirmed the stability of liposomes during a period of 4 weeks when conserved at 4ºC.

4.3.2.2 Stimulation

Cells were incubated at 37ºC, 5% CO_2 with LPS (20 ng/ml) and IFN-γ (400 U/ml) for the time period indicated in table 5.

	Liposome uptake	Liposome tolerability	NO production	Cytokine gene expression		Cytokine protein production
Used cells	monocytes	monocytes	peritoneal macrophages	monocytes		
Liposomes	TRITC-lipos	Lipos 1	Lipos 1	Lipos 2	Lipos 3	Lipos 5
Incubation time	1-24 h	4 h	4 h	4 h		4 h
Stimulation time	-	20 h	20 h	2 h		2 h & 20 h
	↓	↓	↓	cells ↓		↓ supernatants
	Fluorescence microscopy	Cell viability (trypan blue)	Nitrate assay	PCR	Microarray	ELISA

Tab. 5: Overview of in vitro studies

Cells and liposome formulations, and incubation or stimulation times used for each in vitro experiment

4.3.3 Liposome uptake and effects of liposomes on monocyte/ macrophage viability

4.3.3.1 Measurement of liposome uptake

Human monocytes were incubated with 20 µl fluorescence-labeled liposomes in black culture plates. After 1, 3, 6, and 24 h adherent cells were washed tree times with warm PBS and the uptake of liposomes detected by fluorescence microscopy. These experiments was performed in close collaboration with Reiner Schulte.

.

4.3.3.2 Measurement of cell vitality

For the assessment of cell viability, isolated Mφ were incubated for 4 h at 37ºC, 5% CO_2 with different liposome formulations and then stimulated with LPS (20 ng/ml) for 20 h. Adherent cells were washed five times with warm PBS and stained with 20 µl trypan blue in 100 µl medium. Viability was measured by counting at least 100 cells per well and determining the percentage of viable cells (trypan blue-negative). Results were expressed as the mean of 6 wells per liposome.

4.3.4 Determination of nitrite production

Rat PM (7×10^5 cells/ well) were first pre-incubated with liposomes for 4 h at 37ºC, 5% CO_2, and then stimulated for 20 h with LPS/IFN-γ; cell free supernatants were harvested by centrifugation for 6 min at 9800 rpm, immediately shock frozen in liquid nitrogen and stored at -70ºC until further processing. The amount of nitrite in the supernatant, an indicator for the activity of inducible nitric

oxide synthase (iNOS) was determined by the GRIESS reaction as described previously (Mentzel and Bräuer, 1998).

The standard reference curve was prepared with a serial, two-fold dilution row of nitrite (starting at 0.1 mM nitrite standard) in RPMI-medium, and 100 µl of each standard dilution was dispensed in duplicates in a 96-well-plate. Samples were dispensed in triplicates and medium was used as blank reference. GRIESS reagent (100 µl; 1:1 mixture of 1% sulfanilamide in 5% H_3PO_4 and 0.1% N-1-naphtyletylenediamine-dihydrochloride) was added to all standards or sample containing wells. The samples were then incubated for 10 min at RT in the dark, and absorbance was then measured in an ELISA-reader using a 570 nm filter (reference filter: 620 nm).

4.3.5 Microarrays

4.3.5.1 RNA isolation

Adherent monocytes (1×10^8) were incubated and stimulated as described above in 10 cm plates. Cells were lysed with 600 µl lysis-buffer (RTL-buffer/1% β-mercaptoethanol) and stored in 2.0 ml Eppendorf-tubes at -20ºC for further processing. RNA was isolated following a standardized protocol. Briefly, 600 µl of 85% ethanol were added to the sample/lysis-buffer mixture, administered to the binding column and washed by centrifuging 350 µl RW1 buffer through the column. A DNA-digestion step was performed by incubating the samples with 10 µl DNAse1 in 70 µl RDD buffer on the column for 30 min at 30ºC in a thermomixer. The silicate membrane of the column was then washed twice with 700 µl RW1 buffer and twice with 700 µl RPE buffer by centrifugation. RNA was eluted with 100 µl RNAse free water and immediately stored at -20ºC.

4.3.5.2 RNA quality control

RNA processing, labeling and hybridization was performed in collaboration with Dr. Stuhlmüller and N. Tandon in the Institute of Clinical Immunology and Rheumatology, Charité, Berlin.
RNA quality was validated by analyzing the 18S and 28S subunits of total RNA, using the RNA 6000 Nano LabChip kit and the Bioanalyzer 2100 (Agilent), according to the manufacturer's instructions. RNA samples (1 µl) were processed by gel electrophoresis and detected using a fluorescence marker. RNA concentrations and purity were calculated with the corresponding software. The exact concentration was measured in a 1 µl RNA sample, using a spectrophotometer (Nano Drop 1000; NanoDrop), analyzing in the wavelength range from 220 nm to 350 nm. The absorption measured at 260 nm allowed the RNA quantification in ng/ml, the

absorption ratios at 260 nm/280 nm and 260 nm/230 nm were determined for quality control, concretely, to determine whether RNA was free from protein and/or phenol contamination.

4.3.5.3 Amplification and purification of cDNA

Amplification was performed using 2 µg total RNA from each sample, adding 7 µl RNase-free water, 2 µl first strand buffer, 4 µl dNTP mix, 1 µl oligo (dT) primer, 1 µl reverse transcriptase and 1 µl RNase-inhibitor, and reverse transcribing the cDNA first strand for 2 h at 42ºC. Subsequently, 2 µl DNA polymerase, 10 µl second strand buffer, 4 µl dNTP mix, 1 µl RNase-H were added, and cDNA second strand synthesis and RNA digestion were performed by incubation for 2 h at 16ºC. For cDNA purification, the samples were mixed with 250 µl binding buffer, placed on a binding column, centrifuged (1 min at 10,000 x g), washed by centrifuging with 500 µl washing buffer (2 min at 10,000 x g) and finally eluted 2 x with 20 µl DNase-free, RNase-free and preheated water (at 70˚C). The final volume was adjusted to 14 µl by Speedvac vacuum centrifugation.

4.3.5.4 Aminoallyl-aRNA synthesis and cleanup

For aminoallyl-aRNA (AA-aRNA) synthesis, 2 µl UTP, 4 µl aaUTP, 12 µl NTP mix, 4 µl T7-polymerase reaction buffer and 4 µl T7 polymerase mix were added to the cDNA samples and the samples were incubated for 20 h at 37ºC. During this transcription, both non-labeled dUTP and labeled Aminoallyl-dUTP nucleotides were integrated in to the synthesized AA-aRNA. Remaining cDNA was eliminated by digestion with 2 µl DNase1 for 1 h at 37ºC.

AA-aRNA samples were then mixed with 58 µl nuclease-free water, 350 µl binding buffer and 250 µl ethanol, placed on binding columns, centrifuged for 1 min, and washed for further 2 min with 650 µl washing buffer. AA-aRNA was then eluted 2 x with 100 µl preheated water and finally adjusted to a volume of 50 µl by vacuum centrifugation. Quality control and quantification of concentration were performed, as described previously, using Bioanalyzer and NanoDrop, respectively (4.3.5.2).

4.3.5.5 Labeling of the Aminoallyl-aRNA

A total of 10-15 µg AA-aRNA were adjusted to a volume of 7 µl, supplemented by 9 µl binding buffer and 4 µl of the corresponding fluorophore diluted in DMSO, and incubated for 1 h at 27ºC. The reaction was stopped by incubation for a further 60 min with 4.5 µl 4 M hydroxylamine.

The AA-aRNA of the non-stimulated control Mφ was then labeled with Cy5 (red) while the AA-aRNA of the LPS/IFN-γ-stimulated Mφ (either incubated without liposomes, with PBS-lipos, or with DxM-lipos) were labeled with Cy3 (green). For each patient, three different microarray

measurements were performed by directly comparing the respective control to the 3 different samples of stimulated Mφ.

Cleanup was performed as described under 4.3.5.4 and the concentrations of Cy-AA-aRNA were quantified using the NanoDrop 1000. The fluorophore incorporation (FOI) was also calculated using the software of the NanoDrop 1000 after measuring the relative fluorescence of the samples at 550 nm (Cy3) and 650 nm (Cy5) and thereby determining the concentration of each marker. Detection limits were set in the range 0.2-100 pmol/µl (Cy3) and 0.12-60 pmol/µl (Cy5), as described by the manufacturer. The FOI per 1000 nucleotides was calculated using the following formula:

$$FOI= \frac{c[dye\} * 324.5}{c[aRNA]}$$

In order to obtain an equivalent signal for both samples on the array, the RNA samples used for the hybridization were adjusted to an equal FOI.

4.3.5.6 Hybridization

RNA samples of stimulated and liposome-treated cells, with an FOI equivalent to that of the control cells, were mixed with the RNA of the respective control cells. 1 µg human COT1-DNA and 1 µg poly d(A)40-60mer was added to the samples in order to minimize non-specific binding to the repetitive sequences of the microarray, and the samples were adjusted to a final volume of 2 µl. Subsequently 35 µl of preheated DIG-Easy-Hyp buffer (Roche) were added to the samples on the microarray glass slide. To create optimal humidity conditions, the hybridization chamber was rinsed twice with 20 µl of water and twice with 20 µl of DIG-Easy-Hyp buffer, and the microarray was then incubated for 48 h in a 46ºC water bath in the dark.

Following the hybridization, the microarray-plates were prepared for scanning by washing twice for 20 min with a 0.2 x SSC - 0.1% SDS - 0.2mM DTT solution and twice for 5 min with a 0.2 x SSC - 0.2 mM DTT solution and centrifuged for 10 min at 220 x g.

4.3.5.7 Data analysis

First steps of data analysis and normalization were performed in collaboration with Christian Hummert (Dept. of Molecular and Applied Microbiology, HKI, Jena).

The microarrays were scanned with a laser at wavelengths of 543nm (Cy3) and 633 nm (Cy5) to measure the maximum fluorescence of each dye. The laser-intensity of the scanner (ScanArray™ Lite, Packard Bioscience) was set to 95% for all measurements and the photomultiplier was regulated automatically for the signal and background intensities.

The data of the array, represented as an image of digital pixels corresponding to the intensities of the different color channels, was read by the TIGER Spotfinder software. An automatic normalization was achieved by equalizing the gene-replicates (n = 16) for the control and reference genes, β-actin and GAPDH, across the chip. Data were then background-corrected, the probes showing high background signal were removed, and the standard deviation for each sequence was calculated. For each sequence (corresponding to one signal spot) the ratio of the signal intensities of the different stimulated samples (Cy3; green) and the control samples (Cy5; red) gave a first approximation of the effect of treatment on the expression of different genes.

4.3.6 Assessment of cytokine mRNA expression: conventional RT-PCR

4.3.6.1 RNA Isolation

Adherent monocytes (1×10^8) were incubated and stimulated as described above in 10 cm plates. Cells were lysed with 1 ml Tri Reagent and stored in 2.0 ml Eppendorf-tubes at -20ºC if not immediately processed.

Lysates were warmed up to RT for 5 min before RNA isolation. A total of 0.2 ml chloroform were added to the samples, which were then incubated at RT for 5 min and centrifuged at 4ºC for 15 min at 12000 x g in order to separate hydrophilic and lipophilic phases. The RNA-containing aqueous phase on the top of the gradient, was placed in a new collecting tube and 0.5 ml isopropanol were added. The RNA was pelleted by centrifugation (10 min, 4ºC, 12,000 x g). After removal of the supernatant, the pellet was mixed with 1.5 ml 75% ethanol and centrifuged for 12 min at 7,600 x g. Finally, the RNA was air-dried and resuspended in 30 μl RNAse-free water. The RNA content was quantified by measuring the absorbance at 260 nm. RNA samples were stored at -70ºC and equalized to the same total RNA content before conducting further experiments.

4.3.6.2 cDNA transcription

Reverse transcription was performed by adding 1 μl Oligo-dT-Primer to 5 μg RNA (in 11 μl RNAse free H_2O) and heating for 10 min at 70ºC. Then 4 μl 5 X first strand buffer, 2 μl 0.1 M DTT, and 1 μl 10 mM dNTPs were added to the samples, and these were incubated for 2 min at 42ºC before adding 1 μl of Super Script II reverse transcriptase. Samples were then incubated for 50 min at 42ºC and finally heated to 70ºC for 15 min. Synthesized cDNA was stored at –20ºC.

4.3.6.3 Conventional RT-PCR

The principle of PCR (polymerase chain reaction) is based on DNA replication, and allows the amplification of a DNA fragment with a known sequence, by using complementary end segment sequences (primer). The amplification procedure consists of an initial heating step to denaturize DNA, followed by a cooling step to the primer-specific annealing temperature, to allow attachment of the primers to the single DNA strands, and a final heating step to complete the replication of the complementary DNA strand by the DNA polymerase. After n repetitive cycles, 2n identical DNA fragments are obtained.

The PCR reaction mixture consisted of 1 μl transcribed cDNA template, 10 X PCR buffer, 50 mM MgCl$_2$, respective sense and antisense primers and Taq DNA-polymerase in a total volume of 25 μl. The reactions were carried out in an Eppendorf "Mastercycler Personal". "Master Cycler Gradient" was used to determine the ideal annealing temperatures for each primer, which usually lies 5ºC below the primer-specific melting temperature (Tm) and which is calculated using the following formula:

Tm = 69.3 + (0.41 × % GC) – 650/n (n = number of nucleotides in primer)

The optimal number of cycles for each cytokine PCR was determined by amplification kinetics in order to avoid saturation of the PCR reaction by PCR products (tab.6).

gene	sense primer	antisense primer	annealing temp.	cycles
TNF-α	CTT CCT TCA CAT ACT GAC C	AAG TCT GTG GGA GTT GGA GA	56.0ºC	27
IL-1β	ACC AAC CTC TTC GAG GCA CA	TCT CTC AGG ACA CGA CTT AC	57.7ºC	25
IL-6	CTC CTT TCT CAG GGC TGA G	AAC ACC TCT CCT CAA GTA	56.0ºC	29
IL-10	CTG AGA CCA AGA CCC AGA CAT CAA GG	GCC TAG ACC CCG AGA CCC TAT CGA CTG	54.0ºC	35
IL-15	GGA TTT ACC GTG GCT TTG AGT AAT GAG	GAA TCA ATT GCA ATC AAG AAG TG	58.5ºC	36
IL-18	ACC TCA GAC CTT CCA GAT CG	GTA CGG GAG TTA GGG TCG	58.0ºC	27
Aldolase	TCA TCC TCT TCC ATG AGA CAC TCT A	TTA TGC CAG TAT CTG CCA GCA GAA T	58.0ºC	40

Tab. 6: Overview of PCR conditions

Primer pairs, corresponding annealing temperature, and number of cycles used for each gene amplification

4.3.6.4 Agarose gel electrophoresis

All gel electrophoreses were performed with 1.5% agarose gel in 1 x TBE-buffer. Agarose was weighed (1.05 mg), dissolved in 70 ml 1 × TBE by heating, and 5 µl ethidium bromide were added to the liquid gel. The gel was poured in a horizontal chamber, wells were formed with a comb, and once polymerized, the gel was transferred to an electrophoresis chamber filled with 1 x TBE. The DNA samples were mixed with xylenecyanol (1/10 of sample volume) and 10 µl of the mixture were loaded into each well. A 1 kb ladder was used as a molecular weight marker. Electrophoresis was performed at 120 V for 20-30 min, DNA bands were then photographed under UV light and processed with a gel documentation system (Herolab E.A.S.Y.RH-3, Wiesloch, Germany). Gene expression was determined by measuring the density of the bands using Scion Image Software (Scion Corporation; Frederick, Maryland, USA). Results of stimulated but untreated cells were arbitrarily defined as 100%. Quantification was not performed until all cDNA's had been adjusted to equal aldolase mRNA content using semiquantitative RT-PCR. On the basis of the present data, there was no experimental indication for the regulation of aldolase upon stimulation.

4.3.7 Cytokine production

Adherent monocytes (1×10^8) were incubated for 4 h and stimulated for 2 h, as described above, in 10 cm plates. Cell-free supernatants were harvested by centrifugation for 6 min at 990 x g, and immediately stored at –70ºC until further processing.

The concentrations of IL-1β, IL-6 and TNF-α were determined by sandwich enzyme-linked immunosorbent assay (ELISA, tab. 7).

Microtiter ELISA-plates (96 well) were coated with 100 µl capture antibody and incubated overnight at 4ºC to allow antigen binding. The capture solution was then removed and remaining protein binding sites were blocked with 300 µl/well blocking buffer (3 % BSA/PBS) for 2 h at RT in a humid atmosphere. Microtiter plates were washed three times with washing buffer (PBS/0.05% Tween) and 100 µl sample or 100 µl cytokine standard (diluted in 1% BSA/PBS/0,05% Tween) were added per well and incubated for 2 h at RT in a humid atmosphere. After washing another four times with PBS-Tween, 100 µl biotinylated detector antibody (diluted in 1% BSA/PBS-Tween) were added and incubated for 1 h at RT. The plates were washed four times, 100 µl Avidin-Horseradish Peroxidase (Av-HRP) were added and incubated for 30 min at RT. Unbound conjugate was removed by washing eight times with PBS-Tween and 100 µl substrate (OPD-solution) were added and left to react in the dark for 30 min. The reaction was stopped by adding 50 µl /well H_2SO_4 (1 M). Optical density was read in an ELISA-reader with a measuring filter at 492 nm (reference filter

620 nm). The concentrations were calculated from the measured absorbance values using the Fluostar Software.

	TNF- α	IL-1β	IL-6	IL-10	IL-15
capture antibody	anti-hum TNF-α	anti-hum IL-1β	anti-hum IL-6	anti-hum IL-10	anti-hum IL-15
dilution	1:250	1:250	1:250	1:250	1:250
detection antibody	biotinylated anti-hum TNF-α	biotinylated anti-hum IL-1β	biotinylated anti-hum IL-6	biotinylated anti-hum IL-10	biotinylated anti-hum IL-15
dilution	1:250	1:250	1:250	1:500	1:250
standard	rec hum TNF-α	rec hum IL-1β	rec hum IL-6	rec hum IL-10	rec hum IL-15
concentration	500 pg/ml	1000 pg/ml	300 pg/ml	500 pg/ml	500 pg/ml
distributor	BD Biosciences San Diego CA				

Tab. 7: Overview of antibodies and corresponding dilutions used for different cytokine ELISAs
Hum: human, rec: recombinant

4.4 In vivo studies: adjuvant arthritis

All in vivo studies, except for the dose response experiment (expt.4, fig. 5), as well as the cell harvesting, cell culture, and sample isolation resulting from these, were performed in the Department of Physiology, Pharmaceutical Institute, Universidad de Barcelona, in collaboration with Dr. A. Franch, Dr. M. Castell and Dr. F. Perez-Cano.

4.4.1 Chemicals

Mycobacterium butyricum (Mb) suspension for the induction of AA:
100 mg M. butyricum, desiccated (Difco Laboratories, Detroit Michigan, USA)
0.5 ml isotonic NaCl solution
20 ml vaseline

Plethysmometer solution:
36.5 ml isotonic NaCl solution
157.5 µl triton
32.5 µl isoctanol
in 250 ml Aqua bidest.

Mb solution:

2 mg/ml Mb (Difco Laboratories) in PBS ([Mb] = 387 µg/ml after sonication and centrifugation)

Decalcification solution:

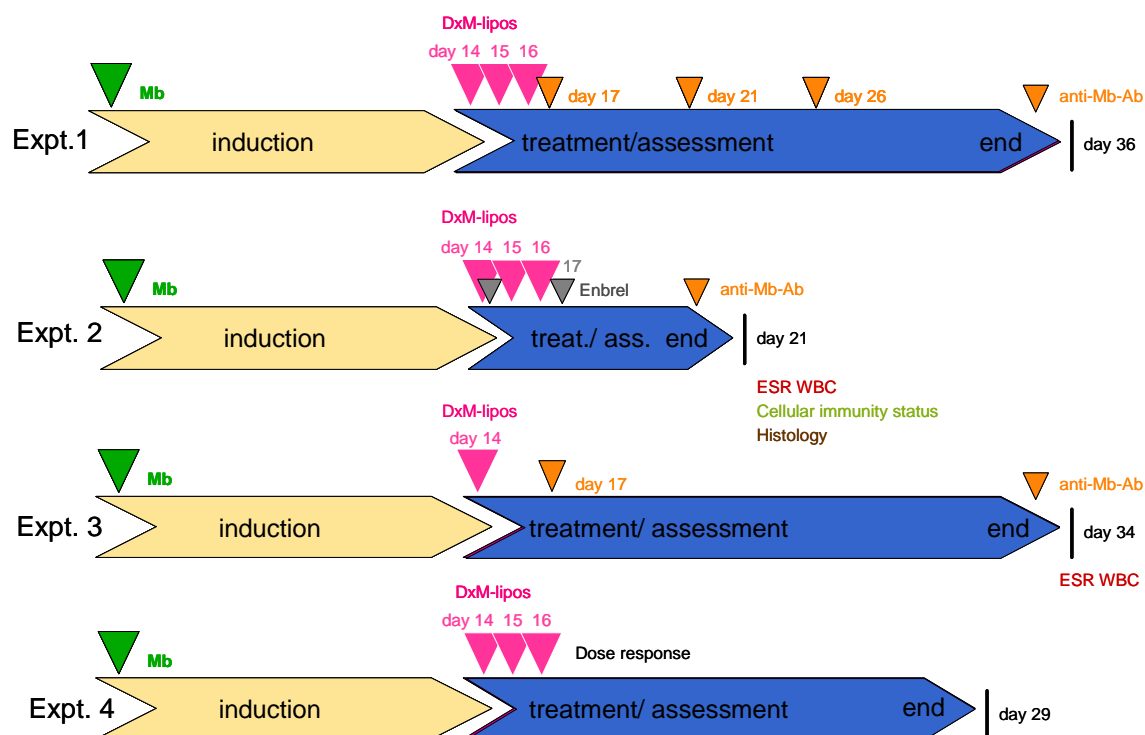85 ml 25-32% HCl

70 ml 85% formic acid

70 g hydrated $AlCl_3$

Fig. 5: Summary of the in vivo studies (experimental design)

Chronology of adjuvant arthritis induction (Mb, day 0), treatment days with DxM-lipos (days 14-16; or day 14, expt. 3) or Enbrel® (days 14, 17), sample isolation and performed studies for each of the 4 experiments (days 17, 21, 26, 34 or 36; red arrow heads).

4.4.2 Animals

Female Lewis rats (7-8 weeks of age) were obtained from Harlan (Barcelona) and housed three to four animals per cage under standard conditions, with food and water ad libitum, constant temperature (20 ± 2ºC), humidity (55%) and a 12 hours light/12 hours dark cycle. The animals were allowed two weeks to adjust to the housing conditions prior to the studies which were performed in accordance with the Institutional Guidelines for the Care and Use of Laboratory Animals established by the Ethics Committee for Animal Experimentation of the University of Barcelona.

33

4.4.3 Experimental design

4.4.3.1 Induction of adjuvant arthritis

On day 0, rats were intradermally injected into the tail base with 0.5 mg of heat-killed *Mycobacterium butyricum* (Mb) in 0.1 ml of liquid vaseline. The control group was not immunized.

4.4.3.2 Treatment of adjuvant arthritis

Dexamethasone liposomes

Only animals developing clear signs of arthritis on day 14 (arthritic score > 2) were used for further studies. On days 14, 15, and 16 of AA, rats were anesthetized by isofluran inhalation and treated intravenously (i.v.) with dexamethasone-liposomes (DxM-lipos) containing 1 mg/kg body weight dexamethasone (DxM, tab. 8). Control groups were injected with 1 mg/kg body weight of free DxM or an equal volume of PBS (arthritic control) or PBS-containing liposomes (PBS-lipos) into the tail vein. The healthy control group received no treatment. Since the mean body weight of the rats on day 14 was 250 mg, the administered dose of 1 mg/kg DxM usually corresponded to 250 µg.

Treatment	injected volume	concentration	dose
DxM-lipos	2 µl/g body weight	500 µg/ml DxM	1 mg/kg body weight
Free DxM	2 µl/g body weight	500 µg/ml DxM	1 mg/kg body weight
PBS-lipos	2 µl/g body weight	matched lipid amount	
PBS	2 µl/g body weight		

Tab. 8: Treatment conditions for DxM-lipos, free DxM, PBS-lipos, and PBS

For the dose response study, animals were treated with 3 different concentrations of DxM-lipos or free DxM (0.01 mg/kg, 0.1 mg/kg, or 1 mg/kg). This experiment (expt. 4) was performed in close collaboration with Dr. D. Pohlers at the Institute of Pathology (Prof. Bräuer, University Hospital, Jena).

Experiment	formulation	administration days	dose
Expt. 1	4	14-15-16	1 mg/kg body weight
Expt. 2	3	14-15-16	1 mg/kg body weight
Expt. 3	3	14	1 mg/kg body weight
Expt. 4	5	14-15-16	1 mg/kg, 0.1 mg/kg, 0.01 mg/kg b.w.

Tab. 9: Treatment conditions and formulation of DxM-lipos used for each experiment
b.w.: body weight

<u>Enbrel®</u>

Enbrel® (Etanercept), a recombinant TNF-α-receptor:Fc fusion protein (Weyth-Pharma GmbH, Münster, Germany), is a biological therapy approved in Germany for the treatment of RA, juvenile chronic arthritis, and other rheumatic diseases. The therapeutic dose in humans is 25 mg (0.3 mg/kg in an individual with 75 kg body weight) twice a week. The same concentration (0.3 mg/kg, tab. 10) was obtained by diluting Enbrel® with saline buffer before administration. For TNF-α-receptor therapy, animals were anesthetized and injected subcutaneously (s.c.) with 0.3 mg/kg body weight of Enbrel®, or a mouse-anti-hum-CD4 mAb in matched concentrations as a negative control, on days 14 and 17 of AA. Previous FACS analysis excluded an interaction between the anti-hum-CD4 mAb and rat CD4$^+$ lymphocytes.

Treatment	injected volume	concentration	dose
Enbrel®	2 µl/g body weight	150 µg/ml	0.3 mg/kg body weight
anti-hum-CD4 mAb	2 µl/g body weight	150 µg/ml	0.3 mg/kg body weight

Tab. 10: **Treatment conditions of Enbrel® and anti-hum CD4 mAb**

4.4.3.3 Assessment of clinical parameters

Assessment of the time course of AA was performed by measuring body mass (precision scale), arthritis score (blinded grading of each paw from 0 to 4 according to the extent of edema and erythema of the periarticular tissue, as well as the deformation of the joint; maximal score per animal:16), and hind paw volume (water plethysmometer; LI 7500 Letica, Spain). Except for the healthy control group, the results were normalized for all groups on day 14, and the hind paw volume was expressed as the mean of both hind paws.

4.4.4 Histology

Hind paws were removed on day 21, skinned, and fixed in 3% paraformaldehyde. Specimens were then decalcified with an aluminum-chloride solution, subsequently processed with increasing concentrations of ethanol (70% - 100%), xylene, and finally embedded in paraffin. Microtome sections (2-3 µm thickness) of decalcified joints were deparaffinized with xylol, ethanol solutions of decreasing concentrations, and finally stained with hematoxylin and eosin (HE).

The severity of arthritis was examined by blinded grading of several pathological parameters, such as acute inflammation, chronic inflammation, and joint and bone destruction. Acute and chronic soft tissue alterations in fat and muscle were scored in order to evaluate the expansion of the inflammation. Table 11 shows the criteria for the different histological parameters).

The preparation of the histology slides and their evaluation was performed in the laboratory of Prof. Dr. Bräuer, by Dr. Gajda, from the Institute of Pathology (University Hospital Jena).

Histological parameters		*Score*
Acute Inflammation/criteria		max. 8
exsudate	normal	0
	single granulocytes	1
	moderate	2
	extensive	3
infiltration of the synovial membrane	normal	0
	few granulocytes	1
	diffuse – moderate	2
	dense	3
+ fibrin is present		+ 1
+ periarticular tissue is affected		+ 1
Chronic Inflammation/criteria		max. 9
synovial hyperplasia	slight hyperplasia / activation of ≤ 50% of lining cells	1
	partial hyperplasia & activation of lining cells	2
	pronounced hyperplasia	3
mononucl. infiltration of synovial membrane	normal	0
	few	1
	moderate	2
	dense	3
periarticular structures (fibrosis, infiltration)	slight fibrosis / infiltration	1
	moderate	2
	pronounced fibrosis / dense infiltration	3
Cartilage & bone destruction (each)		max. 3 each
	below 10 %, local	0,5
	10 - 20 %	1
	20 - 40 %	1,5
	40 - 60 %	2
	60 - 80 %	2,5
	over 80 %	3

Tab. 11: Histology scoring system

Details of the histology evaluation score and the corresponding quantification used for joint rating.
(According to Dr. Gajda and Prof. Dr. Bräuer)

4.4.5 Hematological parameters

4.4.5.1 Erythrocyte sedimentation rate

Blood samples were obtained from the retro-orbital plexus of anesthetized rats on day 21 of AA, to determine the erythrocyte sedimentation rate (ESR). For this purpose, 1 ml of blood was treated with tri-sodium citrate and left to sediment for 1 h in capillaries (Tapval™ tubes), finally the distance between the serum meniscus and the erythrocyte level was measured in mm.

4.4.5.2 White blood count and differential leukocyte count

Retro-orbital blood samples were also used to determine the total and differential leukocyte count. The white blood cell count was determined automatically using a Coulter Counter JT hemocytometer (Hialeah, USA) calibrated for rat blood; the differential white blood count was assessed by manual enumeration of Pappenheim (or Wright-Giemsa) stained blood cell smears. At least 100 cells were counted per smear.

4.4.6 Assessment of the immune status

4.4.6.1 Determination of serum antibodies

Blood samples were obtained from the retro-orbital plexus of anesthetized rats on days 17, 21, 26, and 36. Sera were obtained by centrifugation for 5 min at 13,000 rpm and removal of the blood clot; sera were then stored at -70ºC for further analysis.

Serum antibodies against *M.butyricum* (Mb) were measured by ELISA as described previously. Briefly, microplates were coated with Mb solution (3 µg/ml) and 1% BSA/PBS/0.05% Tween was used as a blank reference; the samples were diluted 1:1.000 and 1:10.000 (in 1% BSA/PBS/0.05% Tween). For preparation of the standard, sera of sensitized rats (PBS-treated group) were pooled and serially diluted from 1:1000 to 1:64000. The Ig concentration of the standard pool from day 17 of AA was arbitrarily set to 1. The conjugated peroxidase-marked anti-rat Ig was diluted 1:16.000; 0.4 mg/ml OPD in citrate buffer was used as the substrate and the absorbance of the microplates was measured at 492 nm. This experiment was performed in close collaboration with the laboratories of Prof. Dr. Bräuer, Institute of Pathology (University Hospital, Jena)

4.4.6.2 Delayed-type hypersensitivity

To assess the delayed-type hypersensitivity, (DTH), 50 µl *M. butyricum* (1.5 mg/ml) and 50 µl PBS, respectively, were injected intradermally into the left and right ear on day 19 (i.e., 48 h prior to sacrifice). The ears of the anesthetized rats were cut, weighed, and the DTH expressed as the x-fold enlargement in comparison to the control ear.

4.4.6.3 Isolation of spleen and lymph node lymphocytes

Spleen and popliteal lymph nodes (pop LN), the first draining node of the arthritic hind paw, were obtained on day 21 from sacrificed rats. Spleen cell suspensions were prepared by passing the samples through stainless steel sieves, centrifuging for 4 min at 1600 rpm, and eliminating the erythrocytes by hypotonic lysis (consecutive resuspension in 1 ml sterile PBS, 8 ml H_2O, and 1 ml 10 x PBS). Cells were then centrifuged for 4 min at 1600 rpm and resuspended in RPMI medium.

Pop LN lymphocytes were passed through stainless steel sieves and sterile gauze to eliminate conjunctive tissue. After centrifugation for 10 min at 1600 rpm, cell suspensions were resuspended in RPMI medium and the lymphocyte count was performed using Fast Read® chamber slides.

4.4.7 Isolation and stimulation of peritoneal macrophages

Peritoneal macrophages were harvested on day 21 by peritoneal lavage with 20 ml ice-cold PBS in order to detach the PM from the peritoneal wall. The cells were then centrifuged, washed, and resuspended in RPMI medium. Single cell suspensions were seeded at 2×10^6 cells per well in 12-well plates, incubated for 2 h incubation at 37ºC, and washed with warm PBS. The adherent PM were then stimulated with LPS (1 µg/ml). Cell-free supernatants were harvested after 24 h and stored at -70ºC for further analysis. Cytokine analysis were performed by ELISA as described previously (4.3.7, tab. 12). Each sample was diluted 1:10 and 1:100.

	TNF-α	IL-1β	IL-6
capture antibody dilution	anti-rat TNF-α 1:250	anti-rat IL-1β 1:200	anti-rat IL-6 1:250
detection antibody dilution	biotinyl. anti-rat TNF-α 1:250	biotinyl. anti-rat IL-1β 1:200	biotinyl. Anti-rat IL-6 1:250
standard concentration	recomb. rat TNF- α 2000 pg/ml	recomb. rat IL-1β 4000 pg/ml	recomb. rat IL-6 5000 pg/ml
distributor	BD Biosciences Pharmingen San Diego, USA	R&D Systems Minneapolis, USA	BD Biosciences Pharmingen San Diego, USA

Tab. 12: Overview of antibodies and corresponding dilutions used for different cytokine ELISA
Biotinyl.: biotinylated, recomb.: recombinant

4.5 Statistics

Differences among groups were analyzed using the Mann-Whitney U-Test and considered statistically significant for $p \leq 0.05$. The Spearman rank correlation test was used to analyze correlations among experimental variables. Analyses were performed using the SPSS 13.0™ program (SPSS Inc.; Chicago, IL, USA).

5. RESULTS

5.1 In vitro studies

5.1.1 Liposome uptake

Comparison of microscope images under normal light and with a fluorescence filter allowed us to visualize the uptake of fluorescence labeled liposomes by monocytes (fig. 6). These results confirm the uptake of liposomes by monocytes shown by electron microscope images in previous studies (Schmidt-Weber, 1996). Cells show different intensities of fluorescence due to different levels of activation, and presumably different liposome uptake.
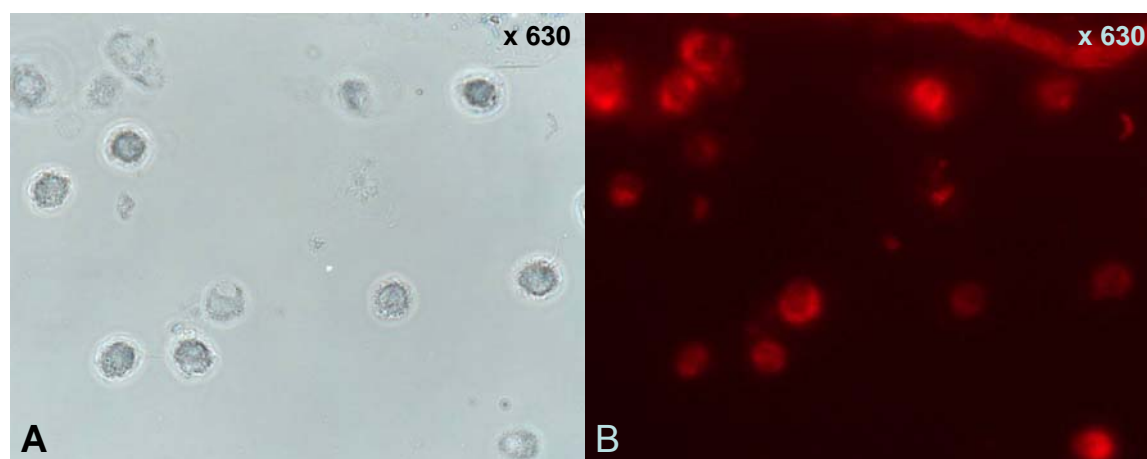

Fig. 6: Uptake of liposomes by human blood monocytes
Uptake of TRITC-lipos by non-stimulated monocytes after incubation for 6 h. Pictures were taken under normal light (A; x 630) and with a fluorescence filter (B; x 630; 540 nm excitation / 590 nm emission).

5.1.2 Liposome toxicity

In vitro assays with human peripheral blood monocytes incubated for 24 h in medium and stimulated for 20 h with LPS showed a maximal death rate of 1%, which corresponds to the natural death rate under cell culture conditions. Supplementary incubation with liposomes for 4 h was also well-tolerated by monocytes, with the maximal death rate remaining below 2%. Measurements of cell viability showed no significant differences between monocytes incubated with PBS, drug-free PBS -lipos or DxM -lipos in different dilutions (up to 1/100).

5.1.3 Nitrite production of rat peritoneal macrophages

Effects of stimulation:

Rat peritoneal macrophages (PM) were incubated for 4 h in medium and subsequently stimulated for 20 h with LPS and IFN-γ. The nitrite production of these cells was then measured as a reference for the activity of the inducible nitric oxide synthase (iNOS). The mean nitrite production of the LPS/IFN-γ control was 27.4 +/- 0.4 μM.

Effects of liposomes:

Pre-incubation with DxM-lipos significantly inhibited the iNOS induction by LPS/IFN-γ, decreasing the production of nitrite by 55% compared to the LPS/IFN-γ stimulated PM (p ≤ 0.01; fig. 7). PBS-lipos also significantly reduced the nitrite production by 17% compared to the stimulated group (p ≤ 0.01). The effect of DxM-lipos was significantly stronger than that of PBS-lipos in standard concentrations (p ≤ 0.05; fig 7). Higher dilutions of PBS-lipos had no effects, while DxM-lipos showed significant reduction of nitrite production up to dilutions of 1:100 (p ≤ 0.01 vs. LPS/IFN-γ and p ≤ 0.05 vs. PBS-lipos for DxM-lipos at 1:10 and 1:100; data not shown)
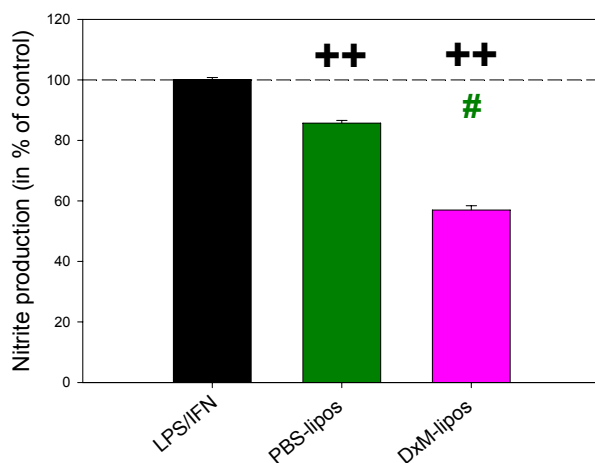

Fig. 7: Reduction of nitrite production by DxM-liposomes

Nitrite production by rat peritoneal macrophages after pre-incubation with DxM-lipos (50 μM), or PBS-lipos (equivalent lipid concentration; both 4 h) and subsequent stimulation with LPS/IFN-γ (20 h; n = 3 for all groups).
++ p ≤ 0.01 vs. LPS/IFN, # p ≤ 0.05 vs. PBS-lipos; Mann-Whitney U-test

5.1.4 Cytokine mRNA expression

5.1.4.1 Microarray analysis

RNA quality control

Exact quantification and optimal quality control of the isolated RNA is required to guarantee good quality of Microarray data and to minimize technical variability among different samples and chip runs. For this purpose, the ratios of absorbance at 260 nm and 280 nm (A260/A280) and at

260 nm and 270 nm (A260/A270) were measured with the NanoDrop throughout the processing of the sample RNA for hybridization and the results are shown in table 13.

RNA quality-control parameters							
Samples	total RNA		AA-aRNA		Cy-AA-aRNA		
	A260/A280	A260/A270	A260/A280	A260/A270	A260/A280	A260/A270	FOI
patient 1							
LPS/IFN	2.06	1.24	1.93	1.28	1.73	1.16	45.84
PBS-lipos	2.08	1.24	1.93	1.27	1.69	1.13	46.41
DxM-lipos	2.09	1.24	1.93	1.27	1.73	1.18	40.78
patient 2							
LPS/IFN	2.10	1.26	1.95	1.28	1.75	1.14	42.42
PBS-lipos	2.09	1.24	1.93	1.27	1.72	1.14	44.94
DxM-lipos	2.13	1.26	1.93	1.27	1.76	1.16	40.66
patient 3							
LPS/IFN	2.09	1.25	1.92	1.27	1.76	1.17	38.46
PBS-lipos	2.10	1.27	1.93	1.27	1.76	1.15	40.96
DxM-lipos	2.13	1.25	1.94	1.27	1.72	1.16	42.97

Tab. 13: Quality control parameters of RNA samples for microarray hybridization

Ratio of absorbance at 260 nm and 280 nm (A260/A280) and at 260 nm and 270 nm (A260/A270) of isolated total RNA, AA-aRNA and Cy-AA-aRNA for each patients sample and fluorophore incorporation (FOI) of AA-aRNA samples after Cy3 labeling.

Total RNA from all samples showed optimal absorbance ratios with A260/A280 > 2.0 and A260/A270 > 1.2 (optimal values range between 1.8 – 2.2 and 1.1 – 1.3 respectively). These quality control criteria were also achieved for all AA-aRNA samples. Cy-AA-aRNA also showed very good values for A260/A270, and values within the acceptable limits for A260/A280 and were therefore suitable for hybridization.

Microarray analysis

For each gene, the expression ratio was calculated by dividing the raw data from the Cy3-labeled samples (stimulated cells) by the raw data for the same gene from the Cy5-labeled samples (non-stimulated cells). In addition to this per-gene normalization, a series or per chip normalization was performed, the data was then background-corrected and finally log-transformed in order to obtain a normal distribution of the expression values. Probes which yielded an elevated noise were excluded from further analysis. An average of 330 genes were expressed in both stimulated and non-stimulated monocytes, however, the expression values of the majority of the genes were not significantly different between the different cells.

Monocyte genes down-regulated by incubation with DxM-lipos

After data normalization, the fold-change of all genes was compared in samples only stimulated or in DxM-lipos and PBS-lipos incubated samples compared to their paired stimulated samples was calculated. A total of 21 genes had a relevant decrease in expression compared to LPS/IFN-γ stimulated monocytes (fig. 8). IL-1 RA, IL-1β, IL-1α, TNF-α were the most down-regulated genes, followed by COX-1, IL-6, Heparin-binding EGF, and HLA-DR. Most genes with decreased expression in DxM-lipos incubated monocytes were also decreased with PBS-lipos, though in a less pronounced way. Interestingly, some genes showed an increased expression with PBS-lipos such as CD 14-Myeloid cell specific glycoprotein, IL-1β and IL-1α.
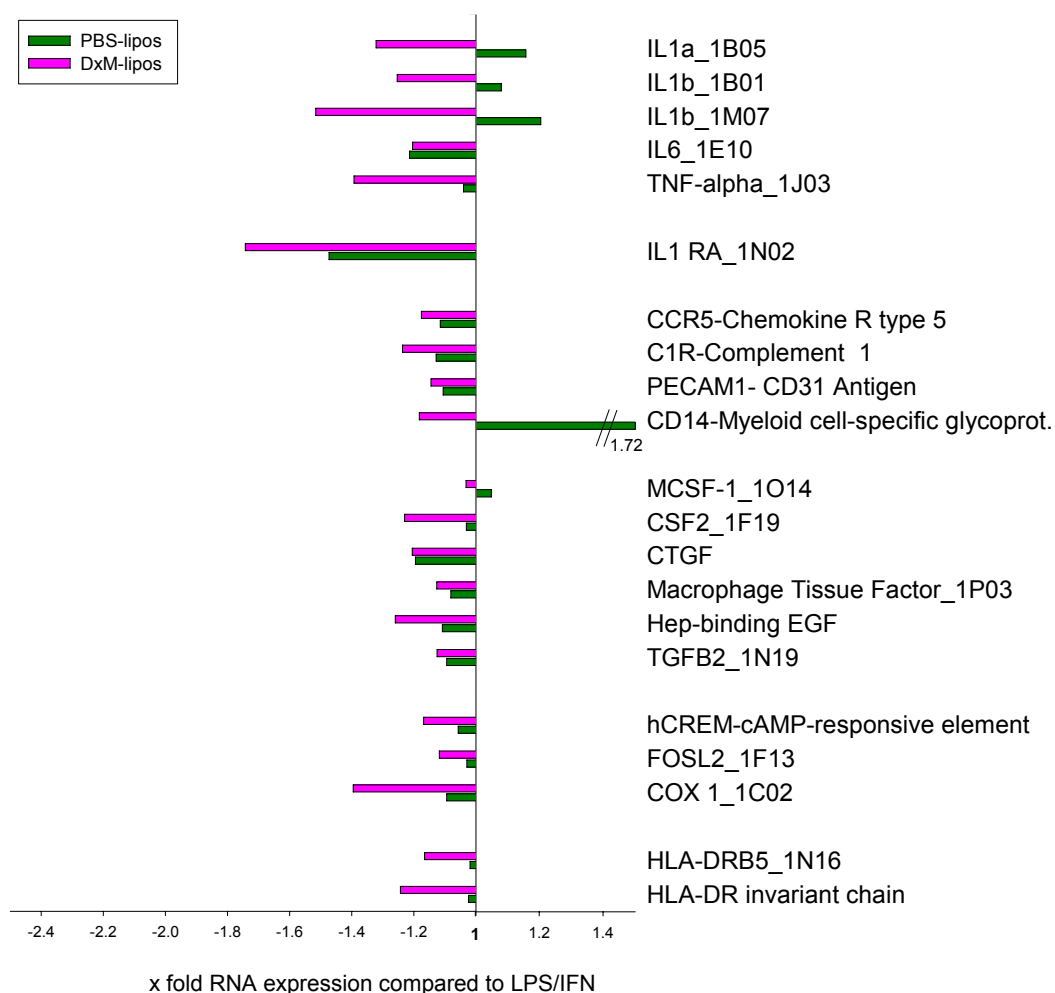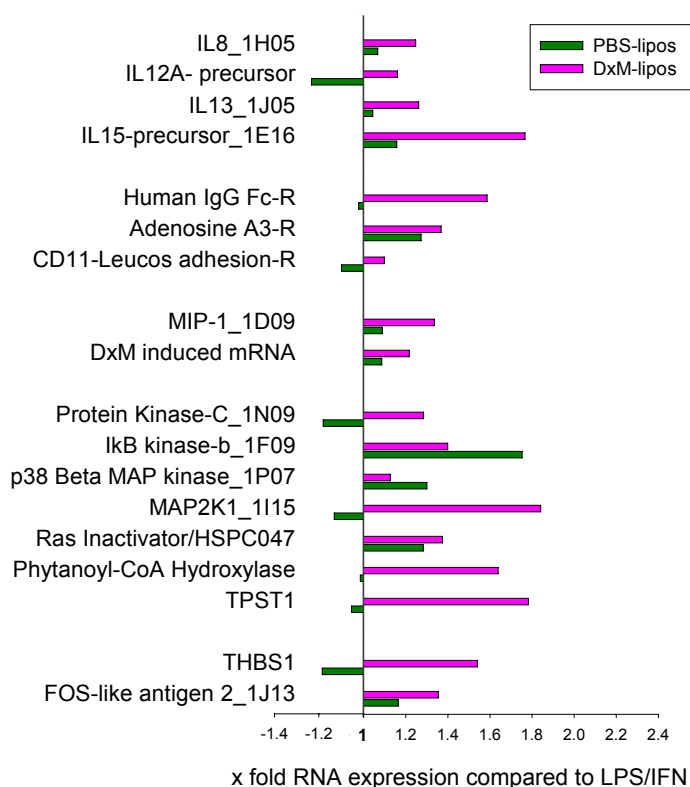

Fig. 8: Overview of down-regulated genes in monocytes incubated with DxM-liposomes

Fold-change analysis of genes with a decreased expression in monocytes incubated with DxM-lipos. Positive values represent a fold change increase and negative values a fold change decrease compared to monocytes only stimulated with LPS/IFN-γ. The expression ratio of LPS/IFN-γ was set to 1 (n = 3).

Monocyte genes up-regulated by incubation with DxM-lipos

After comparison of DxM-lipos incubated monocytes and LPS/IFN-γ stimulated monocytes, 18 genes showed a relevant up-regulated expression (fig. 9). Most markedly activated genes were IL-15, human IgG Fc-R, MAP2 kinase 1 and TPST1 followed by Phytanoyl-CoA Hydroxylase and THBS1. Apart from IkB and p38 MAP kinase, which presented an enhanced mRNA expression with PBS-lipos, the expression of the up-regulated genes in DxM-lipos incubated monocytes were not strikingly influenced by PBS-lipos.

Fig. 9: Overview of up-regulated genes in monocytes incubated with DxM-liposomes

Fold-change analysis of genes with an increased expression in monocytes pre-incubated with DxM-lipos. Positive values represent a fold change increase and negative values a fold change decrease compared to monocytes only stimulated with LPS/IFN-γ. The expression ratio of LPS/IFN-γ was set to 1 (n = 3).

Statistical analysis of microarray data

Microarray analysis identified a large number of over- and under-expressed genes with a relevant fold-change, which were then analyzed for statistical significance using the Mann-Whitney U-test.
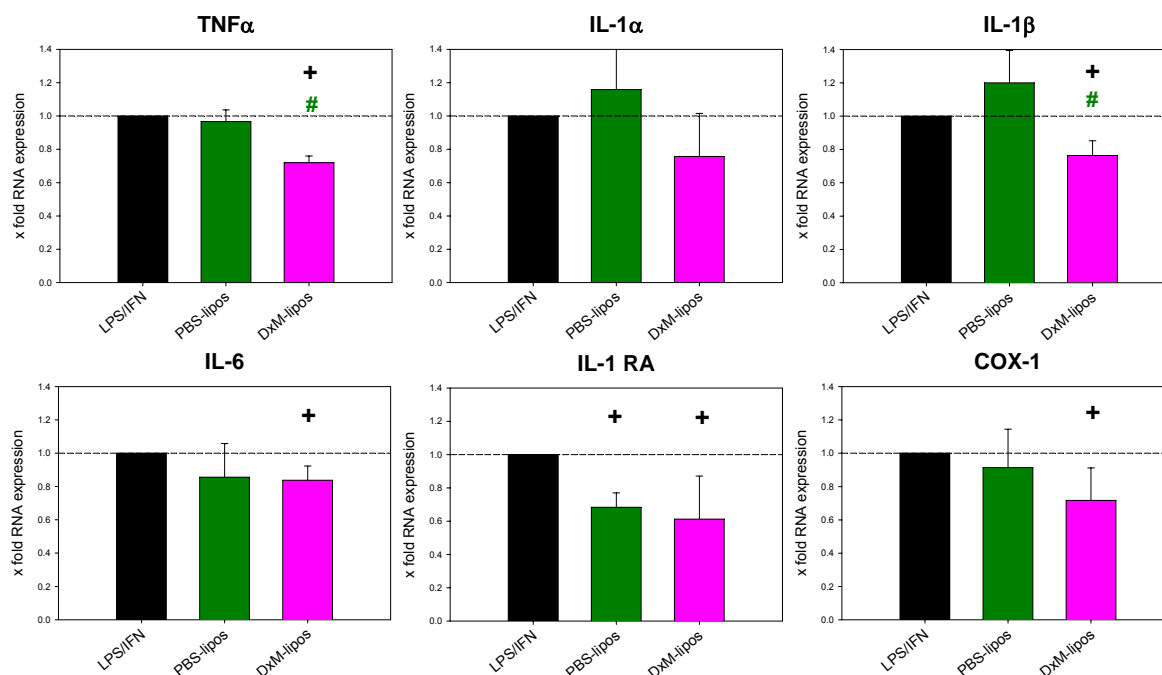
Fig. 10: Statistical analysis of gene expression from Microarray data

mRNA expression of pro-inflammatory cytokines TNF-α, IL-1α, IL-1β and IL-6 as well as IL-1 receptor antagonist (IL-1RA) and Cyclooxygenase-1 (COX-1) in human blood monocytes pre-incubated with DxM-lipos in comparison to monocytes only stimulated with LPS/IFN-γ (n=3).
+ p ≤ 0.05 vs. LPS/IFN, # p ≤ 0.05 vs. PBS-lipos; Mann-Whitney U-test

After statistical analysis, the number of identified down-regulated genes by DxM-lipos was reduced to 5. Down-regulation of both TNF-α and IL-1β expression by DxM-lipos incubation was significant compared to PBS-lipos and LPS/IFN-γ (p ≤ 0.05; fig. 10). DxM-lipos significantly inhibited IL-6, IL-1RA, and Cox-1 activation (p ≤ 0.05 vs. LPS/IFN-γ), while expression of IL-1α, which was numerically decreased by 30 % compared to PBS-lipos, was not statistically significant.

5.1.4.2 Conventional RT-PCR

In order to validate Microarray results we performed PCR studies for the significantly down-regulated genes in DxM-lipos pre-incubated monocytes compared to LPS/IFN-γ stimulated monocytes. For this we focused this part of the study on the interleukin family, extending the range of investigated genes by including IL-10, IL-15 and IL-18, cytokines with known pathophysiological importance in RA

Stimulation effects:

As a positive control, human peripheral blood monocytes were preincubated with medium and then stimulated for 2 h with LPS and IFN-γ. Quantities of cytokine mRNA were determined by

normalizing to the corresponding mRNA quantity of the house keeping gene aldolase. For this, the band density of the cytokine and aldolase samples were measured using the Scion Image software. The calculated cytokine mRNA values of the stimulation control (LPS/IFN-γ) were expressed as 100%.

Liposome effects:

TNF-α

PBS-lipos reduced the TNF-α mRNA expression by 20%, however, without a significant difference (fig. 11). In contrast, DxM-lipos significantly inhibited TNF-α expression by approximately 50% (p ≤ 0.05 vs. LPS/IFN-γ). The reduction of TNF-α expression was significantly stronger by DxM-lipos than that by PBS-lipos (p ≤ 0.05; fig. 11).

IL-1β

IL-1β mRNA expression was non-significantly reduced by PBS-lipos (10%) and significantly reduced by pre-incubation with DxM-lipos (50%; p ≤ 0.05; fig. 11). Again, the DxM-lipos were significantly more effective than PBS-lipos (p≤0.05).
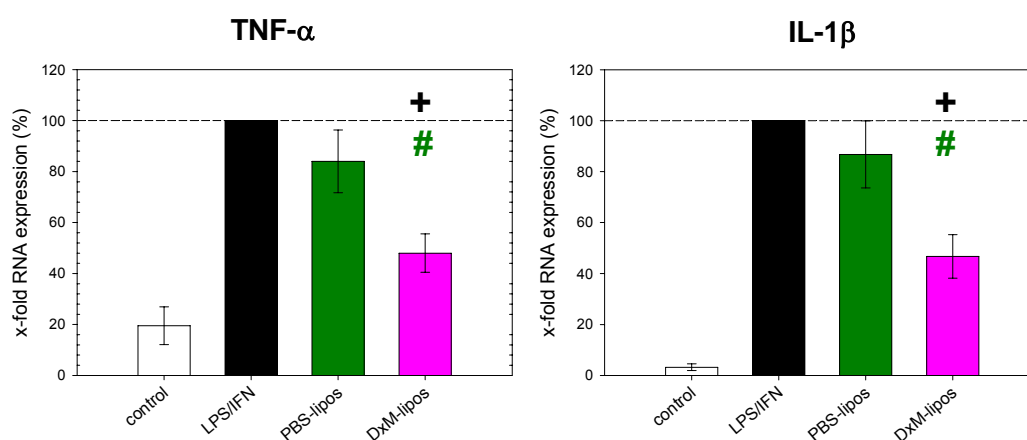
Fig. 11: Reduction of mRNA expression in stimulated monocytes by PBS- or DxM-liposomes
mRNA expression of the pro-inflammatory cytokines TNF-α and IL-1β in LPS/IFN-γ stimulated monocytes following pre-incubation with DxM-lipos (50 µM) or PBS-lipos, both in comparison to stimulated control (n = 4 each).
+ p ≤ 0.05 vs. LPS/IFN, # p ≤ 0.05 vs. PBS-lipos; Mann-Whitney U-test

IL-6

Both PBS-lipos and DxM-lipos significantly inhibited the IL-6 mRNA expression compared to stimulated control (p ≤ 0.05); however, the reduction by DxM-lipos (50%) was stronger than that by PBS-lipos (20%), a difference approaching statistical significance (p ≤ 0.08; fig. 12)
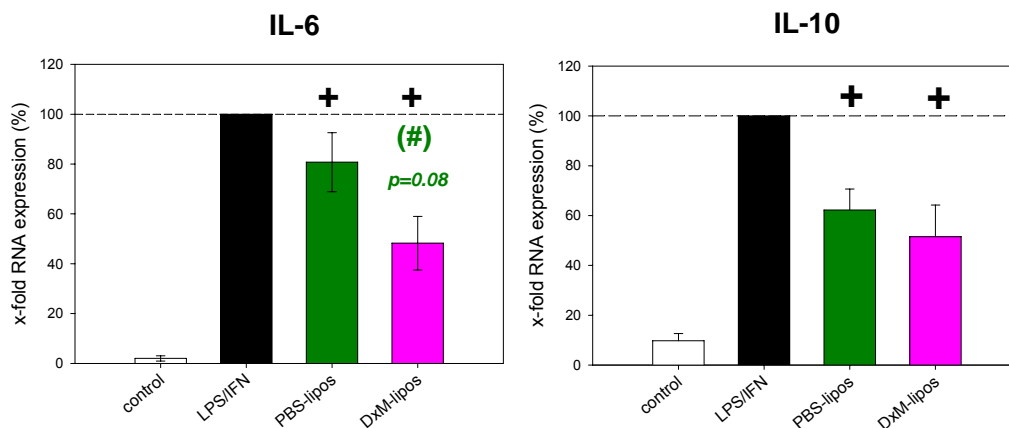
Fig. 12: Reduction of mRNA expression in stimulated monocytes by PBS- or DxM-liposomes
mRNA expression of the pro-inflammatory cytokines IL-6 and IL-10 in LPS/IFN-γ stimulated monocytes following pre-incubation with DxM-lipos (50 µM) or PBS-lipos, both in comparison to stimulated control (n = 4 each).
+ p ≤ 0.05 vs. LPS/IFN, # p ≤ 0.05 vs. PBS-lipos; Mann-Whitney U-test

IL-10

Pre-incubation with both PBS- and DxM-liposomes resulted in a significant inhibition of IL-10 mRNA expression (40% and 50% respectively; fig. 12), without significant differences between the two liposome preparations.

IL-15

IL-15 mRNA expression was significantly augmented by PBS-lipos (3.5 fold) and significantly reduced by DxM-lipos (50%; p ≤ 0.05; fig. 13).
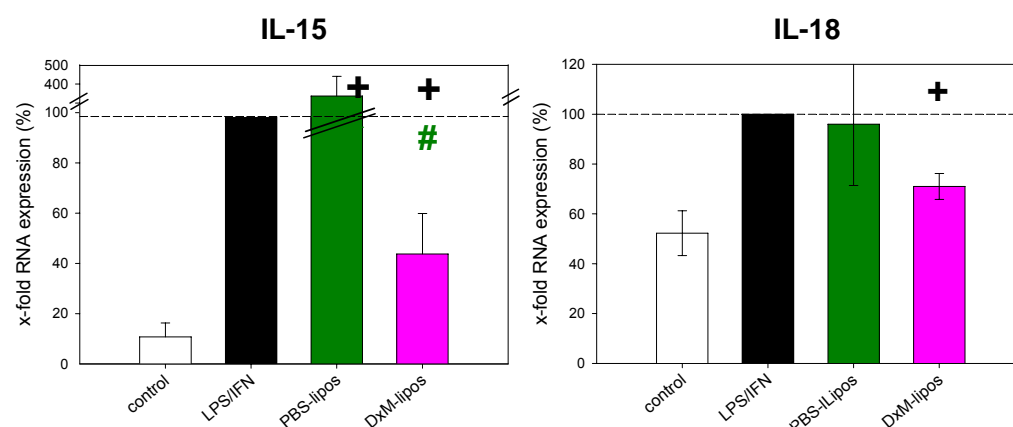

Fig. 13: Reduction of mRNA expression in stimulated monocytes by PBS- or DxM-liposomes
mRNA expression of the pro-inflammatory cytokines IL-15 and IL-18 in LPS/IFN-γ stimulated monocytes following pre-incubation with DxM-lipos (50 µM) or PBS-lipos, both in comparison to stimulated control (n = 4 each).
+ p ≤ 0.05 vs. LPS/IFN, # p ≤ 0.05 vs. PBS-lipos; Mann-Whitney U-test

IL-18

PBS-lipos had no effect on IL-18 mRNA expression, whereas DxM-lipos significantly reduced the IL-18 expression (25%; . p ≤ 0.05; fig.13).

In summary, PBS-lipos significantly inhibited only IL-6 and IL-10 mRNA expression while IL-15 expression was even significantly augmented. In contrast, DxM-lipos significantly reduced the mRNA expression of all analyzed cytokines (TNF-α, IL-1β, IL-6, IL-10 and IL-15 expression approximately 50%; IL-18 by 25%). The difference between the effects of DxM-lipos and PBS-lipos were significant for TNF-α, IL-1β, and IL-15 (p ≤ 0.05) and borderline significant for IL-6 (p ≤ 0.08). This shows that DxM-lipos are potent tools for the inhibition or pro-inflammatory cytokine production in stimulated cells

5.1.5 Cytokine production

The production of cytokines by monocytes cultured under the same conditions as for the PCR studies were investigated by ELISA

Stimulation effects:

As a positive control, human monocytes were pre-incubated for 4 h in medium and then stimulated for 20 h with LPS/IFN-γ. Table 14 shows the absolute protein concentration in the monocytes of the negative control (only incubated with medium) and the LPS/IFN-γ control for the different cytokines.

Both TNF-α and IL-6 protein were significantly increased after LPS/IFN-γ stimulation (p ≤ 0.05 vs. negative control) while IL-10 was only slightly and non-significantly augmented, and IL-15 was unaffected.

Cytokine production of controls (pg/ml)			
	negative control		LPS/IFN-γ control
TNF-α	0.00 +/-	0	226.40 +/-	60.18
IL-1β	0.00 +/-	0	0.00 +/-	0
IL-6	1.20 +/-	0.67	1648.57 +/-	425.93
IL10	192.00 +/-	43.46	276.16 +/-	71.95
IL-15	410.05 +/-	101.22	407.04 +/-	100.25

Tab . 14: Mean cytokine production +/- SEM of non-stimulated and stimulated human monocytes

<u>Lipsome effects:</u>

<u>TNF-α:</u>

PBS-lipos did not significantly reduce (and even numerically enhance) the TNF-α production in stimulated monocytes (fig. 14). In contrast, TNF-α was significantly reduced by DxM-lipos, both compared to the stimulated control and stimulated monocytes pre-incubated with PBS-lipos (p ≤ 0.05; fig. 14).

<u>IL-1β:</u>

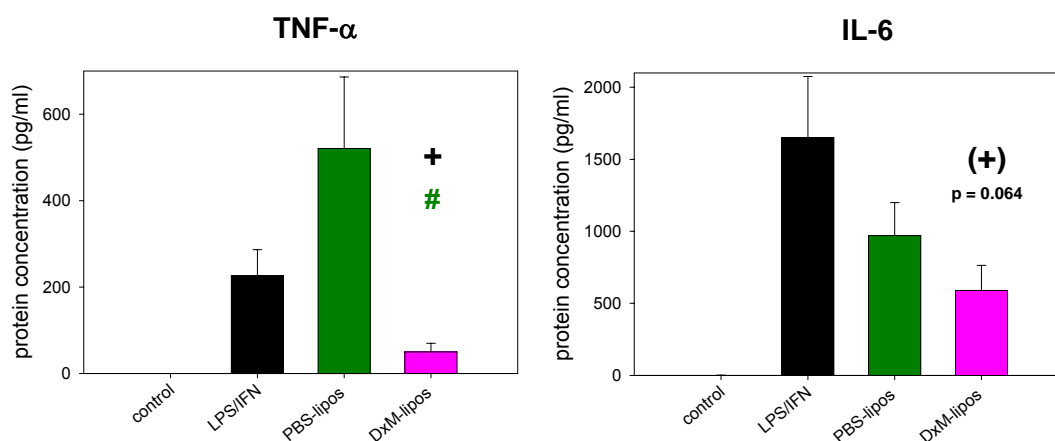No IL-1β concentrations were measured in the supernatants of any sample group except for the PBS-lipos incubated monocytes of one patient (data not shown).

Fig. 14: Cytokine production in stimulated monocytes by PBS- or DxM-liposomes
TNF-α and IL-6 production in LPS/IFN-γ stimulated monocytes following pre-incubation with DxM-lipos (50 µM) or PBS-lipos, both in comparison to stimulated control (n = 3 each).
+ p ≤ 0.05 vs. LPS/IFN, # p ≤ 0.05 vs. PBS-lipos; Mann-Whitney U-test

<u>IL-6:</u>

Both PBS-lipos and DxM-lipos numerically inhibited the IL-6 production compared to the stimulated control(by 40% and 65% respectively); however, only the reduction observed with DxM-lipos approached statistical significant (p = 0.064; fig. 14)

<u>IL-10:</u>

Incubation with both PBS- and DxM-lipos resulted in a numerical inhibition of IL-10 secretion (by 25% and 30% respectively), however without significant differences in comparison to the stimulated control (fig. 15).
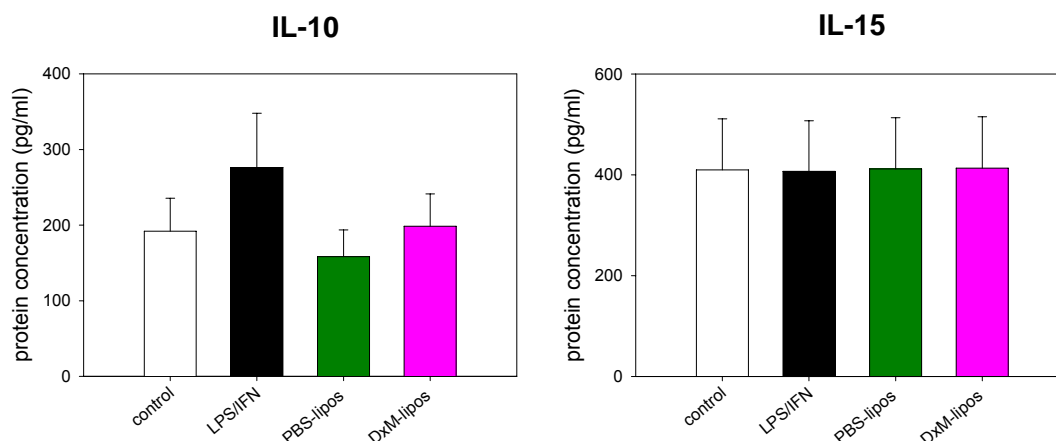
Fig. 15: Cytokine production in stimulated monocytes by PBS- or DxM-liposomes
IL-10 and IL-15 production in LPS/IFN-γ stimulated monocytes following pre-incubation with DxM-lipos (50 µM) or PBS-lipos, both in comparison to stimulated control (n = 3 each).
+ p ≤ 0.05 vs. LPS/IFN, # p ≤ 0.05 vs. PBS-lipos; Mann-Whitney U-test

IL-15:

The IL-15 concentrations were unaffected by stimulation or by pre-incubation of stimulated cells with PBS- or DxM-lipos (fig. 15).

5.2 In vivo studies in the animal model of adjuvant arthritis

5.2.1 Clinical results

5.2.1.1 Effects of treatment with PBS- or DxM-liposomes

Effects of buffer control:

In all experiments, the values of AA animals treated with the buffer control PBS, are shown for comparative purposes.

The clinical course of AA showed a significantly increased arthritis score and paw volume starting on day 14 after induction, which both reached their maximum on day 23, and decreased continuously thereafter; however, both parameters remained above the baseline values until day 34 (fig. 16).
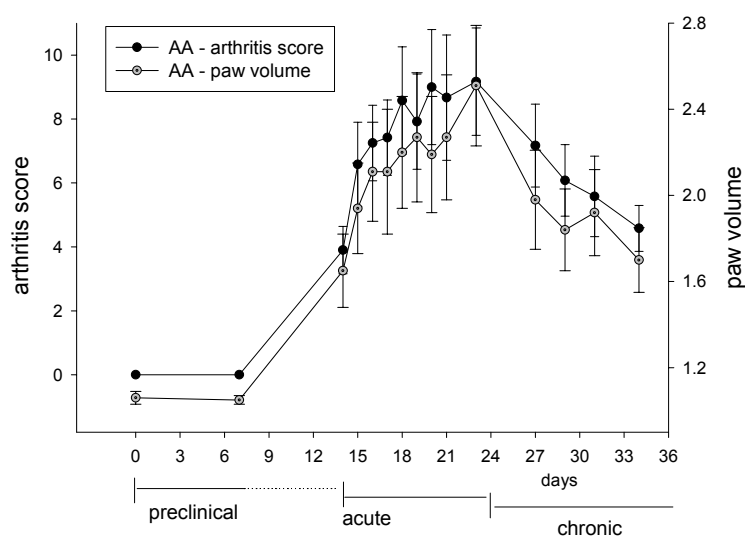
Fig. 16: Time course of adjuvant arthritis (AA)
Time course of arthritis score and paw volume after induction of AA by intradermal injection of 0.5 mg heat-killed *Mycobacterium butyricum* (Mb) on day 0 (n = 6; data corresponds to fig. 20; expt. 3)*.*

According to these results, the clinical course of the disease can be subdivided into the following phases: -1) a preclinical phase (from day 0 to 7); -2) an acute phase (days 14 to 23) and -3) a chronic phase (from day 24 onwards). Although the severity of disease varied between different experimental series, this time course was always reproduced.

Effects of PBS-liposomes

PBS-lipos remained completely ineffective and showed no significant differences for any parameter in comparison to the PBS control throughout the entire experiment; PBS-lipos even induced a transient, numerical increase of the arthritis score (day 14 to 24)and the paw volume (day 26 to 32; fig. 17A-B), with increases of 23% and 2% respectively on day 19 compared to the AA control group (tab. 15). The body weight in the AA group treated with PBS-lipos was comparable to that of the PBS-treated control group (fig. 17C).

Effects of free DxM

Treatment with matched doses of free DxM (3 x 1 mg/kg) only transiently reduced the arthritis score by 51% ($p \leq 0.05$ on days 16 and 17; minimum mean score 1.5 on day 17) and the paw volume by 65% (only numerically; minimum mean score 1.13 on day 19), with a strong rebound and overshoot effect starting 2 days after the end of the treatment (increase of the arthritis score by 4%; day 28; fig. 17 and tab. 15). The body weight dropped transiently but not significantly after DxM treatment.
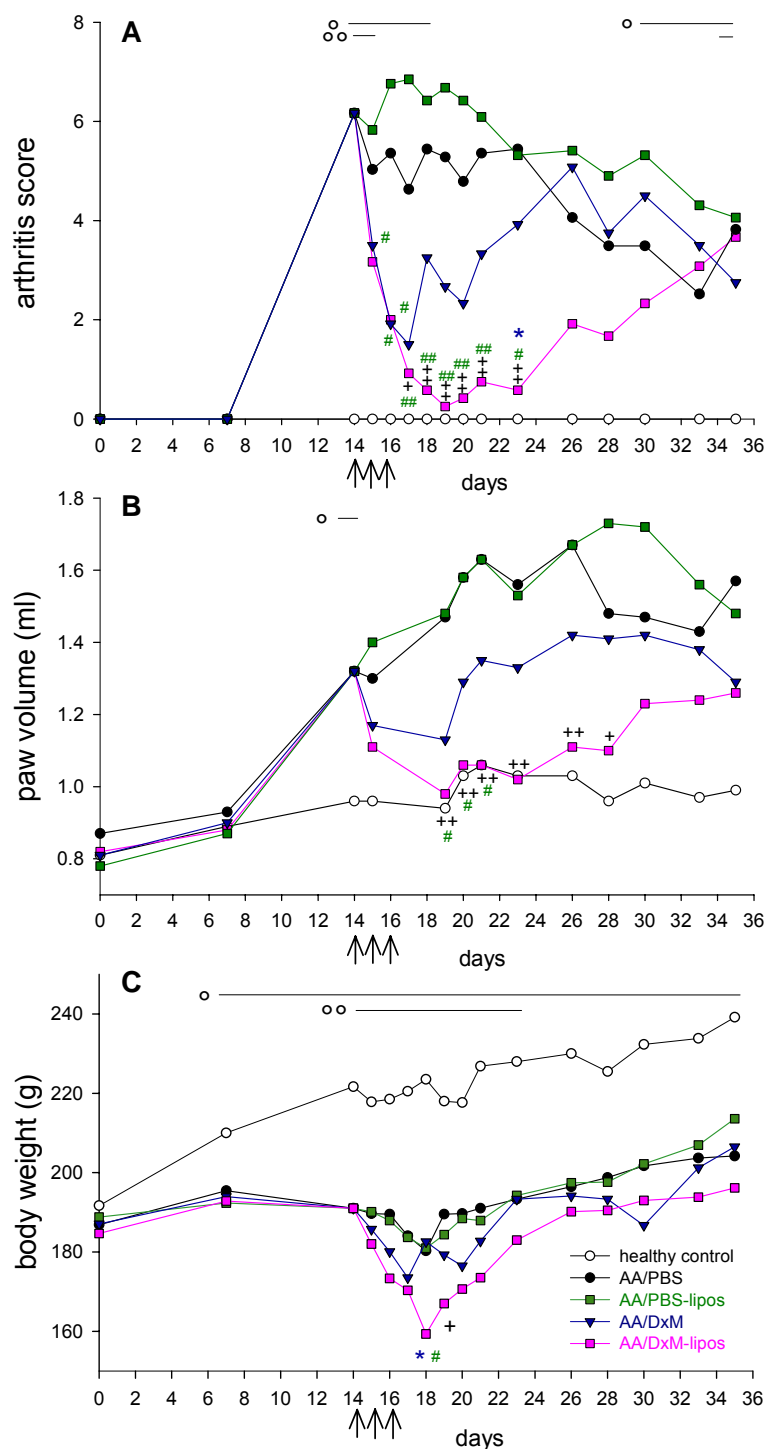
50

Fig. 17: Clinical effects of PBS-liposomes, free DxM, and DxM-liposomes in adjuvant arthritis
Effect of treatment with 3 x 1mg/kg, free DxM or 3 x 1mg/kg DxM-lipos on arthritis score (A), paw
volume (B) and body weight (C); all groups were normalized to the same mean value for each
parameter on day 14 (n = 6; expt. 1).
+ p ≤ 0.05, ++ p ≤ 0.01 vs. AA/PBS; # p ≤ 0.05, ## p ≤ 0.01 vs. PBS-lipos; * p ≤ 0.05 vs. AA/DxM; o p
≤ 0.05, oo p ≤ 0.01 vs. control; Mann-Whitney U-test.
↑ administration days of PBS, PBS-lipos, DxM and DxM-lipos

Effects of DxM-liposomes:

Short term i.v. treatment with DxM-lipos on days 14, 15 and 16 (total of 3 mg/kg body weight in 3 days) resulted in a strong, significant, and long-lasting suppression of arthritis score ($p \leq$ 0.01, days 17-23; minimum mean score of 0.25 and 95% reduction on day 19) and paw volume ($p \leq 0.001$, days 19-27 and $p \leq 0.05$,day 28; minimum swelling of 0.98 ml and 92% reduction on day 19) in comparison to PBS treated AA controls (fig. 17 and tab. 15). Both parameters achieved almost normal levels and there were no significant differences between AA rats treated with DxM-lipos and normal controls for the arthritis score (day 19 to 28) and the paw volume (from day 15 onwards). On day 28, i.e., 2 weeks after the initiation of treatment, DxM-lipos still reduced the arthritis score by 54% and the paw volume by 73%. After a transient, significant drop (days 19-20), the body weight of DxM-lipos-treated rats returned to the levels of PBS treated rats. On day 23 DxM-lipos was significantly more effective in suppressing the arthritis score than free DxM ($p \leq 0.05$, fig. 17A).

Similar results were obtained in a second and third experimental series with maximal score and paw volume reduction by DxM-lipos on day 19 of 90% and 87% (fig.18 and tab. 15; expt.2), or of 96% and 86% (fig. 19 and tab. 16; expt.4), respectively, confirming the validity of the data.

Reduction of clinical parameters

Expt.1	arthritis score		paw volume	
Treatment	day 19	day 28	day 19	day 28
AA/PBS	--	--	--	--
AA/PBS-lipos	+ 23%	- 36%	+ 2%	+ 47%
AA/DxM	- 51%	+ 4%	- 65%	- 13%
AA/DxM-lipos	- 95%	- 54%	- 92%	- 73%
Expt. 2/3	arthritis score		paw volume	
Treatment	day 19	day 29*	day 19	day 29*
AA/PBS	--	--	--	--
AA/PBS-lipos	+ 15%		+ 23%	
AA/DxM	- 67%		- 52%	
AA/DxM-lipos	- 90%		- 87%	
AA/Enbrel	- 18%	- 5%	+ 6%	+ 3%
AA/anti-human CD4 mAb	- 10%	- 31%	+ 23%	- 35%
*AA/DxM-lipos 1x *	- 48%	- 15%	- 63%	- 35%

Tab. 15: Reduction of clinical parameters by DxM-lipos on day 19 and 28 of adjuvant arthritis
Reduction of arthritis score and paw volume on day 19 (maximal efficacy of therapy) and day 28 after treatment with DxM (3 x 1 mg/kg; days 14, 15, 16) or DxM-lipos (3 x 1 mg/kg; day 14, 15, 16) compared to the PBS-treated group (expt. 1 corresponds to the data in fig. 17). For comparison, the effect of treatment with Enbrel® (2 x 0.3 mg/kg; days 14, 17; expt. 2 corresponds to the data in fig. 18) or single-dose DxM-lipos (1 x 1 mg/kg; day 14; expt. 3 corresponds to the data in fig. 20) are shown.
 * results from a separate group of animals (expt. 3) with similar disease severity on day 19/20 as the animals from expt. 2.

5.2.1.2 Comparison with Enbrel®

S.c. treatment with Enbrel® on days 14 & 17 (0.3 mg/kg bodyweight), had no effect on arthritis score or paw volume. There were no significant differences between PBS-treated, Enbrel®-treated or anti-human-CD4 treated AA rats (fig. 18). Similar results were obtained in an additional experiment with a 10 x higher dose of Enbrel® (3 mg/kg body weight) and over a longer period of time (expt. 3, tab. 15).
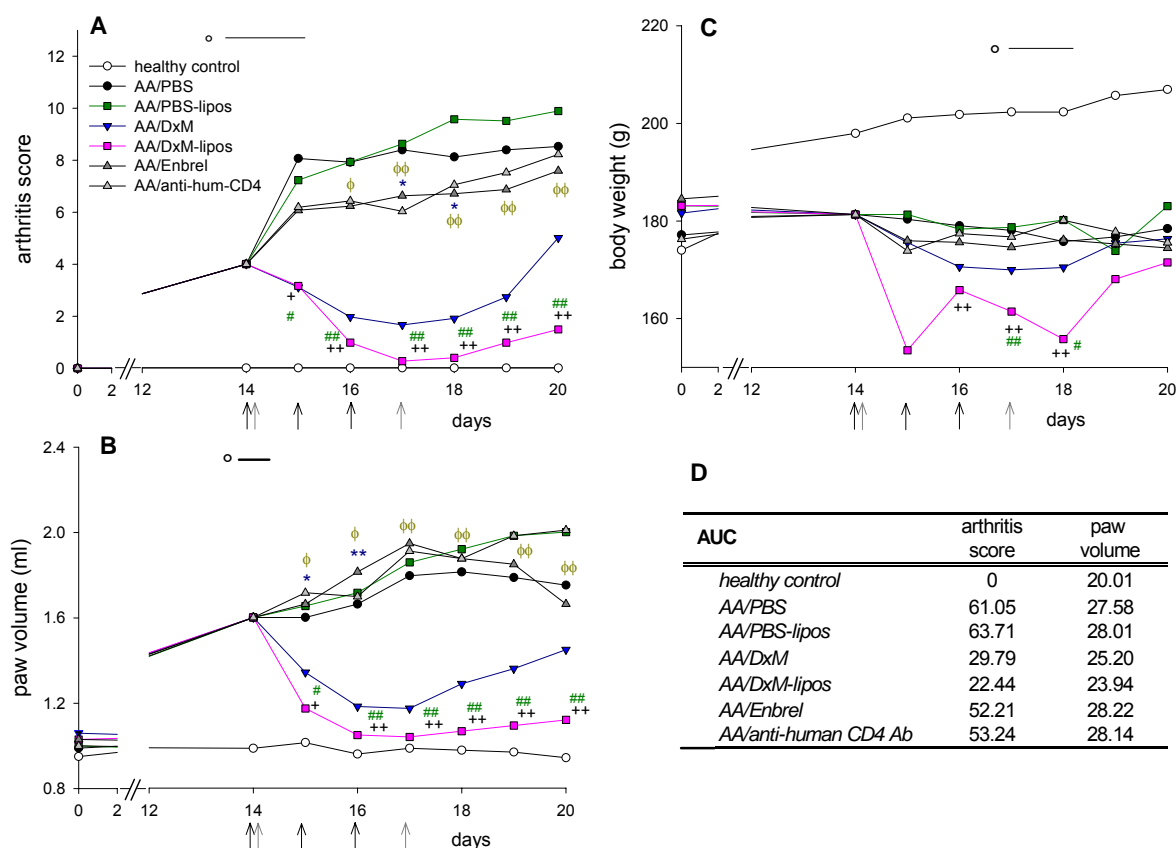

Fig. 18: Comparison of the clinical effects of DxM-liposomes and Enbrel® in adjuvant arthritis
Effects of treatment with DxM-lipos (3 x 1 mg/kg) or Enbrel® (2 x 0.3 mg/kg) on arthritis score (A), paw volume (B), and body weight (C); all groups were normalized to the same mean value for each parameter on day 14 (n = 8 for all groups, except AA/Enbrel and AA/anti-human CD4, both n = 6; expt. 2). Panel D summarizes the respective areas under the curve from graphs A and B.
p ≤ 0.05, ++ p ≤ 0.01 vs. AA/PBS; # p ≤ 0.05, ## p ≤ 0.01 vs. PBS-lipos; * p ≤ 0.05, ** p ≤ 0.01 vs. AA/DxM; φ p ≤ 0.05, φφ p ≤ 0.01 vs. AA/Enbrel; o p ≤ 0.05, oo p ≤ 0.01 vs. control in comparison to AA/Enbrel; Mann-Whitney U-test; ↑ administration days of PBS, PBS-lipos, DxM, and DxM-lipos; ↑ administration days of Enbrel® and anti-human CD4 Ab.

I.v. treatment with DxM-lipos (total dose of 3 mg/kg) had a significantly stronger anti-inflammatory effect in AA than s.c. therapy with a TNF-α receptor (Enbrel®; total of 0.6 mg/kg) resulting in significant differences for paw volume (p ≤ 0.05 or ≤ 0.01, days 15-20) and arthritic score (p ≤ 0.05 or ≤ 0.01, days 16-20). Even the same total dose of free DxM (3 mg/kg) was

more efficient than Enbrel® (paw swelling: $p \leq 0.05$, days 16-17; arthritis score: $p \leq 0.05$, days 17-18; fig.18). Treatment with a single injection of DxM-lipos (1 mg/kg) on day 14 also proved to be more efficient in controlling arthritis than Enbrel® therapy; the reduction of arthritis score and paw volume were significantly stronger on days 15-17 ($p > 0.05$; data not shown). The body weight was not affected by Enbrel® administration, showing similar values as in arthritic control animals.

5.2.1.3 Effects of dose reduction

The efficacy of DxM-lipos was tested in another experimental study, in order to evaluate the possibility of a mono-dose therapy and to determine the minimal therapeutically efficacious dexamethasone dose. For this purpose, rats were injected 3 x with different concentrations of DxM-lipos (1 mg/kg, 0.1 mg/kg or 0.01 mg/kg DxM) or once with DxM-lipos 1 mg/kg.

<u>Dose response</u>

Dose response studies (fig. 19A-C) showed a significant decrease of arthritis score and paw volume, as well as longer lasting effects, with increasing DxM-lipos concentrations: while low-dose DxM-lipos (0.01 mg/kg) had little anti-inflammatory effects, medium-dose DxM-lipos 0.1 mg/kg) significantly reduced the paw volume in acute AA ($p \leq 0.05$, days 16-21) and high-dose DxM-lipos (1 mg/kg) significantly decreased both arthritis score and paw volume in acute and chronic AA ($p \leq 0.01$, days 15-27). Inhibition of arthritis score and paw volume was significantly stronger after high-dose DxM-lipos than after low-dose DxM-lipos administration ($p \leq 0.05$ or $\leq$ 0.01, days 16–24) and even after medium-dose DxM-lipos ($p \leq 0.05$, days 16, 17, 19, and 21 for the arthritis score, and day 19 for the paw volume). The decrease of body weight also was dose dependent.

The differences between liposomal and free DxM were potentiated with increasing concentrations. The reduction of the arthritis score was augmented by 10% when comparing low-dose DxM-lipos treatment to the same dose of free DxM, by 13% when comparing medium-dose DxM-lipos to free DxM and by 27% in the case of high-dose DxM. This led to significant differences between high-dose DxM-lipos and free DxM for the reduction of the arthritis score ($p \leq 0.05$, days 16-19; D), the paw volume ($p \leq 0.05$, day 18; E), but also the body weight ($p \leq 0.05$, days 17-18; F).
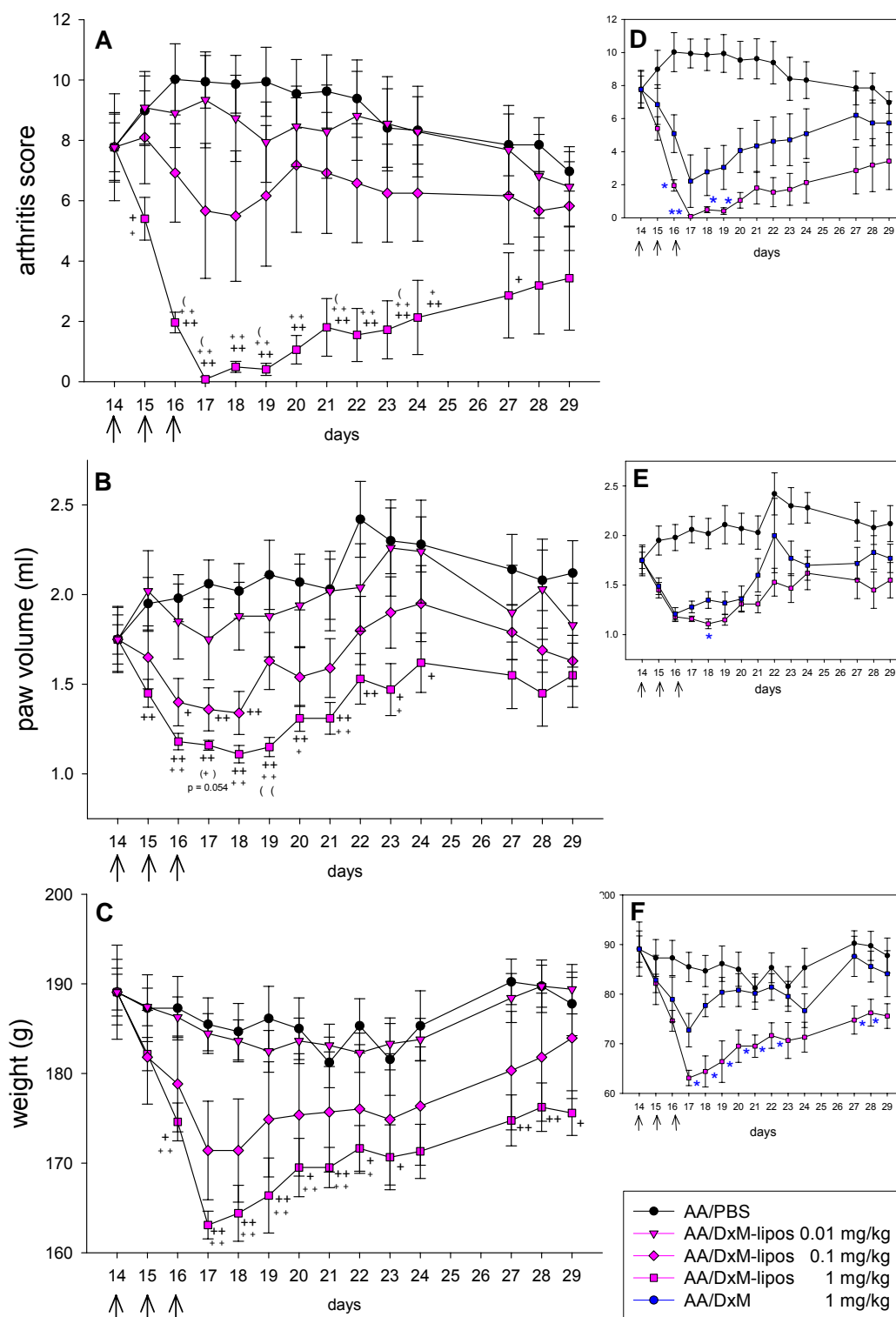
Fig. 19: **Dose dependence of therapy with DxM-liposomes in adjuvant arthritis**
Dose response of DxM-lipos treatment (3 x 1 mg/kg, 3 x 0.1 mg/kg, 3 x 0.01 mg/kg; A-C) and comparison between treatment with DxM-lipos and free DxM (3 x 1 mg/kg; D-F); all groups were normalized to the same mean value for each parameter on day 14 (n = 6; expt. 4).
$+$ $p \leq 0.05$, $++$ $p \leq 0.01$ vs. AA/PBS; $+$ $p \leq 0.05$, $++$ $p \leq 0.01$ vs. AA/DxM-lipos 0.01 mg/kg; $($ $p \leq 0.05$ vs. AA/DxM-lipos 0.1 mg/kg; $*$ $p \leq 0.05$, $**$ $p \leq 0.01$ vs. AA/DxM; Mann-Whitney U-test
$\uparrow$ administration of PBS- and DxM-lipos

Reduction of clinical parameters

Treatment		arthritis score		paw volume	
		day 19	day 28	day 19	day 28
AA/PBS		--	--	--	--
AA/DxM	0.01 mg/kg	- 10%	+ 6%	- 18%	- 12%
AA/DxM	0.1 mg/kg	- 25%	- 4%	- 34%	+ 9%
AA/DxM	1 mg/kg	- 69%	- 27%	- 71%	- 23%
AA/DxM-lipos	0.01 mg/kg	- 20%	- 13%	- 21%	- 5%
AA/DxM-lipos	0.1 mg/kg	- 38%	- 28%	- 44%	- 36%
AA/DxM-lipos	1 mg/kg	- 96%	- 59%	- 86%	- 58%

Tab. 16: **Reduction of clinical parameters by DxM-lipos on day 19 and 28 in adjuvant arthritis**
Reduction of arthritis score and paw volume on day 19 (maximal efficacy of therapy) and day 28 after treatment with DxM (3 x 1 mg/kg, 3 x 0.1 mg/kg, 3 x 0.01 mg/kg) or DxM-lipos (3 x 1 mg/kg, 3 x 0.1 mg/kg, 3 x 0.01 mg/kg) compared to the PBS-treated group (expt. 4; corresponds to the data in fig. 19)

Single dose therapy with DxM-liposomes

Single dose therapy with DxM-lipos (1 mg/kg) on day 14 resulted in a significant, but short-lasting reduction of the arthritis score ($p \leq 0.05$ on day 15; $p \leq 0.08$ on days 16-17 vs. AA/PBS), with a minimum mean arthritis score of 2.3 on day 15 and of the hind paw volume ($p \leq 0.05$ day 15; $p \leq 0.06$ vs. AA/PBS days 16-17 and 19), with a minimum volume of 1.3 ml on day 15 (fig. 20). There were no significant differences for the paw swelling between single dose DxM-lipos treated rats and normal controls from day 16-18. On day 19, arthritis score was reduced by 48% and the paw volume by 63%, i.e., an effect comparable to that of 3 x treatment with 0.1 mg/kg DxM-lipos (tab. 16). Treatment with single dose of DxM-lipos showed no significant increased weight loss compared to buffer treatment (fig. 20).
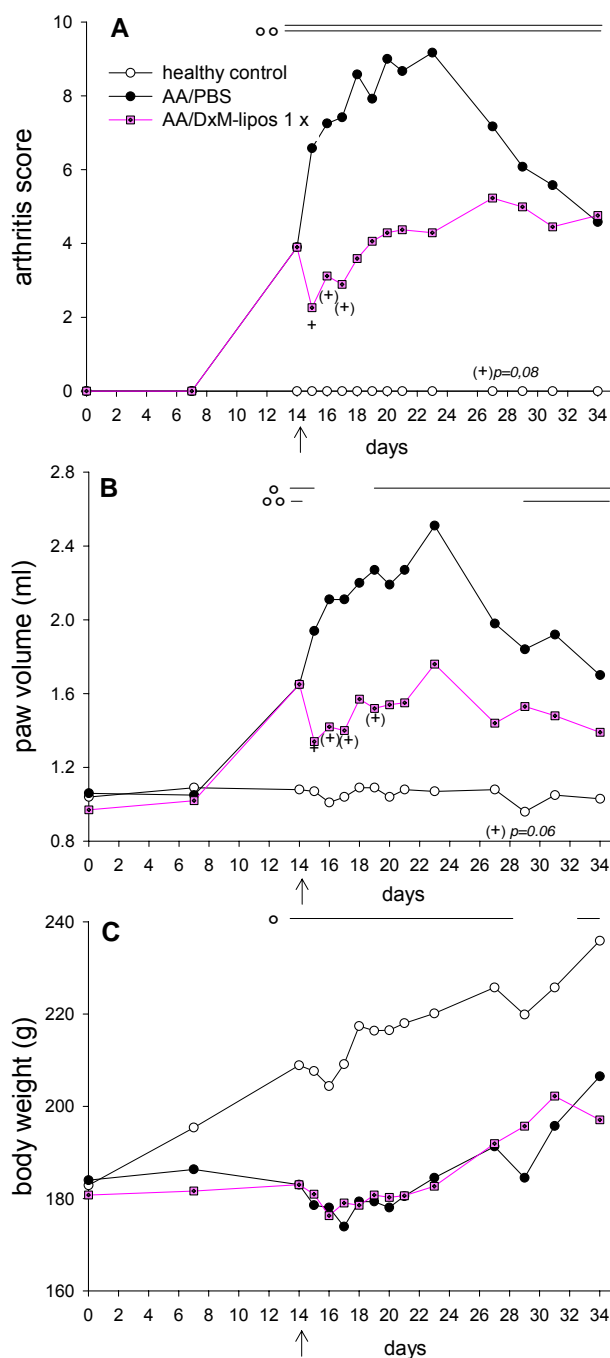
Fig. 20: Clinical effects of single dose DxM-liposome therapy in adjuvant arthritis
Effect of treatment with 1 x 1 mg/kg DxM-lipos on arthritis score (A), paw swelling (B), and body weight
(C); all groups were normalized to the same mean value for each parameter on day 14 (n = 6; expt. 3).
+ $p \leq 0.05$, (+) $p \leq 0.08$ vs. AA/PBS; Mann-Whitney U-test; ↑ administration of PBS- and DxM-lipos

The paw volume on day 19 showed a highly significant, positive correlation with the swelling
measured before treatment (day 14; $p \leq 0.005$, $r_s > 0.87$ in all cases). The regression line
gradient for rats treated 3 x with high-dose DxM-lipos was k = 0.33, showing that 3 x
administration of DxM-lipos strongly controlled the swelling even in the case of advanced

adjuvant arthritis. The regression line gradient of 3 x treatment with DxM-lipos was smaller than that of 1 x treatment with DxM-lipos, indicating the dose-dependent effect of DxM-lipos on paw volume. Rats treated 1 x with DxM-lipos or 3 x with free DxM showed similar gradients: k = 0.9 and 0.86 respectively, and therefore comparable efficacy for the therapy of arthritis (fig. 21).
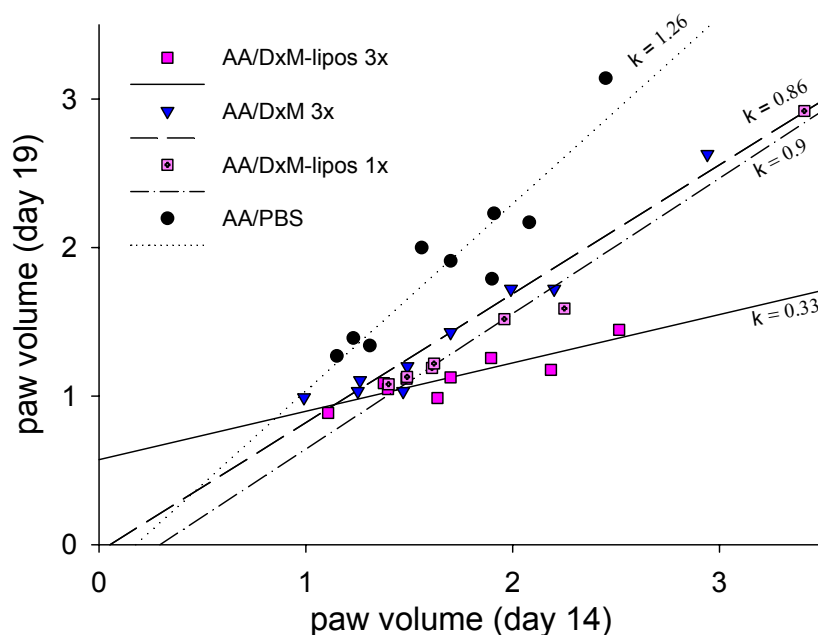
AA/PBS	AA/DxM 3 x	AA/DxM-lipos 3 x	AA/DxM-lipos 1 x
rs = 0.90	rs = 0.97	rs = 0.87	rs = 1
p = 0.001	p = 0.000	p = 0.002	p = 0.000
k = 1.26	k = 0.86	k = 0.33	k = 0.9

Fig. 21: Correlation between the paw volume on different days during the time course of adjuvant arthritis
Correlation (Spearman rank test, rs) between the paw volume on day 19 (maximal efficacy of treatment) and day 14 (prior to treatment) of individual rats treated with high-dose DxM-lipos (3 x 1 mg/kg; days 14, 15, 16; n = 8; or 1 x 1 mg/kg; day 14; n = 6), free DxM (3 x 1 mg/kg; days 14, 15, 16; n = 8) or PBS (3x; days 14, 15, 16; n = 8). The solid, dashed and dotted lines are the regression lines, k represents the regression gradient.
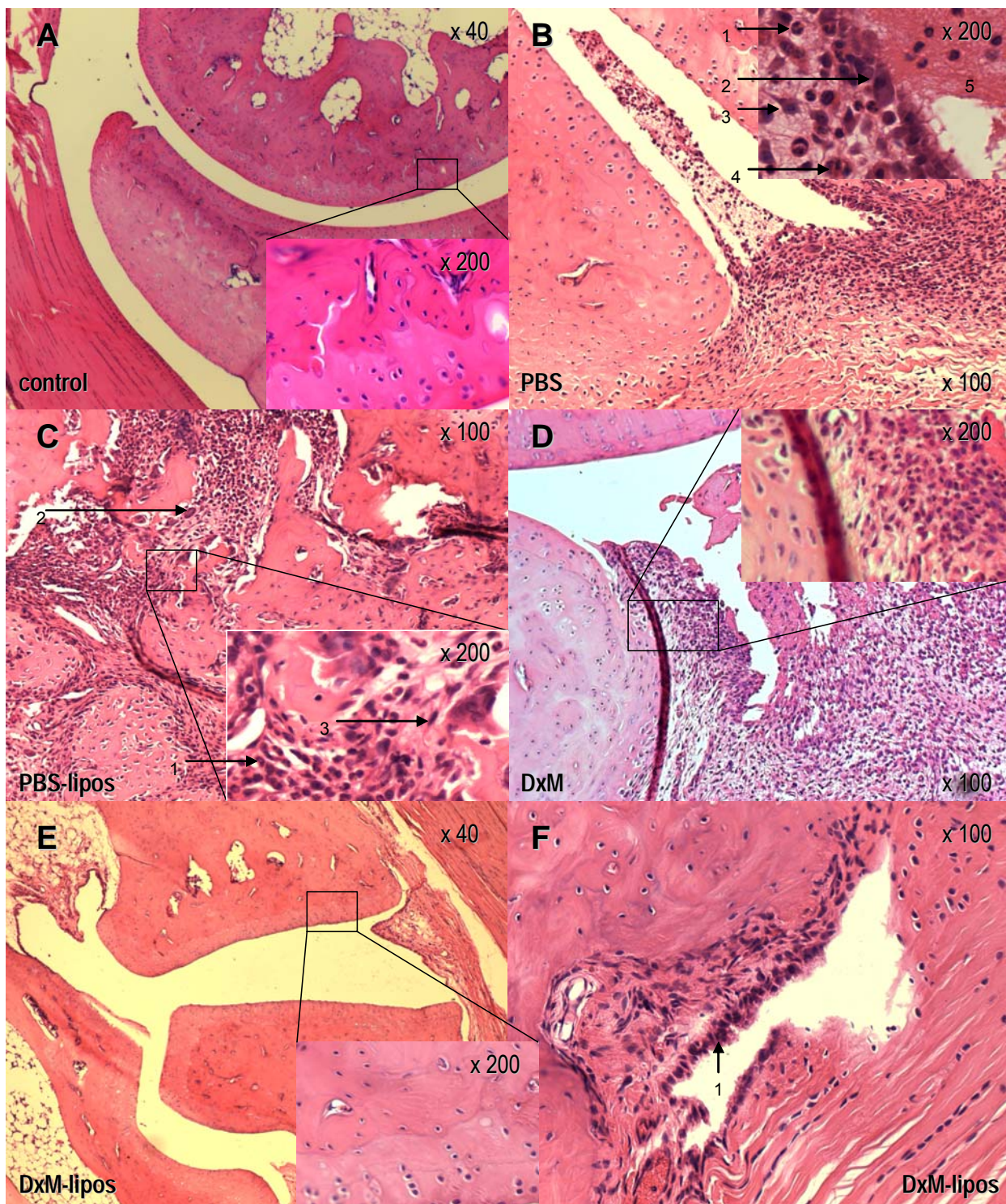
5.2.2 Histology

Fig. 22: Histological assessment of the effects of treatment with DxM-liposomes in adjuvant arthritis (day 21)
Images of HE (hematoxilin and eosin) stained joint sections from healthy control rats (A) and AA rats after treatment with PBS (B, 1 = PMN, 2 = lymphocyte, 3 = dendritic cell, 4 = osteoclast, 5 = fibrin), PBS-lipos (C, 1 = PMN, 2 = osteoclast, 3 = fibroblast), free DxM (3 x 1 mg/kg; D), or DxM-lipos (3 x 1 mg/kg; E-F, 1 = hyperplasia of synovial lining layer ; expt. 2)

Histology pictures of control animals show healthy joints, i.e., cartilage with a smooth surface and vital chondrocytes, a clear border between bone and cartilage as well as normal periarticular fatty and muscle tissue without any signs of cellular infiltration (fig. 22A). In contrast, the joints of arthritic animals are highly deformed, with severe bone affectation (osteomyelitis and osteoclast-activation) and approximately 50% bone and cartilage loss, massive infiltration of the joint space and periarticular tissue, with acute and chronic inflammatory cells (PMN and lymphocytes, respectively), hyperplasia and prominent nucleoli of the synovial lining cells, and proliferation of fibroblasts (fig. 22B). Joints of PBS-lipos treated animals showed the same characteristics (fig. 22C). In contrast, several of these characteristics were reduced or even absent after DxM- or DxM-lipos-treatment. Joints of animals treated with free DxM showed good bone and cartilage presentation, but infiltration of the joint space with lymphocytes was still prominent (fig. 22D). Although a certain joint deformation persists in animals treated with DxM-lipos, bone and cartilage structures seem to be intact, with smooth surfaces, and little infiltration with PMN (fig. 22E). The synovial membrane still presents some signs of chronic inflammation, hyperplasia of the synovial lining, and lymphocyte infiltration, thereby to a lower extent than in free DxM treated rats (fig. 22F). In addition, DxM-lipos significantly reduced acute inflammation and infiltration of periarticular tissue (data not shown).

Histology score:

Quantification of histological parameters showed a pronounced degree of acute and chronic inflammation, as well as cartilage and bone destruction in PBS-treated arthritic animals (sum score of 9.63; fig. 23). PBS-lipos did not significantly modify the histopathological features in AA. Application of free DxM had similar effects as administration of DxM-lipos, with scores significantly lower than those in PBS- and PBS-lipos-treated animals. Treatment with DxM-lipos (3 x 1 mg/kg) significantly reduced this score to a value of 3.18; the acute inflammation and the bone/cartilage destruction showed the most prominent reduction (both approx. 70%, and 64% for chronic inflammation; fig. 23B-D). There were no significant differences between AA rats treated with DxM-lipos and normal controls for the different histological parameters. Compared to Enbrel® which reduced the histology score by 40% (especially due to the inhibition of joint destruction). DxM-lipos-therapy was more effective in reducing the histological signs of inflammation and destruction.
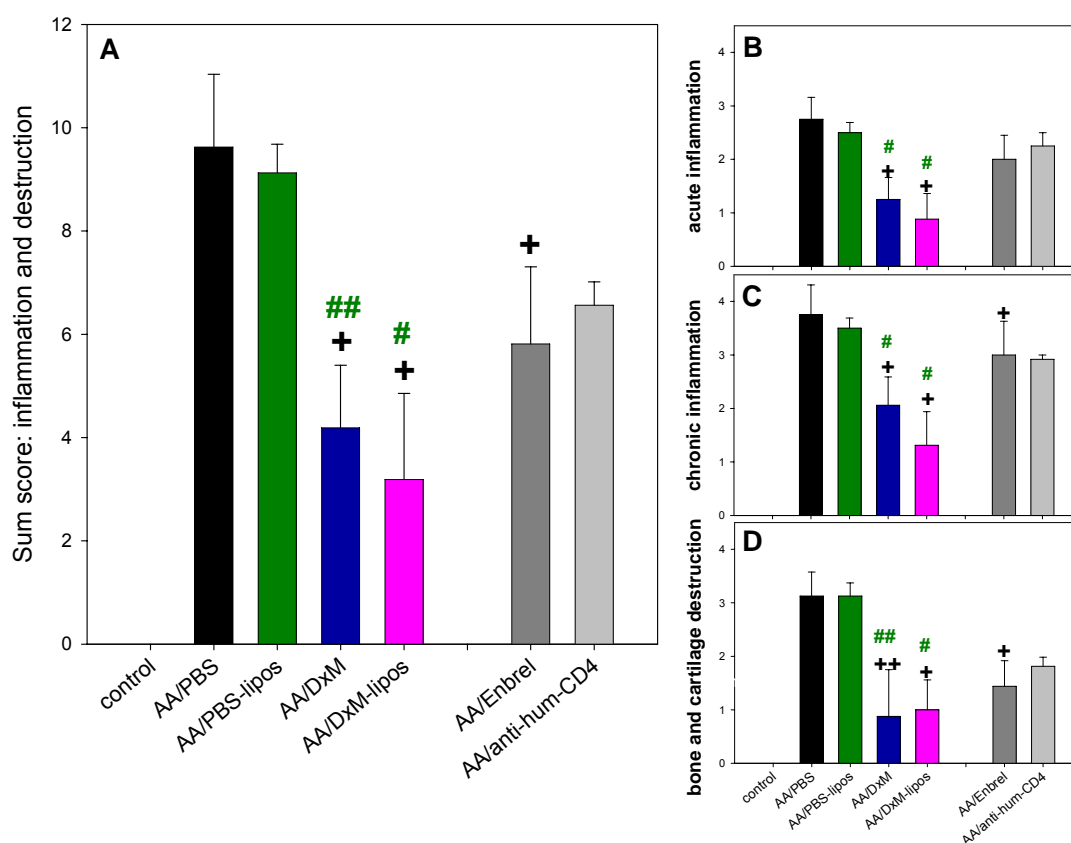
Fig. 23: Quantification of histological parameters in adjuvant arthritis (day 21)

Effects of treatment with PBS, PBS-lipos, free DxM (3 x 1 mg/kg) DxM-lipos (3 x 1 mg/kg; n = 8) or Enbrel® (2 x 0.3 mg/kg; n = 6) on the histology sum score (A) and individual histology parameters (B, acute inflammation: C, chronic inflammation; D, bone and cartilage destruction; data correspond to the images of fig. 22; expt. 2)
+ p ≤ 0.05, ++ p ≤ 0.01 vs. AA/PBS; # p ≤ 0.05, ## p ≤ 0.01 vs. PBS-lipos; o p ≤ 0.05, oo p ≤ 0.01 vs. control; Mann-Whitney U-test

5.2.3 Hematological results

The systemic hematological effects of treatment with DxM-lipos and Enbrel® were evaluated by determining the erythrocyte sedimentation rate (ESR) and the white blood count (WBC) on day 21 of adjuvant arthritis.

.

5.2.3.1 Erythrocyte sedimentation rate

The ESR, measured as a parameter of systemic inflammation, was significantly increased in arthritic animals compared to healthy controls in the acute (day 21) and chronic (day 34) phase of AA (approx. 6-fold in both cases; fig. 24).

Free DxM and PBS-lipos did not inhibit the ESR on day 21, which remained above 2 mm/h as in the PBS-treated arthritic control group (fig. 24A).Treatment with DxM-lipos (3 x 1 mg/kg) significantly reduced the ESR by more than 60% ($p \leq 0.05$ compared to AA/PBS) approaching normal levels on day 21 (fig. 24A). The ESR was significantly lower than that after treatment with PBS-lipos ($p \leq 0.01$). In addition, the ESR was reduced to almost normal levels in the chronic phase of AA (day 34) by a single dose of DxM-lipos (1 mg/kg; fig. 24B).

Treatment with Enbrel® significantly reduced the ESR by 65% ($p \leq 0.01$ vs. AA/PBS; fig. 24A) on day 21 and remained numerically lower than in the AA/PBS group on day 34 (data not shown). There were no differences in the ESR between animals treated with DxM-lipos or Enbrel®.
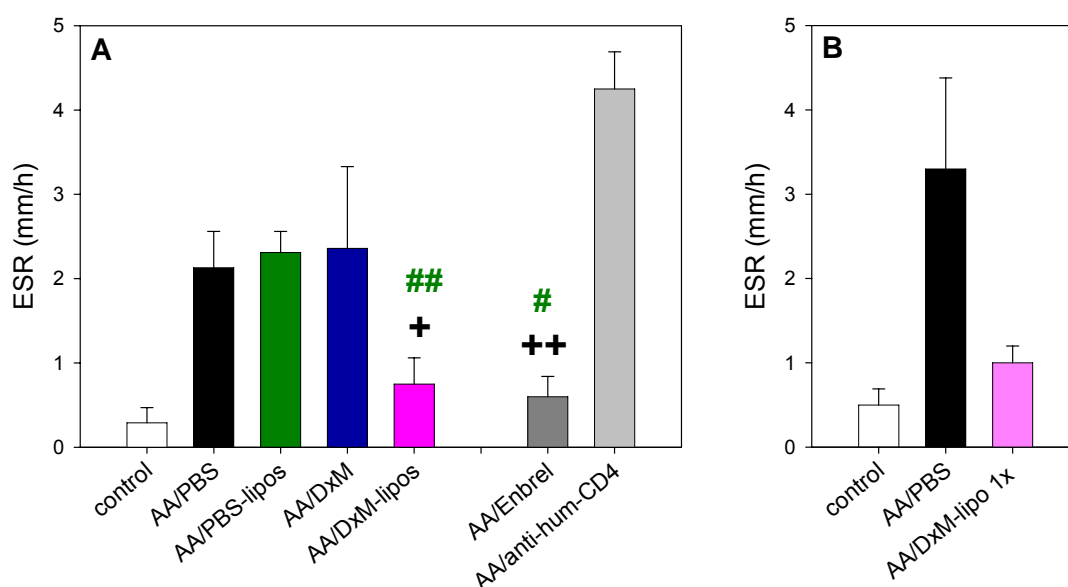

Fig. 24: Erythrocyte sedimentation rate (ESR) on days 21 and 34 of adjuvant arthritis

Effects of treatment with PBS, PBS-lipos, free DxM 3 x 1 mg/kg), DxM-lipos (3 x 1 mg/kg, n = 8) or Enbrel® (2 x 0.3 mg/kg; n = 6) on day 21 (A; expt. 2) or single dose DxM-lipos (1 x 1 mg/kg, n = 6) on day 34 (B; expt. 3)
+ $p \leq 0.05$, ++ $p \leq 0.001$ vs. AA/PBS; # $p \leq 0.05$, ## $p \leq 0.01$ vs. PBS-lipos; Mann-Whitney U-test

5.2.3.2 White blood count and differential leukocyte count

AA was characterized by a systemic leukocytosis on day 21 with a 2.5-fold increase WBC compared to healthy controls ($\approx 5 \cdot 10^9$ cells), and a normalization of WBC on day 34 (fig. 25). PBS-lipos and free DxM only numerically decreased the circulating leukocytes by 20-30%. Inhibition of the leukocytosis by DxM-lipos was significantly stronger than that by PBS-lipos ($p \leq 0.05$; fig. 25A). DxM-lipos completely reduced the leukocytosis in arthritic animals ($p > 0.01$ in comparison to AA/PBS group), leading to a normal WBC ($1.7 \cdot 10^9$ leukocytes). Treatments with

Enbrel® significantly reduced the WBC ($p \le 0.05$ in comparison to arthritic control group), although the inhibition was significantly stronger in DxM-liposomes-treated rats than in Enbrel®-treated rats ($p \le 0.05$)
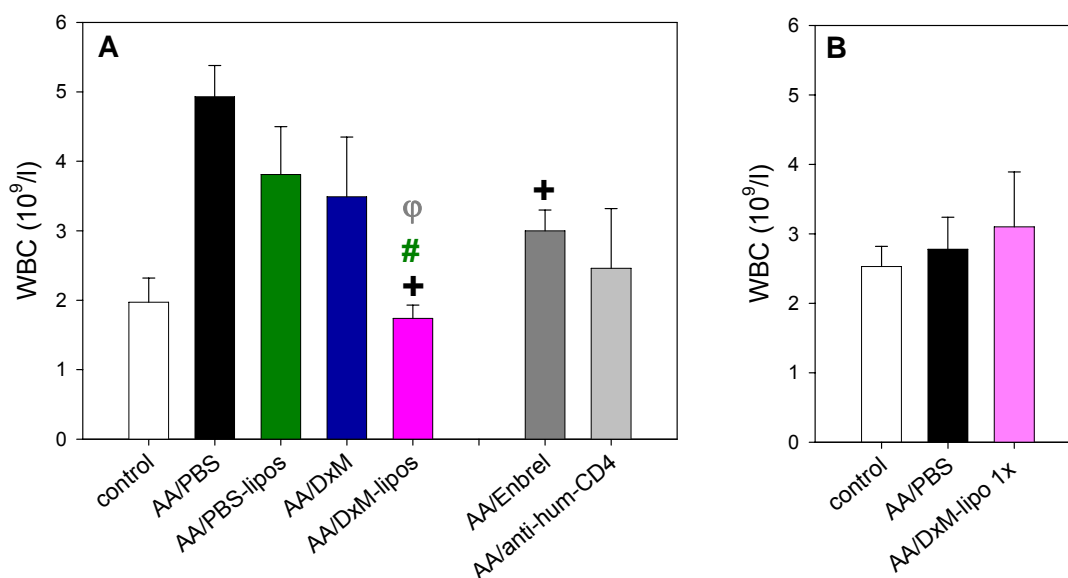

Fig. 25: White blood count (WBC) on days 21 and 34 of adjuvant arthritis

Effects of treatment with PBS, PBS-lipos, free DxM (3 x 1 mg/kg), DxM-lipos (3 x 1 mg/kg, n = 8) or Enbrel® (2 x 0.3 mg/kg; n = 6) on day 21 (A; expt. 2) or single dose DxM-lipos (1 x 1 mg/kg, n = 6) on day 34 (B; expt. 3)
+ p ≤ 0.05, ++ p ≤ 0.001 vs. AA/PBS; # p ≤ 0.05 vs. PBS-lipos; φ p ≤ 0.05 vs. AA/Enbrel; Mann-Whitney U-test

Differential WBC

In addition to the increase of the total WBC (see fig. 26), adjuvant arthritis lead to a significant and relative neutrophilia (i.e., an increase of the PMN from 19% in the control group to 48% in the PBS-treated AA rats) and a corresponding relative lymphopenia (i.e., decrease from 77% in control group to 48% in PBS-treated AA rats; fig. 26A-B). PBS-lipos had no effects on the absolute values or the relative percentages of lymphocyte or PMN. Despite their clear therapeutic efficacy, both free DxM and DxM-lipos lead to a further, significant decrease of the absolute numbers and relative percentages of lymphocytes (down to 33% and 29%, respectively) and the corresponding increase of the relative percentages of PMN and monocytes (up to 57% and 64%, respectively for PMN; fig. 26A-B).

The reduction of lymphocytes and PMN was more effective with DxM-lipos (p ≤ 0.01 for the abs. lymphocyte count, p ≤ 0.05 for the abs. PMN count vs. AA/PBS) than with free DxM (p ≤

0.05 for the abs. lymphocyte count vs. AA/PBS). The lymphocyte percentage was significantly lower after free DxM or DxM-lipos than in PBS-treated AA rats (p ≤ 0.01) and PMN percentages were significantly higher in AA/DxM-lipos and AA/DxM groups vs. AA/PBS (p ≤ 0.01 and p ≤ 0.05 respectively; fig. 26B).
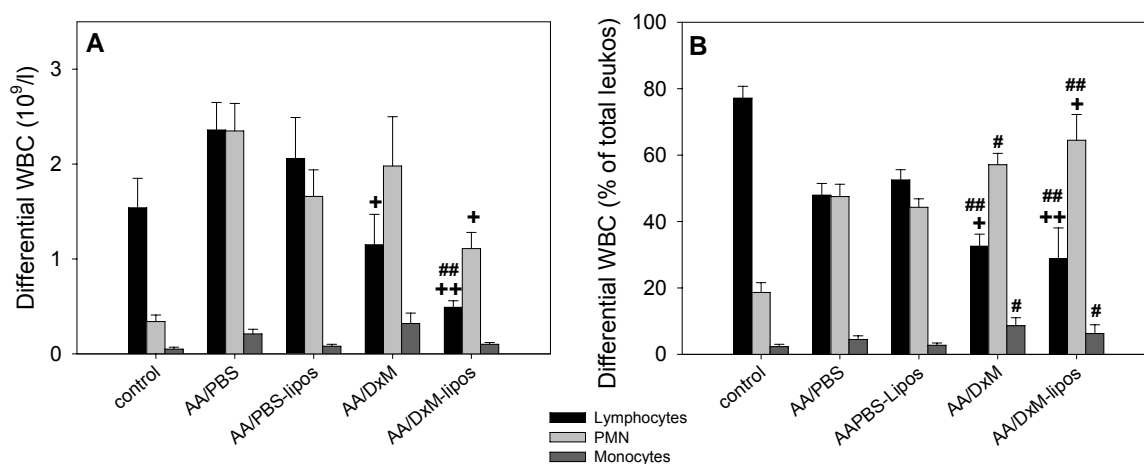

Fig. 26: Differential WBC on day 21 of adjuvant arthritis
Differential WBC in absolute values (A) and relative percentages of leukocytes (B) after treatment with PBS, PBS-lipos, free DxM (3 x 1 mg/kg) or DxM-lipos (3 x 1 mg/kg; n = 8; expt. ,2).
+ p ≤ 0.05, ++ p ≤ 0.01 vs. AA/PBS; # p ≤ 0.05, ## p ≤ 0.01 vs. PBS-lipos; Mann-Whitney U-test.

5.2.4 Immune status

The humoral immune status was monitored by measuring the levels of serum anti-Mb antibodies throughout the experiment. The systemic cellular immunity was evaluated by determining the DTH and by analyzing the total number of lymphocytes in circulating blood and spleen. Local periarticular reactions were measured by determining the total number of lymphocytes in popliteal lymph nodes (pop LN), the first draining lymph node of the affected hind paw joint.

5.2.4.1 Serum anti-Mb-antibodies

Specific antibodies were measured in duplicates in 1:1000 and 1:10,000 diluted sera and the values obtained for arthritic controls on day 17 were set to 100%. The test validity was verified by measuring serum specific antibodies in healthy control rats not injected with Mb, which all showed only a minimal response (≤ 7% +/- 3% ; fig. 27A-B).

Serum anti-Mb-Ab showed a constant increase during the acute phase of AA and then stabilized at a high level in the chronic phase. Animals treated with DxM-lipos had lower levels of specific Ig throughout the entire course of the disease, their quantity was significantly reduced from day 26 onwards and reached normal levels on day 36 (p ≤ 0.01 vs. AA/PBS and vs. AA/PBS-lipos on day 26 and 36; fig. 27A). No significant differences were observed between DxM-lipos and free DxM, although the decrease of serum Ab was more rapid after DxM-lipos therapy (p=0.085 on day 26 vs. AA/DxM). Single dose therapy with DxM-lipos did not significantly the reduce specific antibodies on day 17, but the levels were reduced to some degree on day 34, although not as strikingly as the 3x treatment with DxM-lipos (fig. 27B).
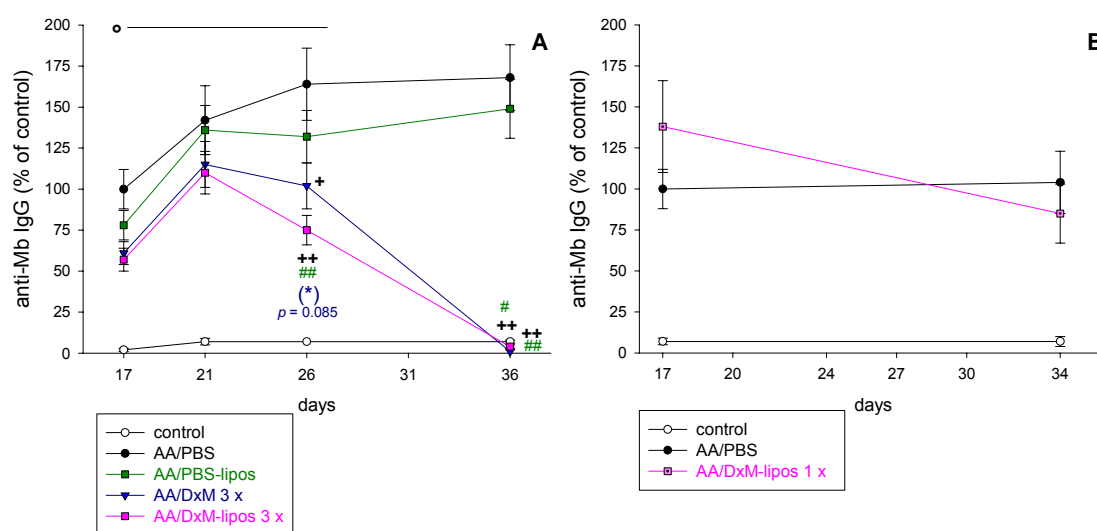

Fig. 27: Specific antibody response on days 17 – 36 of adjuvant arthritis

Levels of specific anti-Mb Ig after treatment with PBS, PBS-lipos, free DxM or DxM-lipos (3 x 1 mg/kg, n = 6; A; expt. 1) or single dose DxM-lipos (1 x 1 mg/kg, n = 6; B; expt. 3)
+ p ≤ 0.05, ++ p ≤ 0.01 vs. AA/PBS; # p ≤ 0.05, ## p ≤ 0.01 vs. AA/PBS-lipos; * p ≤ 0.05 vs. AA/DxM ; o p ≤ 0.05 vs. control; Mann-Whitney U-test

On day 21, the day with the maximal clinical efficacy of DxM-lipos, the specific antibodies were reduced by 20% by both free DxM and liposomal DxM, although there were no significant differences compared to AA/PBS (fig. 28). PBS-lipos and Enbrel® showed no effect on the antibody levels.
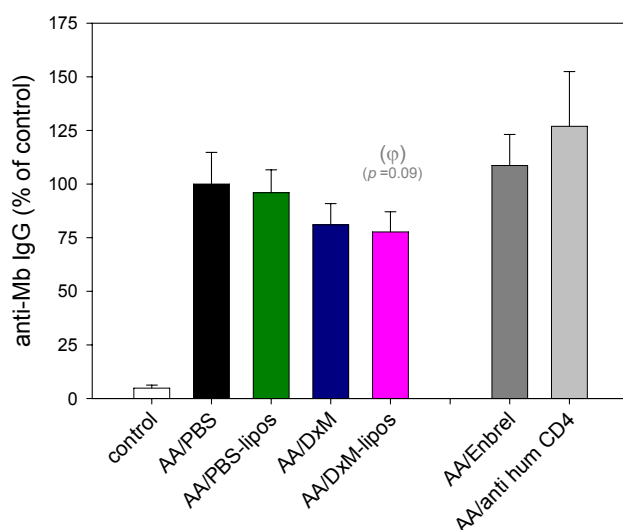
Fig. 28: Specific antibody response on day 21 of adjuvant arthritis

Effects of treatment with PBS, PBS-lipos, free DxM or DxM-lipos (3 x 1 mg/kg, n = 8), or Enbrel® (2 x 0.3 mg/kg; n = 6; expt. 2) φ p ≤ 0.05 vs. AA/Enbrel; Mann-Whitney U-test

5.2.4.2 Delayed-type hypersensitivity

Little reaction was observed 48h after intradermal injection of Mb solution in the ear. The ratio between the left injected ear and the right control ear in PBS treated rats was 1.04 +/- 0.08 (fig. 29). No significant differences were observed on day 21 between healthy animals and arthritic controls. Therapy with PBS-lipos, free DxM, or Enbrel® had no effect on the DTH. Only animals treated with DxM-lipos showed a significantly higher DTH than normal and arthritic controls, with a ratio of 1.42 (p ≤ 0.05; fig. 29).
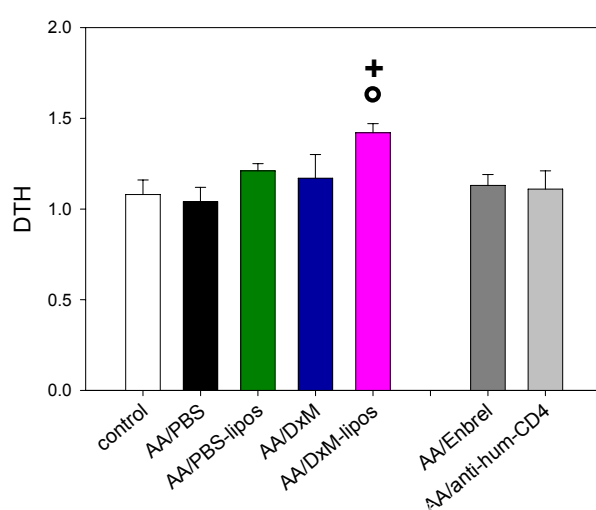

Fig. 29: Delayed-type hypersensitivity (DTH) on day 21 of adjuvant arthritis

Effects of treatment with PBS, PBS-lipos, free DXM or DxM-lipos (3 x 1 mg/kg; n = 8); or Enbrel® (2 x 0.3 mg/kg; n = 6; expt. 2)
+ p ≤ 0.05 vs. AA/PBS; o p ≤ 0.05 vs. control; Mann-Whitney U-test

5.2.4.3 Spleen and lymph node infiltration

Induction of AA resulted in a 3-fold increase of lymphocytes in both spleen and local popliteal LN on day 21.

Spleen lymphocytes:

Free DxM and PBS-lipos had no significant effect on lymphocyte infiltration. Therapy with DxM-lipos significantly reduced the lymphocyte number in the spleen to normal levels (44·10^6 cells; $p \leq 0.05$ vs. AA/PBS & AA/DxM). Enbrel® numerically but not significantly reduced the lymphocyte numbers in spleen (63·10^6 cells; fig. 30B).
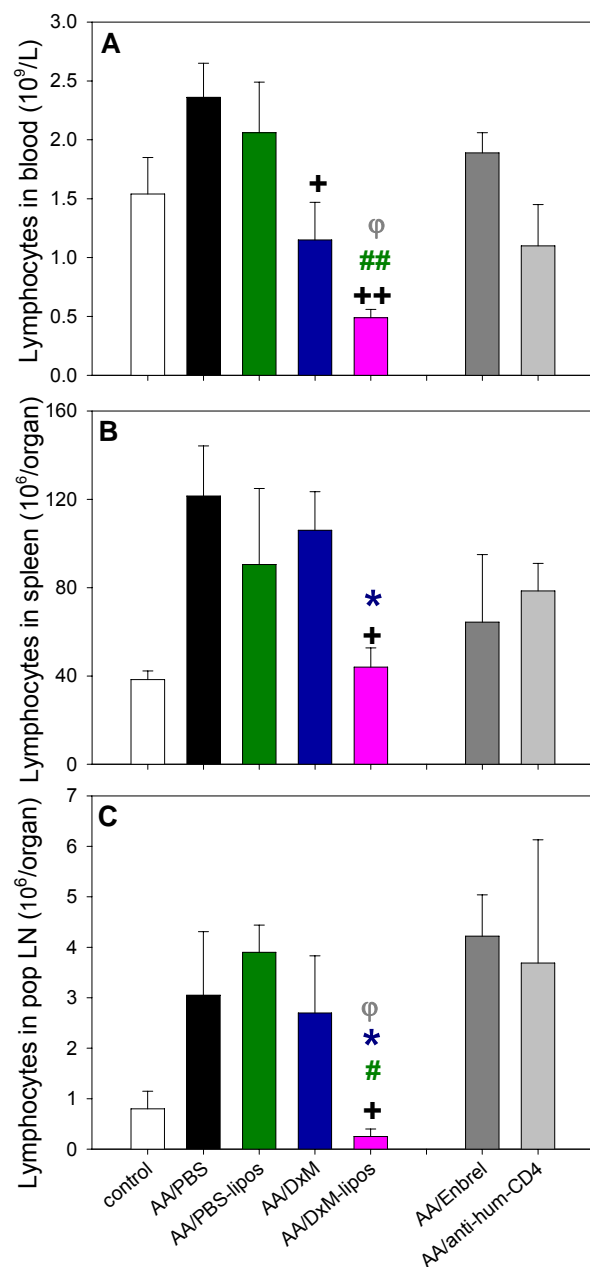

Fig. 30: Effects of DxM-liposomes therapy on lymphocytes on day 21 of adjuvant arthritis

Assessment of lymphocytes in blood (A; n = 8), spleen (B; n = 4) and pop LN (C; n = 4) after treatment with PBS, PBS-lipos, free DxM, DxM-lipos (3 x 1 mg/kg) or Enbrel® (2 x 0.3 mg/kg; expt. 2)
+ p ≤ 0.05, ++ p ≤ 0.01 vs. AA/PBS; # p ≤ 0.05, ## p ≤ 0.01 vs. PBS-lipos; * p ≤ 0.05 vs. AA/DxM ; φ p ≤ 0.05 vs. AA/Enbrel; o p ≤ 0.05 vs. control; Mann-Whitney U-test

Popliteal LN lymphocytes:

PBS-lipos and Enbrel® had no significant effects, beside a slightly increase, on the lymphocyte number in pop LN. Free DxM neither had any effect on the lymphocyte infiltration of pop LN (fig. 30C). Only DxM-lipos treatment prevented the infiltration with lymphocytes in the pop LN (0.25·10^6 cells; $p \leq 0.05$ compared to PBS, PBS-lipos, Enbrel® and even free DxM treated groups), thus achieving numbers of lymphocytes below those of healthy controls (fig. 29C).

Lymphocytes in the blood:

As can be seen from figure A, similar effects were reproduced on circulating lymphocytes: DxM-lipos markedly reduced blood lymphocytes down to $0.49 \cdot 10^9$ cells/l (p ≤ 0.01 vs. AA/PBS & AA/PBS-lipos). Significance also resulted when compared to Enbrel® therapy.

5.2.5 Cytokine production by peritoneal macrophages

Supernatants of non-stimulated and LPS-stimulated peritoneal macrophages (PM), which were obtained from AA rats on day 21 by peritoneal lavage and subsequently stimulated in vitro by LPS, were diluted 1:10 and 1:100 to determine cytokine concentrations. Values of control animals were measured as a reference for the basal production, and in order to evaluate the effects of in vitro LPS stimulation (tab. 17). Unlike for TNF-α and IL-1 β, the IL-6 production did not differ between healthy and PBS-treated AA rats.

Cytokine production of controls (pg/ml)			effect of stimulation
	non-stimulated	LPS-stimulated	x-fold increase
TNF-α	794 +/- 434	2035 +/- 917	2.56
IL-1β	345 +/- 242	4378 +/- 1875	12.69
IL-6	20175 +/- 4849	52557 +/- 13357	2.61

Tab. 17 : Mean cytokine production of controls with or without LPS-stimulation

TNF-α:

No effects on TNF-α secretion were observed in non-stimulated PM; the elevated mean of the Enbrel® group was due to the extremely elevated values of one rat, which were interpreted as an artifact (fig. 31A). In stimulated PM, TNF-α production was reduced by neither PBS-lipos nor free DxM. In contrast, TNF-α secretion was numerically decreased by 40% with DxM-lipos treatment. Only Enbrel® significantly inhibited by 80% TNF-α production (p ≤ 0.05 vs. AA/PBS) reaching normal levels (1095 pg/ml; fig. 31B).

IL-1β:

No significant effects were observed in non-stimulated PM (fig. 31C). IL-1β secretion was numerically reduced by 60% after free DxM treatment and significantly by approximately 70% after PBS- as well as with DxM-lipos treatments (1297 pg/ml and 956 pg/ml respectively; p ≤ 0.05 vs. AA/PPS) in stimulated PM (fig. 31D). Enbrel® therapy also resulted in a significant inhibition of IL-1β production (166 pg/ml; p ≤ 0.01 vs. AA/PPS).

IL-6:

PBS-lipos significantly reduced the IL-6 secretion in non-stimulated PM (7300 pg/ml; $p \le 0.05$ vs. AA/PBS), while no effect was achieved by free DxM (fig. 31E). Treatment with DxM-lipos as well as with Enbrel® significantly reduced the IL-6 production (4866 pg/ml and 1692 pg/ml respectively; $p \le 0.01$ vs. AA/PBS). Similar effects were reproduced in LPS-stimulated PM (fig. 31F). Reduction of IL-6 secretion by PBS-lipos approached statistical significance ($p \le 0.06$), and was significantly inhibited by Enbrel® (24072 pg/ml; $p \le 0.01$ vs. AA/PBS). DxM-lipos also significantly reduced IL-6 production (15619 pg/ml; $p \le 0.01$ vs. AA/PBS), and they were significantly more efficacious than free DxM ($p \le 0.05$; fig. 31F).
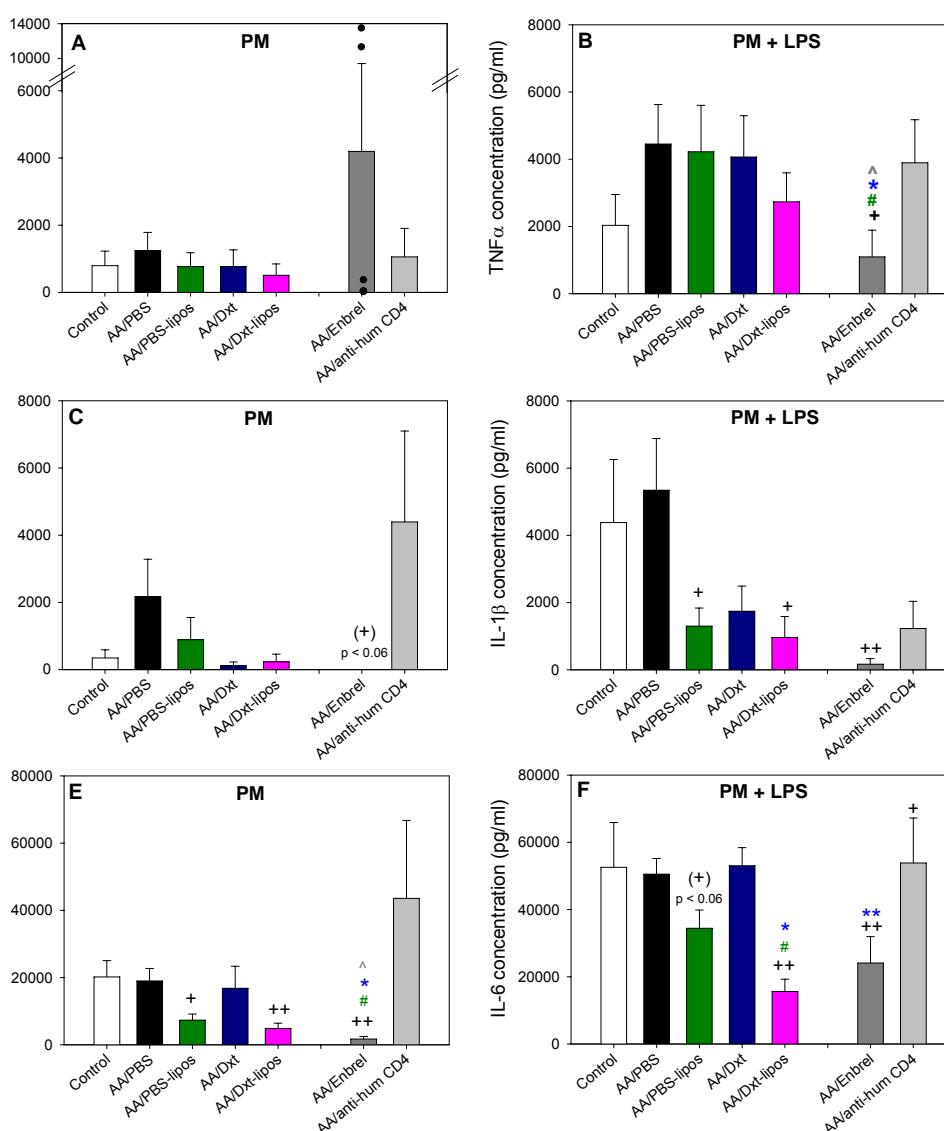
Fig. 31: Cytokine production by peritoneal macrophages on day 21 of adjuvant arthritis
TNF-α (A-B), IL-1β (C-D) and IL-6 (E-F) production by non-stimulated and LPS-stimulated peritoneal macrophages (PM) after treatment with PBS, PBS-lipos, free DxM, DxM-lipos (3 x 1 mg/kg) or Enbrel® (2 x 0.3 mg/kg; n = 4; expt.2).
+ p ≤ 0.05, ++ p ≤ 0.01, (+) p ≤ 0.06 vs. AA/PBS; # p ≤ 0.05 vs. AA/PBS-Lipos; * p ≤ 0.05, ** p ≤ 0.01 vs. AA/DxM ; ^ p ≤ 0.05 vs. anti-human CD4 mAb; Mann-Whitney U-test.

6. DISCUSSION

6.1 Incorporation of DxM-liposomes by macrophages

The aim of using encapsulated DxM as anti-Mφ drug was to increase the DxM uptake by the target cells after systemic i.v. application. Therefore, the features of the liposome vehicle were optimized for enhanced phagocytosis. According to previous studies (Katragadda et al. 2000), the liposomes used in the present study showed optimal characteristics for Mφ uptake, i.e., a negatively charged, PEG-free surface, a DPPC containing bilayer, and a mean size below 200 nm, which is known to accumulate to a greater extent in inflamed joints than larger liposomes (Lowe et al., 1989). Although PEG-ylation is known to decrease the elimination of liposomes from the peripheral blood by the reticulo-endothelial system and thereby to increase the half-live of liposomes in circulation, and, consequently, their accumulation in inflamed joints (Harris and Chess, 2003), PEG-ylation was avoided in this study because of the known induction of allergical and complement activation by PEG-ylated liposomes (Metselaar, 2003). In addition, better anti-inflammatory results were achieved with PEG-free liposomes in previous studies (Schulte, 2003). Fluorescence microscopy images and previous quantitative assays with radioactively labeled liposomes confirmed liposome phagocytosis by Mφ, especially during the first hours of co-incubation in vitro (Schulte; 2003). Both evaluations were performed after thoroughly rinsing the cells in order to avoid false positive results due to loose binding of the liposomes to the Mφ surface.

After in vitro incubations over 24 h with DxM- or with PBS-lipos, no increased cell death was detected; proving the optimal tolerability of both liposome formulations and DxM, and distinguishing them from the cytotoxic effects observed with clodronate-containing liposomes (Richards et al., 1999; Pertermann, 2002). These results confirmed previous studies from our group as well as from other laboratories (Foxwell et al.,1998). We can therefore assume normal cell viability under cell culture conditions and in vivo, despite the fact that GC's induce apoptosis in certain cell types, e.g., activated human peripheral blood lymphocytes (Lanza et al, 1996) or human monocytes (upon incubation with $10^{-6}\mu M$ DxM; Schmidt et al., 1999). This suggests that our in vitro and in vivo results are based on the modulation of molecular functions

rather than on the induction of cell death, consistent with previous descriptions (Yokoyama et al., 1985).

6.2 DxM-liposomes reduce pro-inflammatory effector molecules of macrophages in vitro

In order to avoid loss of Mφ vitality or function, as previously described in our group (Schulte, 2003), all buffy coats and peritoneal macrophages (PM) were processed within 4 h of blood withdrawal or cell harvesting, a time beyond which molecular functions decrease considerably and microarray results can be altered.

In RA, TNF-α is mostly produced by Mφ and believed to be the proximal cytokine in the inflammatory cascade, followed by IL-1β, which mediates most of the articular damage and is also predominantly expressed by Mφ. In addition, elevated levels of IL-6 and NO in synovial fluid are mainly due to Mφ secretion, and the chemoattractants IL-15, and IL-18 assure an auto-activation of these phagocytes (Kinne et al., 2000). The effect of DxM-lipos on the gene expression of these main pro-inflammatory effector molecules has been studied previously using conventional methods (Schmidt, 2001; Pertermann, 2002 and using the same liposome formulation: Schulte, 2003). In the present study, these results were reproduced. The gene expression of TNF-α, IL-1β, IL-6, IL-15, and IL-18 in LPS/IFN-γ stimulated Mφ was significantly reduced by approximately 50% after in vitro pre-incubation with DxM-lipos, and DxM-lipos proved significantly more potent than drug-free PBS-lipos, while the reduction of IL-10 expression by both types of liposomes was similar. This cytokine, believed to function as an anti-inflammatory mediator, may, in the presence of MSCF, contribute to the differentiation of monocytes into TNF-α responsive Mφ in RA (Takasugi et al., 2006), and is therefore an interesting target for anti-inflammatory therapy.

In order to broadly analyze the regulation of gene expression and better understand the mechanism of action of DxM-lipos, we performed a microarray analysis with the RNA of human monocytes, from three healthy donors, in each case after pre-incubation with DxM-lipos and subsequent stimulation.

Cell culture and processing of RNA met all the requirements for good-quality arrays: 1) monocyte isolation within 4 h; 2) sufficient quantity of total RNA in all samples and; 3) fulfilled

criteria of quality control at different stages of RNA processing (Dumur et al., 2004). Despite optimal processing, the chip results displayed a considerable variability between the different arrays. In addition, the gene expression level of the negative control pool was already quite high, and, therefore, the calculated fold-changes of the gene expression in non-stimulated vs. stimulated monocytes (+/- pre-incubated with liposomes) did not achieve the expected levels (Stuhlmüller et al., 2000). Since the monocytes are derived from donors who, despite of being healthy, are continuously facing exogenous and endogenous stimuli, this biological variability cannot be totally excluded. Furthermore, the low number of analyzed chips (n = 3 for each incubation mode) caused an additional problem for the statistical analysis. The expression of genes, whose measured fold-changes between stimulated and DxM-lipos pre-incubated monocytes seemed relevant, was statistically analyzed by means of the Mann-Whitney U-test. Despite these difficulties, we were able to identify a number of genes relevantly over- or under expressed after DxM-lipos incubation, some of which showed statistically significant differences. The most markedly down-regulated genes belonged to the large family of cytokines, i.e., TNF-α, IL-6, IL-1α, IL-1β, its receptor IL-1R1 and its endogenous inhibitor IL-RA, all well-known monocyte/macrophage mediators. Apart from IL-1α and IL-1R1, the decrease of expression by DxM-lipos was statistically significant and also validated by PCR. Other down-regulated genes of interest include: 1) receptors like the chemokine receptor CCR5, known to be increased in both synovial and peripheral blood monocytes in RA (Nissinen et al., 2003) and the complement receptor C1R; 2) growth factors such as the colony stimulating growth factor 2 (CSGF-2), connective tissue growth factor (CTGF) and heparin-binding elongation growth factor (HB-EGF); 3) the cell interaction molecule HLA-DR; and 4) enzymes such as the constitutively induced cyclooxygenase 1 (COX-1). Most of the genes showing a relevantly down-regulated expression after incubation with DxM-lipos have been identified by microarray analysis, as over-expressed in monocytes/macrophages: 1) in activated circulating monocytes from RA patients (TNF-α, IL-6, IL-1β, COX-1; Stuhlmüller et al., 2000), 2) in GCTS (= giant cell tumor supernatant which contains MCSF, GMCSF, IL-1 and IL-6) stimulated, monocyte-derived macrophages (TNF-α, IL-6, IL-1β, CTGF, COX; Albright and González-Scarano, 2004); or 3) in joint extracts of mice in different arthritis models (TNF-α, IL-6, IL-1β, IL-1α, CCR5, C1R, CSGF, CSGF, HLA-DR; Fujikado et al., 2006), pointing out their importance in arthritic diseases.

From the fold-change evaluation of microarray data, we were also able to list a number of genes that seemed to be relevantly induced by DxM-lipos incubation: 1) membrane receptors, such as the human IgG Fc-receptor and the adenosine A3-Receptor; 2) the leukocyte adhesion and migration molecule thrombospondin-1, newly appreciated as a negative regulator of the

production of TNF-α and other cytokines (Doyen et al., 2003); and 3) various intracellular signaling molecules such as IκB, known to be induced by GC's and inhibit nuclear translocation of NF-κB (Auphan et al., 1995), MAP2K1, and protein kinase C. In contrast, the increased expression of IL-15 was not confirmed by our PCR results.

All significant results of microarray analysis were validated with conventional methods (conventional PCR). Some genes, whose expression was not significantly reduced in the array, showed statistically significant modulation in PCR studies (IL-15 and IL-18). In such discrepant studies, established PCR methods are usually accepted as the gold standard to quantitatively evaluate the expression of individual selected genes. Nevertheless microarray analysis, when applied as a screening method, may give a more complete overview of gene activation and inhibition patterns in disease and/or upon therapy and allow to clearly focus subsequent validation studies.

The protein levels of cytokines revealing a significant decrease in mRNA expression (in validating PCR measurements) after DxM-lipos incubation, were determined by ELISA. Consistent with previous studies (Schulte, 2003) and the mRNA expression results, the secreted amounts of TNF-α and IL-6 were significantly reduced, those of IL-10 numerically reduced by DxM-lipos compared to the amounts produced by only stimulated monocytes. Interestingly, IL-1β was not detected in the supernatants of non-stimulated or stimulated monocytes. This may indicate that IL-1β remains in the cytoplasm of the stimulated cells, since cell lysate was not analyzed, or that the translation of mRNA was less efficient than in Mφ (Herzyk et al., 1992). A technical failure was excluded by positive detection of the IL-1β standard.

A clear discrepancy was observed for DxM-lipos between their in vitro and in vivo efficacy in inhibiting the production of TNF-α, IL-1β, and IL-6. The secretion of all three cytokines was reduced to a greater and more significant extent in vivo (PM) than in vitro (monocytes). Several arguments can be used to explain these differences: 1) monocytes and Mφ differ in the regulation of signal transduction pathways (Westra, 2005), 2) in complex diseases like RA, further parameters can influence and promote the efficacy of DxM-lipos in vivo (e.g., over-expression of adenosine receptors may increase the cytokine instability induced by GC's; Fishman et al., 2006); and 3) PM from rats with antigen-induced arthritis and other arthritides are in a pre-activated state (Nissler at al., 2004) and may thus be more susceptible for the action of DxM-lipos.

6.3 Efficacy of DxM-liposomes in vivo

6.2.1 Suppression of joint and periarticular inflammation

AA is known to be a very severe experimental model displaying both systemic and local features, and showing a number of histopathological similarities to RA (Billingham, 1995). The treatment was started on day 14, when the severity of the disease had reached approximately 50% of the maximal level in PBS-treated arthritic controls, thus, treatment was performed in analogy to the clinical situations in RA, in which DxM-lipos treatment would represent a therapeutic rather than a preventive measure. Considering the relative potency of dexamethasone compared to prednisolone (approx. 4 fold), the maximum dose administered in the present study (1 mg/kg/d ≈ 2.5 mg/kg/d predisolone) approaches the therapeutic doses of prednisolone used in RA, i.e., 1,5 mg/kg/d for high dose therapy or 3 mg/kg/d i.v. for pulse therapy (Mahajan and Tandon, 2005).

Therapy with 3 x DxM-lipos in acute stages of AA (days 14-16) significantly suppressed joint swelling and periarticular inflammation in the acute phase by over 90% and in chronic phase by 60%. The anti-inflammatory effects lasted for more than 2 weeks after the end of treatment. These results were not only reproduced in all experiments (expt. 1, 2 and 4), but even the difference compared to treatment with the same dose of free DxM was significantly reproduced in all series, showing the reliability of the results. The same dose of free DxM only had a short-lasting anti-inflammatory effect, showing that encapsulation enhances and prolongs the anti-inflammatory effects of DxM. Previous studies performed in our group (3 x 1 mg/kg of identical DxM-lipos in rat antigen-induced arthritis) similarly showed a significant and long-lasting reduction of clinical parameters by DxM-lipos and confirmed the differences in therapeutic efficacy in comparison to the same dose of free DxM (Schulte, 2003).

Effects of non-specific joint targeting with liposomally encapsulated glucocorticoids has been investigated repeatedly with different GC in different arthritis models. Treatment with 100 µg betamethasone sodium in PGLA nanoparticles, for example, reduced the paw volume in rat adjuvant arthritis by 30% (Higaki et al. 2005). However, single administration of our non-PEG-ylated DxM-lipos reduced the joint swelling by more than 60%. In addition, administration of a single dose of DxM-lipos and of 3 x free DxM showed a comparable clinical course and reduction of arthritis parameters. Correlations between the swelling on day 19 and 14 confirmed this observation and the similarity between the gradients of both regression lines indicate that the liposomal vehicle may permit a dose reduction by at least a factor of 3. The

same dose reduction by encapsulating betamethasone sodium phosphate in PLGA nanoparticles was recently described (Higaki et al. 2005). Furthermore, a strong remission for more than 1 week after a single dose of 10 mg/kg prednisolone-phosphate encapsulated in PEG-ylated liposomes has been shown in rat adjuvant arthritis (Metselaar et al, 2003) and murine collagen type II arthritis (Metselaar et al., 2004). Therapeutic effects of free prednisolone were only achieved using a 10-fold increased dose, a finding also indicating the possibility of considerably reducing the therapeutically efficacious dose by liposomal encapsulation and PEG-ylation. In the present study, dose reduction studies with 3 administrations showed a strongly dose-dependent efficacy of DxM-lipos, with the effects of 1 mg/kg being significantly stronger than those of 0.01 mg/kg, and even 0.1 mg/kg. By judging the long-term effects (day 28), the anti-inflammatory effects of DxM-lipos at 3 x 0.1 mg/kg were stronger than those of free DxM at 3 x 1 mg/kg (reduction of the paw volume was 36% and 23% respectively; reduction of the arthritis score by 28% and 27% respectively), also suggesting a 10-fold increase of DxM efficacy by encapsulation. Furthermore, differences between DxM-lipos and free DxM concerning the clinical efficacy augmented with rising DxM concentrations (additional reduction of the arthritis score on day 19 in DxM-lipos compared to DxM-treated animals was of 10%, 13%, and 27% for treatments with 0.01 mg/kg, 0.1 mg/kg, and 1 mg/kg, respectively), leading to highly significant differences between both treatments at high concentrations.

To our knowledge, this is the first evidence of a nearly 100% remission and a prolongation of the therapeutic benefit over approx. 14 days in the severe model of AA with a dose of 1 mg/kg DxM encapsulated in non-PEG-ylated liposomes, and injected for 3 consecutive days. Avnir et al. (2008) tested their PEG-ylated, methylprednisolone remote loaded liposomes (size 80 nm) in AA by administering 3 x 10 mg/kg on days 10, 14, and 18, achieving a long-term suppression of the arthritis score over 18 days. However, treatment in this study was initiated at a much earlier stage of the disease (day 10), i.e., immediately after the first onset of clinical signs. Such early or preventive treatment is usually more effective than therapy at later steps of arthritis (Yoshino et al., 1990; Billingham et al., 1990).

In order to asses the long-term benefit of short-term therapy with DxM-lipos, we evaluated histological sections of the affected joints and were able to confirm the amelioration of clinical parameters also at the microscopic tissue level, with a significant reduction of histology score. Chronic inflammation is a sign of the severe acute inflammation the joint was submitted to

during the clinical outbreak of AA. The minimal presence of acute inflammation confirms the efficacious suppression of the active inflammatory process in the affected joints by DxM-lipos. Lack of bone and cartilage destruction after treatment with DxM-lipos could result from a prompt therapeutic response to therapy. The effects of free DxM were similar to those of DxM-lipos, which we attribute to the early stage at which the joint extraction was performed (day 21), therefore the clinical rebound effect observed with free DxM on day 19 may not yet have significantly affected the joint structure. Similar protective effects on joint destruction after non-specific targeting of the inflamed synovial membrane have also been described (Metselaar et al., 2004 and Higaki et al., 2005), or after treatment with clodronate liposomes (Richards et al., 1999); in the latter case the effect was attributed to Mφ elimination (Kinne et al., 1995). Knowing that cartilage and bone destruction is directly (Tetlow et al., 1993; Mulherin et al.,1996; Kinne et al. 2000) or indirectly mediated by synovial Mφ, for example via TNF-α, IL-1β, or IL-6 mediated stimulation of fibroblasts (Scott et al., 1997), our histological findings may reflect the inhibition of both Mφ activation and secretion of pro-inflammatory mediators. We were also able to identify osteoclasts, cells derived from the myelomonocytic linage, strongly contributing to bone erosion (Gravallese et al., 1998), in preparations of PBS- or PBS-lipos-treated AA rats, but not in DxM- or DxM-lipos-treated animals. Gross bone deformations in PBS- or PBS-lipos-treated AA rats, prove the aggressiveness and the severity of the disease and also explain the persisting high levels of paw volume throughout the studies (until day 36), which is in contrast to the decreasing arthritis score in chronic stages of AA.

Interestingly, lymphocyte infiltration was markedly reduced in the draining popliteal LN, where total lymphocyte depletion was significantly more prominent after DxM-lipos therapy than after any other treatment. In other words, DxM-lipos reduced the activation of the popliteal LN, a regional mediator of disease and inflammation (Schmidt-Weber, 1999).

6.2.2 Systemic effects

In order to address the question whether DxM-lipos influenced systemic Mφ activation in AA (Johnson et al., 1986), we investigated a number of hematological and immunological parameters. The ESR as well as total and differential WBC were significantly decreased to almost normal levels by DxM-lipos therapy during acute and chronic AA (day 21 & 34), whereas free DxM induced little or no amelioration in systemic inflammation parameters, suggesting an enhanced and prolonged suppression of systemic inflammation in AA by DxM-lipos. The reduction of the ESR by DxM-lipos, which is largely determined by the concentration

of fibrinogen, may be due to direct inhibition of fibrinogen synthesis in the liver, or indirect inhibition via reduced levels of IL-6, IL-1β, and TNF-α, or even to decreased levels of circulating antibodies (Boss and Neeck, 2000; Paulus and Brahn, 2004).

Although leukocytosis in AA was determined by an increase of PMN, reduction of WBC, by both free DxM and DxM-lipos was primarily based on a significant decrease of circulating lymphocytes, an effect achieved to a greater extent by the encapsulated form. Total lymphocytes were reduced to levels below 50% of those in healthy controls ($p \leq 0.01$), suggesting that lymphopenia may be the result of direct GC side effects in addition to indirect effects via Mφ inactivation. GC's, in particular DxM-P, are known to strongly diminish the number of lymphocytes in peripheral blood via two mechanisms (Hochhaus et al., 2001): 1) induction of cell apoptosis; and 2) redistribution to spleen, lymph nodes, bone marrow, and perivascular compartments. However, our results demonstrated significantly lower numbers of lymphocytes in lymphoid organs (systemically in the spleen and locally in the draining pop LN) after DxM-lipos therapy, suggesting that migration to spleen and LN did not occur or only in combination with increased lymphocyte apoptosis at these sites. Since the number of lymphocytes in blood and popliteal LN were reduced (significantly in the case of blood lymphocytes) to levels below those of normal healthy rats, both apoptosis and altered migration to perivascular compartments may contribute to the lymphopenia observed after therapy with free or encapsulated DxM.

Other studies in our group showed high accumulation of DxM-lipos in spleen and lymph nodes after systemic administration in AIA (higher opsonization of non-PEG-ylated liposomes by the reticulo-endothelial system), which may be at least responsible for the systemic effects of DxM-lipos also in AA. The anti-inflammatory effects of DxM-lipos were more pronounced in the pop LN than in the spleen, possibly reflecting the stronger activation of Mφ in the pop LN of AA rats (Schmidt-Weber et al. 1999).

Modulation of cell-mediated immunity was also assessed by evaluating the delayed-type hypersensitivity (DTH) skin response to the arthritogenic Mb, an in vivo parameter of the Th1-dominant immune response (Cher and Mossmann, 1987). Previous AA studies had demonstrated that the DTH peaked a few days before the maximum of arthritis (Schmidt-Weber et al., 1999). In our studies, the DTH was significantly increased on day 21 after DxM-lipos treatment. This augmented cellular response could on one hand be interpreted as a delayed onset of the clinically relevant T-cell response (Schmidt-Weber et al., 1999). On the other hand, DxM-lipos may have induced a shift of the Th1/Th2 balance in AA (Schmidt-Weber

et al. 1999) in favor of the protective T cell reactivity for example by modulating the Mφ cytokine pattern (Mosser, 2003) and inducing a "regulatory" Th1 type DTH (Yang, 2001).

In order to investigate the modulation of the humoral immunity by DxM-lipos, we measured the levels of specific anti-Mb antibodies in rat serum throughout the time course of AA. Interestingly DxM-lipos, as well as free DxM, induced a significant immune suppression after day 21. The delay compared to the effects on the cell mediated immunity is likely due to half-life of the circulating antibodies and the interval needed for modulation of B-cell functions.

To our knowledge this is the first study which reports on the effects of systemic application of a Mφ -targeting drug on PM, cells which are not directly in contact with the circulating blood. Secretion of pro-inflammatory cytokines in non-stimulated or LPS-stimulated PM was significantly (IL-1β and IL-6) or numerically (TNF-α) inhibited by i.v. treatment with DxM-lipos, while only IL-1β was numerically reduced in rats treated with free DxM. This may be due to enhanced extravascular accumulation of the liposomes in the peritoneal cavity, while free DxM distributes rather evenly in different body compartments. In previous studies from our group, indeed, we evidenced the opposite liposome migration, i.e., local anti-inflammatory effects were observed in arthritic joints after intra-peritoneal application of DxM-lipos.

It is interesting to note that DxM-lipos treatment had little effect on TNF-α secretion by PM, suggesting that in this model, if the results from PM are transferable to the arthritic joints (Schmidt-Weber et al., 1999), clinical improvement may not be primarily mediated by reduction of TNF-α but rather by reduction of IL-1β and IL-6. These results do not agree with those achieved in vitro with human peripheral blood monocytes (see above), in which suppression of TNF-α was equal to that of IL-6. However, similar discrepancies between the cytokine production in monocytes and monocyte-derived macrophages have been reported previously (Westra, 2005).

At this point, the question arises whether encapsulation of DxM is safe and whether it decreases or augments side-effects. The aim of this Mφ -targeting vehicle system is to reduce the systemic side-effects of the encapsulated drug. For this purpose, we monitored the body weight of the animals during the time course of AA. The administration of 3 x 1 mg/kg DxM-lipos transiently reduced the body weight, which was significantly lower than in animals treated with free DxM on day 18. This loss of body weight has been described as a rat-specific side-effect of GC (observed at doses above 0.05 mg/kg DxM), mediated by a decreased ribosomal amino acid incorporation in muscle cells (Elliott et al. 1971), and possibly related with relatively

high plasma levels of released DxM (Metselaar, 2003). In addition, a certain extent of cell-mediated as well as humoral immune suppression was induced by DxM-lipos. While the suppression of specific antibodies by DxM-lipos was not stronger than that induced by free DxM, lymphopenia in periphery blood, spleen and popliteal LN was significantly increased after treatment with the encapsulated drug. No other adverse effects were observed in our studies. However, parallel experiments performed in our group with DxM-lipos in mouse CIA, showed that i.v. administration of 4 mg/kg DxM-lipos (comparable to our total dose of 3 mg/kg) did not reduce the endogenous cortisol levels, while the equivalent clinically effective dose of free DxM significantly suppressed endogenous cortisol production. Similar results were observed after intraarticular injection of large-sized or small-sized DxM-palmitate liposomes in AIA (Bonanomi et al., 1987). Therefore our studies suggest that despite systemic administration of DxM-lipos, intravasal DxM levels were low enough not to induce suppression of the hypothalamic-adrenergic axis. Nevertheless, blood DxM levels, as well as kidney and liver function parameters should be measured in future studies to evaluate a possible leakage of DxM from the liposome and to exclude further side effects.

6.4 Comparison to Enbrel®

To our knowledge, this is the first time that the effects of Enbrel® on rat AA have been directly studied. In RA, Enbrel® is given twice a week at a dose of 25 mg (approx. 0,3 mg/kg). In analogy to the treatment with DxM-lipos we administered the human dose s.c. on days 14 & 17, which showed to be completely ineffective against the clinical manifestation of the disease, forcing us to augment the second dose by a factor of 10 in half the animals (3mg/kg); this dose ameliorated the clinical parameters to a slightly higher degree (data not shown). Therapy with DxM-lipos was significantly more effective than anti-TNF-α treatment in AA, however, these results have to be reproached with a question of doubt, since the affinity of Enbrel® to human and rat TNF-α considerably differs. While human TNF-α binds to its receptor as well as to Enbrel® as a trimer (Eck und Sprang, 1989), rat TNF-α seems to bind to Enbrel® as a monomer (Biacore analysis performed by Dr. Hortschansky, HKI, Jena). In contrast, bone and cartilage destruction was significantly reduced after Enbrel® treatment, which points to a possible correlation between synovial TNF-α levels and bone/cartilage erosion (Neidel et al., 1995).

Although Enbrel® failed to significantly influence local joint swelling, positive systemic effects were achieved in the acute phase of AA. Both ESR and WBC were significantly reduced by Enbrel® on day 21; in contrast, the number of lymphocytes in the pop LN was not altered, confirming that Enbrel® had little effect on peripheral sites of inflammation, at least in the present concentrations. The cytokine production in LPS-stimulated PM was significantly reduced by Enbrel®, achieving similar effects as DxM-lipos. As an exception, TNF-α secretion, was only effectively inhibited after Enbrel® therapy. This could be due to an interrupted autocrine stimulation of the PM by endogenous TNF-α through the specific TNF-α receptor.

In summary, the results of systemic parameters and histology proved that Enbrel® did not remain completely ineffective, however, both the reduced binding capacity of Enbrel® to rat TNF-α and a limited pathophysiological importance of TNF-α in the rat AA model may have prevented more profound inhibitory effects of Enbrel® in this model.

6.5 Dual effects of the liposomal vehicle

In order to evaluate the effects of the liposomal vehicle, PBS-containing liposome with matched lipid concentration were tested in all experiments.

Empty, drug free liposomes were not only inefficient in suppressing arthritis, but sometimes showed a slight pro-inflammatory effect in acute and chronic stages of the disease (especially after day 26) and a numerically increased number of lymphocytes in the local pop LN. Previous studies in our group reported a slightly augmented cell death rate in PM incubated with PBS-lipos (Schulte, 2003). These observations were related to the increased phagocytosis of PM compared to PBMC, resulting in greater intracellular lipid accumulation. Similar observations were reported after intramucosal injection of non-PEG-ylated DPPC/Chol liposomes, producing a local and transitory Mφ reaction (Foong et al, 1989). PEG-ylated liposome formulations are known to induce allergic reactions (Albert and Garcia, 1997; Uziely et al., 1995), possibly as a result of complement activation (Szebeni, 2001). However, evidence has shown that, among other factors, liposome size also plays a key role in complement activation. Non-PEG-ylated DSPC/Chol liposomes with a mean diameter of more than 90 nm, induced complement activation (Metselaar et al., 2002), while liposomes with the same composition but a smaller mean size (65 nm) were free of allergic properties. These findings may explain the augmented inflammation and lymphocyte numbers in pop LN observed with PBS-lipos in our studies (200

nm mean size).There have been recent attempts to prevent this lipid toxicity by increasing the drug-lipid ratio, and therefore decreasing the amount of administered liposomes (Avnir et al. (2008).

Interestingly, the expression of the chemoattractant IL-15 was radically increased (3.5 fold) by PBS-lipos in PCR studies, which may promote lymphocyte recruitment in vivo (McInnes et al. 1996) and Mφ stimulation (Badolato et al., 1997), and may therefore be responsible for the numerically increased inflammation compared to PBS-treated arthritic controls. On the other hand, high concentrations of empty liposome vehicle significantly decreased NO secretion, as well as IL-6 expression and production in both Mφ and stimulated PM, indicating some anti-inflammatory properties of drug free liposomes.

Considering these stimulating effects of the liposomal vehicle, which were restricted to the inflamed regions, the anti-inflammatory efficacy of DxM-lipos demonstrates the enhancement of the therapeutic potential of DxM by encapsulation. The fact that the pro-inflammatory reactions to the lipid stimulus were restricted to the local inflammation sites may be due to the presence of activated Mφ, with a higher uptake of liposomes. Increased phagocytic activity in inflamed joints may be triggered by lyso-phosphatidylcholine, a hydrolysis product of liposomal DPPC through phospholipase A, which significantly increases Mφ ingestion (Morito et al., 2000)

7. CONCLUSIONS

The liposomal formulation used in the present study showed high uptake by and lack of toxicity in circulating monocytes/macrophages. This biocompatibility was an essential prerequisite for further *in vitro* and *in vivo* studies

In the fist phase of the study we performed microarray analysis in human monocytes pre-incubated with PBS-lipos or DxM-lipos and subsequently stimulated with LPS/IFN-γ. We obtained a general overview of genes up- or down- regulated by DxM-lipos, identified those which were significantly down-regulated, and successfully validated them with conventional RT-PCR. We conclude that microarray analysis is well suitable as a general screening method to identify relevant gene expression patterns in disease or upon therapy, and that it helps to select individual target genes for validation with more specific and reliable methods (e.g., RT-PCR). In addition, we confirmed that DxM-lipos efficaciously inhibited the production of key pro-inflammatory effector molecules for RA in monocytes/Mφ, both at the mRNA and the protein level.

In our *in vivo* studies, we achieved a pronounced (over 90% reduction) and long-lasting (for more than 14 days) suppression of <u>established</u> rat AA with 3 x 1 mg/kg DxM-lipos treatment, which was confirmed at a clinical and histological level. This prompt anti-inflammatory effect of DxM-lipos would be optimal to control RA flares and the resulting progress of joint deformation. In addition, we demonstrated the superior therapeutic efficacy of our DxM-liposome formulation over that of free, non-encapsulated DxM, both in early and advanced disease stages. With 1 administration of 1 mg/kg DxM-lipos we achieved a 3-fold dose reduction, while in the case of 3 administrations an at least 10-fold dose reduction was obtained. Furthermore, DxM-lipos significantly reduced the systemic activation of monocytes/Mφ in peripheral blood and peritoneal cavity, possibly contributing to the therapeutic benefit in vivo. No relevant side-effects were observed, apart from a partial suppression of the humoral immune response, which is in contrast to the increased T cell mediated, perhaps protective DTH. Finally, the efficacy of DxM-lipos was significantly superior than that of Enbrel®, a drug officially approved for difficult RA cases, even if the comparability between the therapeutic effect in rat AA and RA is questionable.

This Mφ–targeting drug, with the trade name "Micromethason" considerably reduces the therapeutic dose and side-effects, and therefore represents a promising alternative for the

treatment of RA, making potent anti-inflammatory steroids safer for treatment in human diseases. The present study is a good example for translational research with commercial perspectives for the manufacturer Novosom AG. In order to achieve this goal a clinical study with RA patients should be the next step.

Albert DS, Garcia DJ, 1997; Safety aspects of pegylated liposomal doxorubicin in patients with cancer. Drugs, 54, Suppl 4:30-45

Albright AV, González-Scarano F, 2004; Microarray analysis of activated mixed glial (microglia) and monocyte-derived macrophage gene expression. J Neuroimmunol, 157:27-38

Allen TM, 1994; Long-circulating (sterically stabilized) liposomes for targeted drug delivery. TIPS, 15:215-220

Allen TM, Austin GA, Chonn A, Lin L, Lee KC, 1991; Uptake of liposomes by cultured mouse bone marrow macrophages: influence of liposome composition and size. Biochim Biophys Acta, 1061(1):56-64

American College of Rheumatology Subcommittee on Rheumatoid Arthritis Guidelines, 2002; Guidelines for the management of RA: 2002 Update. Arthritis Rheum, 46:328-346

Arend WP, Malyak M, Guthridge CJ, Gabay C, 1998; Interleukin-1 receptor antagonist: Role in biology. Annu Rev Immunol, 16:27-55

Arnett FC, Edworthy SM, Bloch DA, McShane DJ, Fries JF, Cooper NS, 1988; The American Rheumatism Association 1987 revised criteria for the classifcation of rheumatoid arthritis. Arthritis Rheum, 31:315-324

Auphan N, DiDonato JA, Rosette C, Helmberg A, Karin M, 1995; Immunosuppression by glucocorticoids: inhibition of NF-kappa B activity through induction of I kappa B synthesis. Science, 270(5234):232-233

Avnir Y, Ulmansky R, Wasserman, V., Even-Chen, S., Broyer, M., Barenholz, Y., Naparstek, Y., 2008; Amphiphathic Weak Acid Glucocorticoid Prodrugs Remote-Loaded Into Sterically Stabilized Nanoliposomes Evaluated in Arthritic Rats and in a Beagle Dog. Arthritis Rheum, 58(1):119-129

Badolato R, Ponzi AN, Millesimo M, Notarangelo LD, Musso T, 1997; Interleukin-15 (IL-15) induces IL-8 and monocyte chemotactic protein 1 production in human monocytes. Blood, 90:2804-2809

Barnes PJ, 1998; Anti-inflammatory actions of Glucocorticoids: molecular mechanisms. Clin Sci, 94:557-572

Barrera P, Blom A, van Lent PL, von Bloois L, Beijnen JH, van Rooijen N, de Waal M, van de Putte LB, Storm G, van der Berg WB, 2000; Synovial macrophage depletion with clodronate-containing liposomes in rheumatoid arthritis. Arthritis Rheum, 43:1951-1959

Bickel M, Iwai Y, Pluznik DH, Cohen RB, 1992; Binding of sequence-specific proteins to the adenosine- plus uridine-rich sequences of the murine granulocyte/macrophage colony-stimulating factor mRNA. Proc Natl Acad Sci USA, 89:1001-1005

Billingham MEJ, 1995; in "Mechanisms and models in Rheumatoid Arthritis" (B Henderson, JCW Edwards, ER Pettipher, Eds), p 389, Academic Press London

Billingham MEJ, Hicks C, Carney S, 1990; Monoclonal antibodies and arthritis. Agents Actions, 29(1-2):77–87

Bonanomi MH, Velvart M, Stimpel M, Roos KM, Fehr K, Weder HG, 1987; Studies of pharmacokinetics and therapeutic effects of glucocorticoids entrapped in liposomes after intraarticular application in healthy rabbits and in rabbits with antigen induced arthritis. Rheumatol Int, 7(5):203-212

Boss B, Neeck G, 2000; Correlation of IL-6 with the classical humoral disease activity parameters ESR and CRP and with serum cortisol, reflecting the activity of the HPA axis in active rheumatoid arthritis. Z Rheumatol, 59 (Suppl 2):62-64

Braunwald E, Fauci AS, Kasper DL, Hauser SL, Longo DL, Jameson JL, 2001; Harrison's Principles of internal medicine, McGraw-Hill 15th edition, 1928-1936

Bresnihan B, 1999; Pathogenesis of joint damage in rheumatoid arthritis, J Rheumatol, 26:717-719

Buttgereit F, 2001; Mechanism of action and effects of glucocorticoids. Z Rheumatol 60:117-119

Cansell M, Parisel C, Jozefonicz J, Letourneur D, 1999; Liposomes coated with chemically modified dextran interact with human endothelial cells. J Biomed Mater Res, 44:140-148

Carol M, Pelegrí C, Castellote C, Franch A, Castell M, 2000; Immunohistochemical study of lymphoid tissues in adjuvant arthritis (AA) by image analysis; relationship with synovial lesion. Clin Exp Immunol, 120:200-208

Cher DJ, Mossmann TR, 1987; Two types of murine helper T cell clone. II. Delayed type hypersensitivity is mediated by Th1 clones. J Immunol, 138:3688-3694

Crofford LJ, Wilder RL, Ristimaki AP, Sano H, Remmers EF, Epps HR, Hla T, 1994; Cyclooxygenase-1 and -2 expression in rheumatoid synovial tissue. J Clin Invest, 93:1095-1101

Curran RC, Crocker J, 2001; Atlas der Histopathologie, Springer Verlag

Cutolo M, Sulli A, Barone A, Seriolo B, Accardo S, 1993; Macrophages, synovial tissue and rheumatoid arthritis. Clin Exp Rheumatol, 11:331-39

Dinarello CA, Moldawer LL., 2002; Proinflammatory and Anti-inflammatory cytokines in rheumatoid arthritis. 3. edition

Doyen V, Rubio M, Braun D, Nakajima T, Abe J, Saito H, Delespesse G, Sarfati M, 2003; Thrombospondin 1 is an Autocrine Negative Regulartor of Human Dendritic Cell Activation. J Exp Med, 198(8):1277-1283

Dumur CI, Suhail N, Best AM, Archer KJ, Ladd AC, Mas VR, Wilkinson DS, Garrett CT, Ferreira-Gonzalez A, 2004; Evaluation of Quality-Control Criteria for Microarray Gene Expression Analysis. Clin Chem, 50(11):1994-2002

Eck MJ, Sprang SR, 1989; The structure of tumor necrosis factor-α at 2.6 Å resolution. J Biol Chem, 264(29):17595–17605

Elliott P, Peters RF, White AM, 1971; A study of the relationship between glucocorticoid-induced weight loss in rats and the activity of skeletal-muscle and cardiac-muscle ribosomes in vitro. J Biochem, 125(4):106P-107P

Firestein GS, Alvaro-Gracia JM, Maki R, 1990; Quantitative analysis of cytokine gene expression in rheumatoid arthritis. J Immunol, 144:3347-3353

Fishman P, Bar-Yehuda S, Madi L, Rath-Wolfson L, Ochaion A, Cohen S, Baharav E, 2006; The PI3K-NF-κB signal transduction pathway is involved in mediating the anti-inflammatory effect of IB-MECA in adjuvant-induced arthritis. Arthritis Res Ther, 8:R33

Foong WC, Harsanyi BB, Mezei M, 1989; Effect of liposomes on hamster oral mucosa. J Biomed Mat Res, 23:1213-1229

Foxwell B, Browne K, Bondeson J, Clarke C, de Martin R, Brefnnan F, Feldmann M, 1998; Efficient adenoviral infection with IκBα reveals that macrophages tumor necrosis factor α production in rheumatoid arthritis is NF-κB dependant. Proc Natl Acad Sci, 95:8211-8215

Fries JF, Williams CA, Morfeld D, Singh G, Sibley J, 1996; Reduction in long-term disability in patients with rheumatoid arthritis by disease-modifying antirheumatic drug-based treatment strategies. Arthritis Rheum, 39:616-622

Fujikado N, Saijo S, Iwakura Y, 2006; Identification of arthritis-related gene clusters by microarray analysis of two independent mouse models for rheumatoid arthritis. Arthritis Res Ther, 8:R100;

Genovese MC, Bathon JM, Martin RW, Fleischmann RM, Tesser JR, Schiff MH, Keystone EC, Wasko MC, Moreland LW, Weaver AL, Markenson J, Cannon GW, Spencer-Green G, Finck BK., 2002; Etanercept versus methotrexat in patients with early rheumatoid arthritis: two year radiographic and clinical outcomes. Arthritis Rheum, 46:1443-1450

Gravallese EM, Harada Y, Wang JT, Thornhill TS, Juppner H, Goldring SR, 1998; Identification of cell types responsible for bone resorption in rheumatoid arthritis and juvenile rheumatoid arthritis. Am J Path, 152:943-951

Harris JM, Chess RB, 2003; Effect of pegylation on pharmaceuticals; Nat Rev Drug Discov, 2:214-221

Herzyk DJ, Allen JN, Marsh CB, Wewers MD, 1992; Macrophage and monocyte IL-1 beta regulation differs at multiple sites. Messenger RNA expression, translation, and post-translational processing. J Immunol, 149(9):3052-3058

Higaki M, Ishihara T, Izumo N, Takatsu M, Mizushima Y, 2005; Treatment of experimental arthritis with PLGA nanoparticles encapsulating betamethasone sodium phosphate. Ann Rheum Dis, 64:1132-1136

Hochhaus G, Barth J, al-Fajoumi S, Suarez S, Derendor H, Hochhaus R, Mollmann H, 2001; Pharmakokinetics and pharmakodynamics of dexamethasone sodium-m-sulfobenzoate after i.v. and i.m. administration: a comparison with dexamethasone-phosphate. J Clin. Pharmac, 41(4):425-434

Hong KS, Hack JK, Hyun PK, Lee HJ, Byun SM., 1988; Liposomes with anti-inflammatory steroid prednisolone palmitate. Drug Dev, 14:765-777

Isomäki P, Luukkainen R, Saario R, Toivanen P, Punnonen J, 1996; Interleukin-10 functions as a antiinflammatory cytokine in rheumatoid arthritis. Arthritis Rheum, 39:386-395

Johnson WJ, Muirhead KA, Meunier PC, Votta BJ, Schmitt TC, DiMartino MJ, Hanna N, 1986; Macrophage activation in rat models of inflammation and arthritis: Systemic activation precedes arthritis induction and progression. Arthritis Rheum, 29(9):1122-1130

Johnson WJ, DiMartino MJ, Hanna N, 1986; Macrophage activation in rat models of inflammation and arthritis: determination of markers and stages of activation. Cell Immunol, 103(1):54-64

Katragadda A, Bridgman R, Betageri G, 2000; Effect of liposome composition and cholesterol on the cellular uptake of stavudine by human monocyte/macrophage. Cell Mol Biol Letters, 5:483-493

Kawai S, 2003; Current drug therapy for rheumatoid arthritis. J Orthop Sci, 8:259-263;

Kinne RW, Stuhlmüller B, Palombo-Kinne E, Burmester GR, 2000; The role of macrophages in the pathogenesis of rheumatoid arthritis. In: Rheumatoid Arthritis, Oxford University Press: 69-87

Kinne RW, Bräuer R, Stuhlmüller B, Palombo-Kinne E, Burmester GR, 2000; Macrophages in rheumatoid arthritis. Arthitis Res, 2:189-202

Kinne RW, Schmidt-Weber CB, Hoppe R, Buchner E, Palombo-Kinne E, Numberg E, Emmerich F, 1995; Long-term amelioration of rat adjuvant arthritis following systemic elimination of macrophages by clodronate-containing liposomes. Arthritis Rheum., 38:1777-1790

Koch AE, Polverini PJ, Kunkel SL, Harlow LA, DiPietro LA, Elner VM, Elner SG, Strieter RM,1992; Interleukin-8 as a macrophage-derived mediator of angiogenesis. Science, 258:1798-1801

Koning GA, Schiffelers RM, Wauben MHM, Kok RJ, Mastrobatista E, Molema G, 2006; Targeting of angiogrnic endothelial cells at sites of inflammation by treatment with DxM-containing RGD peptide liposomes inhibits experimental arthritis. Arthritis Rheum. 54(4):1198-1208

Langman MJ, 1999; Adverse upper gastrointestinal effects of Rececoxib compared with NSAID's. JAMA, 282:1919-1933

Lanza L, Scudeletti M, Puppo F, Bosco O, Peirano L, Filaci G, Fecarotta E, Vidali G, Indiveri F, 1996; Prednisolone increases apoptosis in *in vitro* activated human peripheral blood T lymphocytes. Clin Exp Immunol, 103(3):482-490

Lazarević-Jovanović B, Dimić M, Dimić A, Marković Z, Pavlović D, Cekić, S, 2004; The values of bone mineral bone density in patients with rheumatoid arthritis syndrome and depression syndrome. Med Biol, 11:20-25;

Lipsky PE, van der Heijde DM, St Clair EW, Furst DE, Breedveld FC, Kalden JR, Smolen JS, Weisman M, Emery P, Feldmann M, Harriman GR, Maini RN, 2000; Infliximab and methotrexate in the treatment of rheumatoid arthritis: Anti-Tumor Necrosis factor Trial in Rheumatoid Arthritis with Concomitant Therapy Study Group. N Engl J Med, 343:1594-1602

Liu H, Pope RM, 2003; The role of apoptosis in rheumatoid arthritis. Curr Opin Pharmacol, 3:317-322

Lowe WG, Amos N, Kellaway IW, Williams BD, 1989; Specific accumulation of technecium-99m radiolabeled, negative liposomes in the inflamed paws of rats with adjuvant induced arthritis: effect of liposome size. Ann Rheum Dis, 48:143-148

Mahajan A, Tandon VR, 2005; Corticoids in Rheumatology: Friendo or Foes; J Ind Acad Clin Med, 6(4):275-280

Mans K, 2005; Maßgeschneiderter cDNA Mikroarray zur Messung der Monozytenaktivierung und zur Diagnose der rheumatoiden Arthritis. Thesis in biotechnology, Fachhochschule Berlin

McInnes IB, al-Mughales J, Field M, Leung BP, Huang FP, Dixon R, Sturrock RD, Wilkinson PC, Liew FY, 1996; The role of interleukin-15 in T-cell migration and activation in rheumatoid arthritis. Nature Med, 2:175-182

Mentzel K, Bräuer R, 1998; Matrix metalloproteinases, IL-6, and nitric oxide in rat antigen induced arthritis. Clin Exp Rheumatol, 16:269-276

Metselaar JM, van den Berg WB, Holthuysen AE, Wauben MH, Storm G, van Lent PL, 2004; Liposomal targetingof glucocorticoids to sinovial lining cells strongly increases therapeutic benefit in collagen type II arthritis. Ann Rheum Dis, 63:348-353,

Metselaar JM, Wauben MH, Wagenaar-Hilbers JP, Boerman OC, Storm G, 2003; Complete remission of experimental arthritis by joint targeting of glucocorticoids with long-circulating liposomes. Arthritis Rheum, 48:2059-2066

Metselaar JM, Sanders S, Van Lamoen R, Van Bloois L, Laverman P, Baranyi L, Savay S, Milosevits J, Wauben MHM, Alving CR, Storm G, Szebeni J, 2002; Complement activation-related hypersensitivity reactions caused by pegylated liposomes, Thesis (chapter 8), Utrecht University

Moreland LW, Schiff MH, Baumgartner SW, Tindall EA, Fleischmann RM, Bulpitt KJ, Weaver AL, Keystone EC, Furst DE, Mease PJ, Ruderman EM, Horwitz DA, Arkfeld DG, Garrison L, Burge DJ,

Blosch CM, Lange ML, McDonnell ND, Weinblatt ME, 1999; Etanercept therapy in rheumatoid arthritis: a randomized controlled trial. Ann Inter Med, 130:478-486

Morito T, Oishi K, Yamamoto M, Matsumoto K, 2000; Biphasic regulation of Fc-receptor mediated phagocytosis of rabbit alveolar macrophages by surfactant phospholipids, Yohoku J Exp Med, 190(1):15-22

Moser DM, 2003; The many faces of macrophage activation. J Leukoc Biol, 73:209-212

Mulherin D, Fitzgerald O, Bresnihan B, 1996; Synovial tissue macrophage populations and articular damage in rheumatoid arthritis. Arthritis Rheum, 39:115-124

Neidel J, Schulze M, Lindschau J, 1995; Association between degree of bone-erosion and synovial fluid-levels of tumor nekrosis factor alpha in knee joints of patients with rheumatoid arthritis. Inflamm Res, 44:217-221

Nishikawa K, Arai H, Inoue K, 1990; Scavanger receptor-mediated uptake and metabolism of lipid vesicles containing acid phospholipids by mouse peritoneal macrophages. J Biol Chem, 265:5226-31

Nissinen R, Leirisalo-Repo M, Tiittanen M, Julkunen H, Hirvonen H, Palosuo T, Vaarala O, 2003; CCR3, CCR5, interleukin 4, and interferon-gamma expression on synovial and peripheral T cells and monocytes in patients with rheumatoid arthritis. J Rheumatol, 30(9):1928-1934

Nissler K, Pohler D, Hückel M, Simon J, Bräuer R, Kinne RW, 2004; Anti-CD4 monoclonal antibody treatment in acute and early chronic antigen induced arthritis: Influence on macrophage activation. Ann Rheum Dis 63:1470-1477

Palmer, D. G., Selvendran, Y., Allen, C., Revell, P. A., Hogg, N., 1985; Features of synovial membrane identified with monoclonal antibodies. Clin. Exp. Immunol., 59:529-538

Paulus HE, Brahn E, 2004; Is Erythrocyte Sedimentation Rate the Preferable Measure of the Acute Phase Response in Rheumatoid Arthritis? (Editorial), J Rheumatol, 31:838-840

Pertermann A, 2002; Hemmung von Monozyten/Macrophagen-Funktionen durch Dexamethason-enthaltende Phosphatidylcholin-Liposomen in vitro. Medical thesis, University of Leipzig

Pettit AR, Thomas R, 1999; Dendritic cells: the driving force behind autoimmunity in rheumatoid arthritis? Immunol Cell Biol, 77(5):420-427

Pham TN, Rahman P, Tobin YM, Khraishi MM, Hamilton SF, Alderdice C, Richardson VJ, 2003; Elevated serum nitric oxide levels in patients with inflammatory arthritis associated with co-expression of inducible nitric oxide synthase and protein kinase C-eta in peripheral blood monocyte-derived macrophages. J Rheumatol, 30(12):2529–2534

Pincus T, Callahan LF, Sale WG, Brooks AL, Payne LE, Vaughn WK, 1984, Severe functional declines, work disability, and increased mortality in seventy-five rheumatoid arthritis patients studied over nine years. Arthritis Rheum, 27(8):864-872

Richards PJ, Williams AS, Goodfellow RM, Williams BD, 1999; Liposomal clodronate eliminates synovial macrophages, reduces inflammation and ameliorates joint destruction in antigen-induced arthritis, Rheum (Oxford), 38:818-825

Sakurai H, Kohsaka H, Liu MF, Higashiyama H, Hirata Y, Kanno K, Saito I, Miyasaka N, 1995; Nitric oxide production and inducible nitric oxide synthase expression in inflammatory arthritides. J Clin Invest, 96(5):2257-2263

Schmidt I, 2001; Hemmung von Monozyten/Macrophagen-Funktionen durch Dexamethason-enthaltende Phosphatidylcholin-Liposomen in vitro, Medical thesis, University of Leipzig

Schmidt M, Pauels HG, Lügering N, Lügering A, Domschke W, Kucharzik T, 1999; Glucocorticoids Induce Apoptosis in Human Monocytes: Potential Role of IL-1ß. J Immunol, 163(9):3484-3490

Schmidt-Weber CB, Pohlers D, Siegling A, Schädlich H, Buchner E, Volk HD, Palombo-Kinne E, Emmrich F, Kinne RW, 1999; Cytokine Gene Activation in Synovial membrane, Regional lymph nodes, and Spleen during the course of Rat adjuvant arthritis. Cell Immunol, 195(1):53-65

Schulte R, 2003; Biochemische und zellbiologische Charakterisierung der anti-inflammatorischen Wirkung von Dexamethason-enhaltenden Liposomen. Thesis; Friedrich Schiller University, Jena

Schulze-Koops H, Davis LS, Kavanaugh AF, Lipsky PE, 1997; Elevated cytokine messenger RNA levels in the peripheral blood of patients with rheumatoid arthritis suggest different degrees of myeloid cell activation. Arthritis Rheum, 40:639-647

Scott BB, Weisbrot LM, Greenwood JD, Bogoch ER, Paige CJ, Keystone EC, 1997; Rheumatoid arthritis synovial fibroblast and U937 macrophage/monocyte cell line interaction in cartilage degradation. Arthritis Rheum, 40(3):490-498

Shannon W, Culverhouse R, Duncan J, 2003; Analyzing microarray data using cluster analysis. Pharmacogenomics, 4(1):41-51

Simon J, Surber R, Kleinstäuber G, Petrow PK, Henzgen S, Kinne RW, Bräuer R, 2001; Systemic macrophage activation in locally-induced experimental arthritis. J Autoimmun, 17:127-136;

Smyth GK, Speed T, 2003; Normalization of cDNA microarray data. Methods, 31:265-273

Stuhlmüller B, Ungethüm U, Scholze S, Martinez L, Backhaus M, Kraetsch HG, Kinne RW, Burmester GR, 2000; Identification of known and novel genes in activated monocytes from patients with rheumatoid arthritis. Arthritis Rheum, 43(4):775-790

Symmons D, 2002; Epidemiology of rheumatoid arthritis: determinants of onset, persistence and outcome. Best Pract Res Clin Rheymatol, 16:707-722

Szebeni J, 2001; Complement activation related pseudoallergy caused by liposomes, micellar carriers of intravenous drugs and radiocontrast agents. Crit Rev Ther Drug Carr Syst, 18:567-606

Szoka F Jr, Papahadjopoulos D, 1978; Procedure for preparation of liposomes with large internal aqueous space and high capture by reverse-phase evaporation. Proc Natl Acad Sci, 75:4194-4198

Takasugi K, Yamamura M, Iwahashi M, Otsuka F, Yamana J, Sunahori K, Kawashima M, Yamada M, Makino H, 2006; Induction of tumour necrosis factor receptor-expressing macrophages by interleukin-10 and macrophage colony-stimulating factor in rheumatoid arthritis. Arthritis Res Ther, 8:R126

Tetlow LC, Lees M, Ogata Y, Nagase H, Woolley DE, 1993; Differential expression of gelatinase B (MMP-9) and stromelysin-1 (MMP-3) by rheumatoid synovial cells in vitro and in vivo. Rheumatol Int, 13(2):53-59

Torchilin VP, Lukyanov AN, 2003; Peptide and protein drug delivery to and into tumors: challenges and solutions. Drug Discov Today, 8:259-266

Tsao PW, Suzuki T, Totsuka R, Murata T, Takagi T, Ohmachi Y, Fujimura H, Takata I, 1997; The effect of dexamethasone on the expression of activated NF-kappa B in adjuvant arthritis. Clin Immunol Immunopathol, 83:173-178

Uziely B, Jeffers S, Isacson R, Kutsch K, Wei-Tsao D, Yehoshua Z, Libson E, Muggia FM, Gabizon A., 1995; Liposomal doxorubicin: antitumor activity and unique toxicities during two complementary phase I studies. J Clin Oncol, 13:1777-1785

Vertut-Doi A, Ishiwata H, Miyajima K, 1996; Binding and uptake of liposomes containing poly(ethylene glycol) derivate of cholesterol (stealth liposomes) by the macrophage cell line J774: influence of PEG contents and its molecular weight. Biochim, Bophys Acta 1278:19-28

Wang P, Wu P, Siegel MI, Egan RW, Billah MM., 1995, Interleukin (IL)-10 inhibits nuclear factor kappa B (NF kappa B) activation in human monocytes. IL-10 and IL-4 suppress cytokine synthesis by different mechanisms. J Biol Chem, 270:9558-9563

Wehling M, 2005; Clinical Pharmacology. Springer Verlag

Westra J, 2005; Experimental studies on signal transduction pathways in rheumatoid arthritis. Medical thesis; University Medical Center Groningen

Wolffe AP, 1997; Transcriptional control. Sinful repression. Nature, 387:16-17

Xie QW, Kashiwabara Y, Nathan C, 1994; Role of transcription factor NF-kB/Rel in induction of nitric oxide synthase. J Biol Chem, 269:4705-4708

Yang X, 2001; Distinct function of Th1 and Th2 type delayed type hypersensitivity: protective and pathological reactions to chlamydial infection. Microsc Res Tech, 53(4):273-277

Yokoyama K, Okamoto H, Watanabe M, Suyama T, Mizushima Y, 1985; Development of corticosteroid incorporated in lipid microspheres .Drugs Exp Clin Res, 11:611-620

Yoshino S, Kinne R, Hünig T, Emmrich F, 1990; The suppressive effect of an antibody to the α/β T cell receptor in rat adjuvant arthritis: studies on optimal treatment protocols. Autoimmunity, 7:255-266

Yui S, Sasaki T, Miyazaki A, Horiuchi S, Yamazaki M, 1993; Induction of murine macrophage growth by modified LDL's. Arterioscler Thromb, 13:331-337

Summary

Background: The abundance and activation of macrophages (Mφ) in the inflamed synovial membrane significantly correlates with the severity of rheumatoid arthritis (RA). Mφ possess widespread pro-inflammatory, destructive and remodeling capabilities that critically contribute to acute and chronic disease. Also, activation of the monocytic lineage is not locally restricted, but extends to systemic parts of the mononuclear phagocyte system. Thus, selective counteraction of Mφ activation remains an efficacious approach to diminish local and systemic inflammation, as well as prevent irreversible joint damage.

Glucocorticoids (GC) represent the most important and frequently used class of anti-inflammatory and immunosuppressant agents in the management of many rheumatologic diseases. Their unequalled efficacy and the difficulty in replacing them with other medications, despite obvious concerns about long-term side effects, emphasizes the need of making them safer. Specific targeting of GC to the synovium has the potential to increase drug efficacy while minimizing extra-synovial toxicity, an approach which has been attempted since the 1970's by liposomal encapsulation of GC. One particular feature of liposomes is that they are efficiently phagocytosed by activated Mφ and can hence be targeted towards the inflamed synovium.

In previous in vitro studies, different dexamethasone-containing liposome formulations (DxM-lipos), varying in composition and size, have been compared for their uptake and efficacy to inhibit activation in Mφ; allowing us to choose the liposome formulation which most successfully fulfilled these parameters for the present study.

Methods and results: First, we verified whether the chosen DxM-lipos formulation was sufficiently ingested by Mφ, and lacked signs of toxicity upon incubation with human monocytes/Mφ isolated from the peripheral blood. These prerequisites were fulfilled, thereafter we analyzed the differential gene expression of LPS/IFN-γ-stimulated Mφ pre-incubated with PBS- or DxM-lipos, by performing microarray analysis. This method, which allows to monitor simultaneously the expression patterns of thousands of genes during cellular differentiation and response, offered a general overview of the genes up- or down-regulated by DxM-lipos, and showed that the expression of some interleukins (TNF-α, IL-1β, IL-6 and IL-1RA) and of the cyclooxygenase 1 were significantly reduced. These results were validated by conventional RT-PCR and by measuring the cytokine secretion by ELISA; thus confirming that DxM-lipos efficaciously inhibited the production of key pro-inflammatory effector molecules in Mφ. In

addition, we evidenced the suitability of performing microarray analysis as a general screening method to identify relevant gene expression patterns in disease or upon therapy and to focus further investigations on selected target genes, based on the relevant microarray findings.

The second part of the present study focused on the efficacy of DxM-lipos in the experimental model of adjuvant arthritis (AA), induced by intradermal injection of Mycobacterium butyricum (Mb) on day 0. Rats with established AA were systemically treated with 3 intravenous administrations of DxM-lipos (1 mg/kg, days 14, 15, 16 post induction), resulting in a significant suppression by 90 – 95% of the clinical parameters, arthritis score and paw volume as well as histological inflammation and joint destruction. In addition, DxM-lipos led to long-lasting amelioration of AA (for more than 14 days) and were significantly more efficacious than drug-free, PBS-liposomes and non-encapsulated DxM, both in acute and chronic disease phases. By performing a dose response study, we furthermore showed that encapsulation increased the efficacy of DxM by at least a factor of 10 compared to free DxM.

Throughout the time course of AA, we monitored several hematological, immunological and systemic Mφ-activation parameters. In the present study, we showed that DxM-lipos treatment significantly inhibited systemic inflammation alterations, such as the erythrocyte sedimentation rate, the increased white blood count, as well as the augmented number of leukocytes, both systemically in the spleen and locally in the popliteal lymph nodes, in contrast to free DxM and PBS-lipos treatment. The circulating lymphocytes and the specific antibody response to the arthritogenic Mb were significantly reduced by DxM-lipos, suggesting a partial immuno-suppressant side-effect. However, inhibition of the systemic monocyte/Mφ-activation also affected the distant peritoneal Mφ, reducing their production of TNF-α, IL-1β and IL-6 in response to systemic DxM-lipos treatment, and in addition to systemic anti-inflammatory effects, possibly contributed to the therapeutic benefit of DxM-lipos

Furthermore, we compared the effects of DxM-lipos treatment (3 x i.v.,1 mg/kg, days 14, 15, 16) to those of Enbrel® (2 x s.c. administration, 0.3 mg/kg, days 14 and 17). Our results showed no significant clinical amelioration of AA after treatment with Enbrel®, a highly-effective anti TNF-α treatment officially approved as an anti-rheumatic drug, and a significantly superior efficacy of DxM-lipos in the experimental model of AA.

Conclusions: The present investigation on this Mφ-targeting drug is an example of translational research, concluding that this new formulation of potent anti-inflammatory steroids has the potential to enhance therapeutic efficacy and limit side-effects of treatment in inflammatory disorders like human RA.

Curriculum vitae

ANDERSON Rebecca
born the 06.04.83 in St Martin d'Hères (F)
English, French and Spanish nationality

Scholarship

- 1989-90:   Kalktaren   **Schlieren**   **CH**
- 1990-91:   Colégio Alemán San Alberto Magno   **Zaragoza**   **E**
- 1991-94:   Ecole Primaire Internationale Houille Blanche   **Grenoble**   **F**
- 1994-2001:   Collège & Lycée International Stendhal

- March 2001: Deutsches Sprachdiplom der Kulturministerkonferenz Stufe II

- June 2001 :   Graduation: Baccalauréat Scientifique (spécialité Biologie)   **F**

University

- from 2001:   Medical school: Friedrich Schiller Universität (FSU)   Jena   D
- SS 2002:   Course: Laser in medicine

- Sept. 03:   1st state exam: Ärztliche Vorprüfung mark: 2.0

- SS 2005:   ERASMUS- exchange semester Universidad Autonoma   **Barcelona**   **E**

- Mai 2008:   2nd state exam: Ärztliche Prüfung mark: 2.0

Clinical rotations

- Aug 2002:   Surgery & Internal medicine (University of Tennessee)   **Knoxville**   **USA**
- March 2003:   Emergency room (University of Tennessee)   **Knoxville**   **USA**
- Sept. 2003:   ICU Internal medicine (Clinica Miguel Enrique)   Havana   Cuba
- March 2004:   Ophthalmology (Clinique St Joseph & Practice Dr. Pellat)   Chambéry   F
- Sept. 2005:   Anesthesia (Klinikum der FSU)   Jena   D
- 3/ 2006:   Pediatrics (Hospital universitario)   Salamanca   E
- 8/06-12/06:   Surgery elective (Gondar college of medical sciences)   Gondar   **Ethiopia**
- 1/07-4/07:   Internal medicine elective (Universidad de Buenos Aires)   **Buenos Aires**   **Argentina**
- 5/07-8/07:   Pediatrics elective (Centre hospitalier universitaire l'Archet 2)   Nice   F

Thesis

- from 2005:   Experimental Rheumatology unit (Prof. Kinne)   Jena   D
                University Hospital FSU in collaboration with the Dpt. of
                Rheumatology, Charite, Berlin (Prof. Stuhlmüller)

- SS 2005:   Research Project: Faculty of Pharmacy, University of   Barcelona   E
                Barcelona (Dr. Franch & Dr. Castell)

Publications

- <u>Sept. 2005</u>:   33. Kongress der deutschen Gesellschaft für Rheumatologie   Dresden   D
  Abstract: "<u>Liposomal encapsulation of water soluble dexamethasone</u>
  <u>enhances & prolongs the anti-inflammatory effects in rat adjuvant arthritis</u>
  R Anderson, A Franch, M Castell, C Pelegri, U Rauchhaus, S Panzer, R W Kinne

- <u>2005</u>:   Ann. Rheum. Dis 64 (2005) 342-344
  <u>CD68 is not a macrophage specific antigen</u> * Authors reply
  JT Beranek, E Kunisch, R Anderson, RW Kinne, R Fuhrmann, A Roth, W
  Lungershausen, U Rauchhaus, S Panzner

- <u>Feb. 2007</u>:   27. European Workshop for Rheumatology and Research   Florence   I
  Abstract: "<u>Liposomal encapsulation of water soluble dexamethasone</u>
  <u>(Micromethason) enhances and prolongs the anti-inflammatory effects</u>
  <u>in rat adjuvant arthritis</u>
  R Anderson, A Franch, M Castell, F Pérez-Cano, U Rauchhaus, S Panzer,
  R W Kinne

<u>Employments:</u>

- 2004- 06:   Docent in histology courses, Medical Faculty, FSU Jena
- 2008:   Medical assistant duties, University Hospital, FSU Jena

Jena, the 25th July 2008   Rebecca Anderson de la Llana

Acknowledgments

Ehrenwörtliche Erklärung

Hiermit erkläre ich, dass mir die Promotionsordnung der Medizinischen Fakultät der Friedrich-Schiller-Universität bekannt ist,

ich die Dissertation selbst angefertigt habe und alle von mir benutzten Hilfsmittel, persönlichen Mitteilungen und Quellen in meiner Arbeit angegeben sind,

mich folgende Personen bei der Auswahl und Auswertung des Materials sowie bei der Herstellung das Manuskripts unterstützt haben: Prof. Dr. med. Kinne

die Hilfe eines Promotionsberaters nicht in Anspruch genommen wurde und dass Dritte weder unmittelbar noch mittelbar geldwerte Leistungen von mir für Arbeiten erhalten haben, die im Zusammenhang mit dem Inhalt der vorgelegten Dissertation stehen,

dass ich die Dissertation noch nicht als Prüfungsarbeit für eine staatliche oder andere wissenschaftliche Prüfung eingereicht habe und

dass ich die gleiche, eine in wesentlichen Teilen ähnliche oder eine andere Abhandlung nicht bei einer anderen Hochschule als Dissertation eingereicht habe.

Jena, den 25. Juli 2008   Rebecca Anderson de la Llana